INVESTIGATION OF VAPOR-LIQUID EQUILIBRIA FOR HYDROGEN-SIX CARBON HYDROCARBONS

By
RICHARD EUGENE THOMPSON

Bachelor of Science
Oklahoma State University
Stillwater, Oklahoma
1951

Master of Science
Colorado School of Mines
Golden, Colorado
1959

Submitted to the faculty of the Graduate School of the
Oklahoma State University of Agriculture and
Applied Sciences in partial fulfillment
of the requirements for the degree
of DOCTOR OF PHILOSOPHY
August, 1963

INVESTIGATION OF VAPOR-LIQUID EQUILIBRIA

FOR HYDROGEN-SIX CARBON HYDROCARBONS

Thesis Approved:

Wayne C. Edmister
Thesis Adviser

R. N. Maddox

John B. West

Clarence M. Cunningham

David L. Weeks

Robert MacVicar
Dean of the Graduate School

PREFACE

In the present work, experimental vapor-liquid equilibrium data were obtained at elevated pressures and temperatures for the binary systems hydrogen-benzene and hydrogen-cyclohexane. The systems were chosen to provide data for the characterization of the effect of the nature of the solvent on gas solubility data. The conditions of measurement were selected, inasmuch as possible, to extend the range of available data for the above systems.

I wish to thank professor Wayne C. Edmister for his patience and guidance during the course of this work. I appreciate sincerely the encouragement and help received from the staff of the School of Chemical Engineering and my fellow graduate students. Particular thanks are due to Mr. William B. Lumpkin, whose help in the experimental work was invaluable. I also wish to express my appreciation to Mrs. L. C. Dennis, who typed this thesis.

The financial assistance of the Esso Research and Engineering Company and the Standard Oil Foundation, Incorporated, is gratefully acknowledged. The Phillips Petroleum Company generously donated the hydrocarbons used in the experimental work.

It is not possible to express adequately to my wife, Marilyn, my appreciation for her devotion and help during these lean years.

TABLE OF CONTENTS

Appendix

Page

LIST OF TABLES

Page

LIST OF FIGURES

Page

CHAPTER I

INTRODUCTION

This study consists of a theoretical and experimental investigation of equilibria between coexisting vapor and liquid phases at elevated temperatures and pressures. The particular systems investigated were the binary systems composed of hydrogen with n-hexane, cyclohexane, and benzene. The experimental data for hydrogen--n-hexane were available (54). Data for the two remaining systems were obtained in the experimental part of this work.

There were several reasons for selecting the above systems for study. Systems containing hydrogen with light hydrocarbons are encountered in petroleum refineries, so that the data obtained here may be of practical use. The hydrocarbons were chosen with the intent of obtaining data to determine the effect of varying solvent nature on hydrogen solubility. Finally, some data were available for comparison, which allowed the experimental apparatus and technique to be checked.

The voluminous literature in the field of vapor-liquid equilibria amply testifies to its importance. The interest in such data has had two aspects: practical and theoretical. From the practical side, data are needed for the design and analysis of operation of chemical plant equipment. Theoretical interest has stemmed from two problems: thermodynamic testing of vapor-liquid equilibrium data, and correlation of existing data for extension to new systems.

The particular type of vapor-liquid equilibrium studied in this work is that in which one of the components is a gas, i. e., is above its critical temperature. Certain difficulties present in any study of vapor-liquid equilibria are more pronounced when one component is a gas. The selection of experimental apparatus and method of analysis of composition of equilibrium phases is more difficult because of the wide difference in volatility of the components. The theoretical problem of hypothetical standard states is more prominent; equilibrium conditions correspond to conditions far removed from those in which the gas can exist as a pure liquid, or the solvent as a pure vapor.

In the following chapter, prior work in vapor-liquid equilibria is reviewed. This review covers experimental methods, methods of analysis of composition, and previous investigations for the systems studied here. In Chapter III, vapor-liquid equilibria theory is discussed, especially as it pertains to the present work. The experimental equipment, precedure, and results are described next. Finally, the data are analyzed and the results of correlation work are discussed.

CHAPTER II

PRIOR INVESTIGATIONS

As stated previously, the literature in the field of vapor-liquid equilibria is voluminous. The review presented below includes only a few aspects of the total field. Emphasis is placed on work in gas-liquid equilibria. Experimental techniques are described first. Methods of analysis of composition are discussed next. In connection with the latter subject, some preliminary work in gas chromatography is reported. Prior studies on systems containing hydrogen with n-hexane, cyclohexane, and benzene are tabulated in the final section.

Experimental Methods

The experimental investigation of vapor-liquid equilibria involves measurement of the pressure, temperature, and composition of coexisting equilibrium phases. Determinations of densities for the equilibrium phases, subcooled liquids, and superheated vapor mixtures are desirable (as discussed in Chapter III), but not necessary for characterizing the equilibrium state.

The experimental problem is simple, in principle. In practice, many difficulties arise, and errors are common. Hipkin (33) has classified these errors as follows:

(1) Theoretical limitations
(2) Operational errors
(3) Sampling errors
(4) Analysis errors

Theoretical limitations are inherent in the design of the apparatus. Attainment of equilibrium must be possible. Operational errors include improper operation of the equilibrium apparatus, incorrect measurement or control of temperature and pressure, and the use of impure materials. The measurement of temperature and pressure will not be discussed.

Sampling errors are difficult to avoid entirely. The problem is to remove representative samples of the equilibrium phases without disturbing the equilibrium appreciably, and without changing the composition of the samples. Sample lines usually are purged and may have to be heated for gas samples in order to avoid partial condensation.

Even if representative samples have been isolated, the possibility of errors in the analysis of the samples is always present. Analysis errors may limit the overall precision of the p-T-x-y data. As Hipkin has stated, there is a tendency to lump all experimental error in this last category. The magnitude of the other errors listed above may be impossible to evaluate, but the possibility of their presence should always be considered.

The experimental techniques used in the determination of vapor-liquid equilibrium data have been reviewed by Barr-David (6), Robinson and Gilliland (71), and Hipkin (33). These techniques may be classified as shown in Table I. These methods are discussed below. In this discussion, it will be implicit that the equilibrium apparatus must be maintained at a constant, uniform temperature during any determination. Comments from the three references mentioned above are incorporated in the discussion.

TABLE I

EXPERIMENTAL METHODS USED IN THE STUDY OF VAPOR-LIQUID EQUILIBRIA

Method	References
Static	
Constant Volume	11, 47, 57, 69
Variable Volume	15, 46
Bubble- and Dew-Point	
Indirect	54, 73
Visual	17, 41, 42
Dynamic Flow	45, 51, 62
Differential	---
Liquid-Recirculation	6, 66
Vapor-Recirculation	5, 70

Static Method

In the simplest application of the static method, a closed vessel of constant volume is used. The vessel is evacuated, filled with the components to be studied, placed in a constant temperature bath, and agitated. Theoretically, equilibrium is attained after sufficient time has elapsed. The equilibrium phases are then sampled, and the samples are analyzed. Lindroos and Dodge (47) and Peter and Reinhartz (57) used constant-volume cells in recent work.

During the removal of samples from the constant-volume cell, the pressure necessarily falls, disturbing the equilibrium. Liquid samples are usually much smaller than vapor samples and are removed first. Pressure decrease is minimized by making the cell volume large with respect to the sample volume. In gas-liquid equilibria at moderate pressures, a decrease in pressure results in an increase in the concentration of the heavy component. Without agitation, the heavy component enters the vapor phase only by diffusion. If the gas-sampling point is far removed from any liquid surface and sampling is rapid, the sample composition should be affected little by the pressure decrease.

Boomer et al. (11) attempted to avoid pressure decrease in sampling by isolating the samples before removal. A constant-volume cell with three horizontal chambers was used. The upper chamber contained only vapor, the middle chamber contained vapor and liquid, and the lower chamber contained only liquid. The chambers were interconnected at each end by lines provided with valves. The cell was rocked intermittantly to attain equilibrium. The valves were then closed, isolating the samples. One drawback of this apparatus was the long time necessary to make a run. An advantage was that equilibrium phase densities were determined from the volumes of the chambers and the masses of the samples.

A second, and more common, way to reduce pressure decrease during sampling is to use a variable-volume cell. Usually the cell contents are confined over mercury. During sample removal, additional mercury is injected to maintain the pressure nearly constant. Recent studies in which the variable-volume cell was used include those of Connolly (15) and Leland et al. (46). Measurement of the volume of mercury injected during sampling, and of the mass of the sample, permits calculation of the equilibrium phase densities.

Rigas et al. (69) used a variable-volume cell that contained a movable piston interposed between the mercury and the cell contents. From the sampling standpoint, this cell was constant-volume, however. The equilibrium samples were withdrawn very quickly into very small, evacuated spaces that were isolated between valves built into the cell body.

Static equilibrium cells have been agitated by three methods. External agitation by rocking the entire cell has been used extensively. All tubing connected to the cell must be flexible in this case. Internal agitation has been accomplished in two ways: (1) stirring paddles operated by an external motor, and (2) magnetic stirrers operated by an external coil. Several mechanical and operational difficulties have been encountered with agitation. Motors and coils immersed in the constant temperature bath may be subjected to severe temperature conditions. On the other hand, external mounting may result in serious heat leaks. Motor-operated stirrers require packing glands, which are sources of pressure leaks in the equilibrium cell.

The static method is equally applicable to gas-liquid and vapor-liquid equilibria, although it has probably been used more for high-pressure gas-liquid studies. The variable-volume cell seems to be more versatile than the constant-volume cell, but is more complicated. The use of mercury as a confining substance limits the temperature range of the variable-volume cell. In the static method, the critical conditions of a mixture cannot be determined directly. Multicomponent mixtures, as well as binaries, may be investigated.

Bubble- and Dew-Point Method

The bubble-and dew-point method is essentially a modification of the variable-volume static method in which sampling is avoided. Two basic variations have been used.

Indirect Method - The work of Sage *et al*. (54, 73) exemplifies the indirect bubble- and dew-point method. The components are weighed or measured volumetrically into a variable-volume cell over mercury and the temperature is stabilized. Pressure is increased in increments by injecting mercury. The volume of the mixture is determined from the amount of mercury injected. This procedure is repeated to very high pressures, passing through the two-phase region. Samples are not withdrawn, since the composition is known. The entire procedure is repeated for several temperatures and compositions. The p-V data for each composition are plotted and the bubble-and dew-points found from breaks in the curves.

The indirect method is quite satisfactory for bubble-point measurements. However, dew-points are often difficult to determine from p-V plots, so that Sage *et al*. usually determined dew-point compositions by withdrawing gas samples from the equilibrium mixture and analyzing these samples.

Visual Method - Kay (41, 42) used a glass capillary in his work, which allowed visual determination of the formation of the first bubble in a liquid and of the first dew from the vapor. The apparatus was much simpler than that used in the indirect method, although two capillaries had to be used to cover the range of densities encountered.

Connolly (17) used an apparatus similar to that of Kay, but used a slightly different technique to observe the dew-point. The dew-point was determined by the appearance of a speck of liquid at the point of contact of a steel stirring ball with the wall of the capillary. The speck pressure is slightly different from the true dew-point pressure. Corrections were made for this effect. Bubble-points were determined from p-V plots.

Both Kay and Sage *et al*. cross-plotted their data on large graphs to determine equilibrium concentrations. Connolly interpolated his bubble-point data by a curve-fitting method. A large number of experimental points are required for either treatment. The method is applicable only to binary mixtures, as can be shown by application of the phase rule.

The bubble- and dew-point method has several advantages. Density data may be obtained for the equilibrium and unsaturated phases. Experimental compositions are usually known without sampling. Critical conditions may be determined rather precisely if the components are very pure.

Dynamic Flow Method

There are several variations of the dynamic flow method, but the basic procedure is that of bubbling a gas slowly through a liquid. Sufficient contact with the liquid should saturate the gas. The exit gas stream is collected and analyzed. A liquid sample may also be withdrawn and analyzed.

One difficulty with the dynamic flow method is that equilibrium may not be attained. Several factors may contribute to this problem. There is a definite pressure drop in the gas phase as it travels through the liquid, due to the hydrostatic head of the liquid. The pressure drop effect should be small at high pressures. Adequate contacting may not be achieved between the phases. Prausnitz and Benson (62) used two liquid vessels in series to avoid this problem, as well as introducing the gas through a fritted-glass sparger. Krichevskii and Sorina (45) used only one vessel, but provided stirring of the cell contents. Michels (51) also used one vessel, but broke the gas up into small bubbles and passed it through a packed section. Insufficient liquid mixing may occur, also, but this can be avoided by allowing the mixture to equilibrate before passing the gas through. Then the liquid should be of uniform composition.

Entrainment of liquid in the gas phase can also produce error in the dynamic flow method. Low flow rates can be used to avoid this problem. Prausnitz and Benson used a glass-wool plug to prevent entrainment. Krichevskii and Sorina used a liquid knock-out chamber.

The dynamic flow method appears to be limited to use with a single liquid component. If a gas is bubbled through a mixed liquid, the liquid components will leave in different amounts in the gas phase. Thus, the liquid-phase composition will change with time. A large liquid volume and small gas rate would lessen the problem. The case of a mixed gas with a single liquid has been studied by Michels (51), who investigated the system ammonia-hydrogen-nitrogen. In the latter study, the mole ratio of hydrogen to nitrogen was held constant at 3:1.

The dynamic flow method allows withdrawal of the gas sample at constant pressure and in large amount. Several samples may be withdrawn at the same conditions, if necessary.

Differential Method

The differential method is no longer used (33) and is not applicable to gas-liquid mixtures, but will be discussed briefly. A mixture of known composition is charged to a distillation flask and boiled. The distillate is condensed in a receiver and analyzed. Either average compositions are used for the distillate and residue, or else a series of distillates are sampled. In the latter case, composition is plotted as function of volume distilled and extrapolated back to zero volume to find the composition in equilibrium with the initial liquid. The question arises as to whether or not the liquid leaving a boiling mixture is in equilibrium with it. It is known that even pure liquids may superheat when boiling. Furthermore, vapor can condense on the walls of the flask and change in composition before entering the condenser.

Liquid-Recirculation Method

In the liquid recirculation method a still is used, as in the differential method, but the vapor is condensed and recirculated to the still. This method is also not applicable with gases. Liquid recirculation has been used at elevated pressures where both components are below their critical temperature, notably by Barr-David (6) and Rao *et al*. (66). The liquid recirculation method suffers from the same drawback as the differential method, that is, boiling in the still. A steady state may be achieved, but not necessarily a true equilibrium state.

Vapor-Recirculation Method

In the vapor-recirculation method, vapor is removed from the top of the equilibrium vessel and recirculated to the bottom. The vapor must be pumped by some means, and must be heated or cooled to the temperature of the cell before reintroduction. Aroyan and Katz (5) and Roberts and McKetta (70) used magnetic pumps to recirculate the vapor in high pressure studies.

Consideration of the vapor-recirculation method shows that it is actually the dynamic flow method in closed-circuit form. Thus, sufficient recycling should give true equilibrium. Furthermore, the vapor-recirculation method has the advantage that it can be used with vapors, as well as gases. This method can also be used with multicomponent mixtures, provided that vapor samples are removed without disturbing the contents of the cell. The latter was accomplished by Aroyan and Katz by the introduction of mercury into the recirculation system during removal of the vapor sample.

The recycled vapor must not condense, since this will change its composition. If the vapor is superheated at room temperature, no difficulty is encountered. But for systems operating at temperatures higher than ambient, the recycle lines and pump must be heated. Roberts and McKetta placed the entire apparatus in an air bath for operation at elevated temperatures.

It may be remarked that vapor-recirculation can also be viewed as a method of agitation for the static method. Indeed, Roberts and McKetta used the method in this way, allowing the phases to remain static for about an hour prior to sampling.

Present Method

Consideration of the above dicussion indicates that in the case of gas-liquid equilibria, there are fundamentally two methods of study with variations on each. These are the dynamic flow and the static methods. Furthermore, liquid samples are almost always drawn more or less instanteously, and at static conditions. The handling of the vapor sample differentiates between the two methods.

The experimental method used in this study is the dynamic flow method. The apparatus used is, for the most part, identical to that of Michels (51) and was purchased from W. C. t'Hart and Zn, Rotterdam. This equipment has several attractive features. Contact with mercury in the equilibrium cell is avoided. Modifications can be made to permit conversion to the vapor-recirculation or static type of operation, and also to permit measurement of volumetric data. The pressure is regulated and measured by the same device. The pressure measuring and regulating equipment obtained with the cell can be adapted for use in other studies, such as p-V-T measurements. A detailed description of the apparatus and experimental procedure is given in Chapter IV.

Methods of Analysis

Conventional methods of analysis, such as refractive indices or liquid densities, cannot be used with gas-liquid samples due to the wide difference in volatilities of the components. Previous investigations were reviewed in as effort to select a suitable method.

Preliminary Work on Gas Chromatography

A method that seemed promising was gas-liquid partition chromatography. Conventional gas chromatographs operate at pressures slightly above atmospheric. In this method, the sample is isolated in small quantity, and then is expanded into the chromatographic column.

In the initial phase of this study, an attempt was made to develop a method for sampling and introduction of equilibrium phase samples into a chromatography unit. The original sampling valve design was based on the desire to obtain densities as well as compositions. It was hoped that a valve could be developed that could eventually be placed directly atop the equilibrium cell in order to isolate known volumes of the samples at equilibrium temperatures and pressures.

A rotary valve, shown in Figure 1, was constructed. Initial operation with the valve was to be outside the constant temperature bath, followed by mounting in the bath if operation proved successful. The valve consisted of two stationary end plates with a rotary center section, all of steel. It was found that to lap a leak-free metal-to-metal surface was very nearly impossible. For this reason, Teflon gaskets were inserted.

The valve could be turned so that either liquid or vapor samples would flow through. Partial rotation trapped the sample. Further rotation connected the sample to the helium supply line that fed the chromatography unit.

Tests performed on the valve showed that it was not satisfactory. The system ethane-benzene was used in these tests. Liquid samples of fair reproducibility were obtained, but vapor compositions

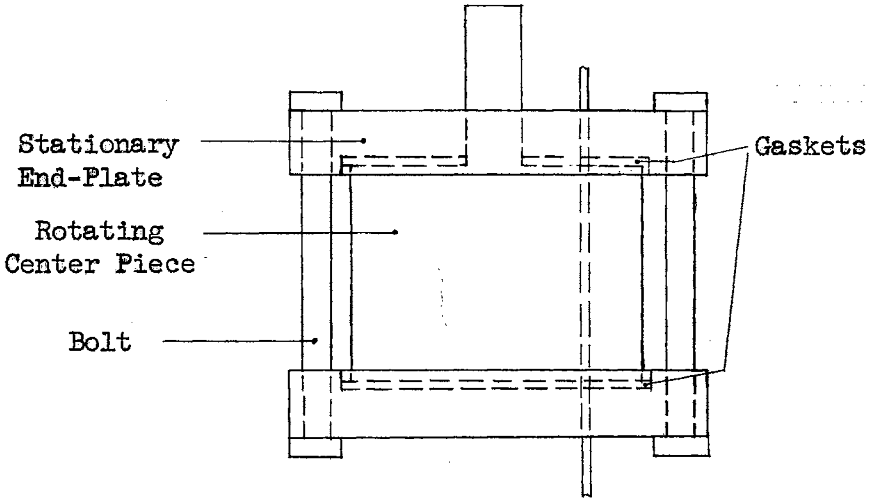

Side View

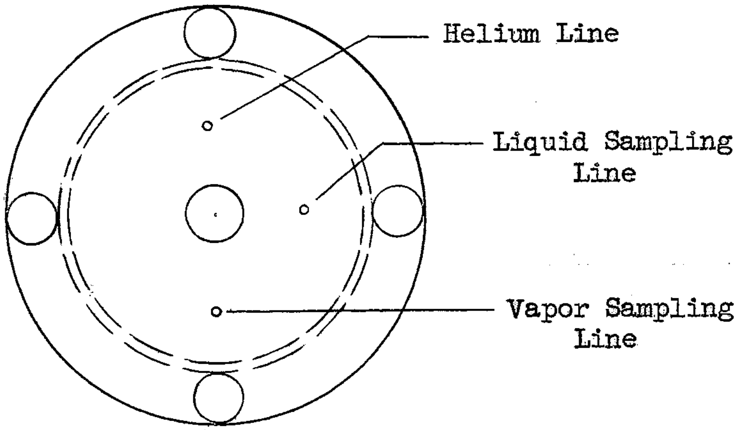

Top View

Figure 1

Gas Sampling Valve

showed extreme variation. The variation in vapor composition was probably due to condensation of benzene in the valve body, since it was not heated. A more serious difficulty developed, however. The Teflon gaskets galled and periodically plugged the capillary connections. Nylon gaskets showed better mechanical stability but were far less self-lubricating, which made the valve extremely difficult to turn. No leakage was observed, but the pressure used was only 150 psig. Because of the difficulties encountered, the above method was abandoned.

The analysis of hydrogen-hydrocarbon mixtures by gas chromatography presents two difficulties. The thermal conductivity of hydrogen is greater than that of the usual carrier gas, helium, while that of the hydrocarbons is less. Even if another carrier gas is used, a reversing switch must be placed in the detector circuit. Furthermore, the holding time of hydrogen in a chromatographic column is very low compared to that of hydrocarbons. A two-section column with switching valve could be used to obtain satisfactory peaks for the hydrogen and hydrocarbon in a reasonable length of time.

Other Methods

Silver (76) used mass spectroscopy in his study of ternary and quaternary mixtures containing the same components used in this study. A suitable mass spectrograph was not available here. Moreover, the precise analysis of mixtures containing hydrogen is difficult on the mass spectrograph. Silver found that several analyses were necessary for each equilibrium sample. The analytic data were treated statistically to obtain equilibrium phase compositions.

Akers et al. (3) utilized built-in thermal conductivity cells in their apparatus to analyze both liquid and vapor phases. This method was peculiarly suited to their apparatus because both liquid and vapor phases were recirculated. Their method was not applicable to the present equipment without extensive modification.

Gas specific gravity has been used to measure sample compositions, after expansion of the samples to low pressure. Aroyan and Katz (5) used this method for analyzing hydrogen-n-butane mixtures. Akers et al. (4) found that this method was not satisfactory for the system nitrogen-n-heptane. The method requires extreme care and is not particularly good for low concentrations.

A general method that has been used in several modifications consists of passing the equilibrium samples through a trap in which the heavy component is retained. The amount of heavy component is found by weighing the trap. The amount of gas is determined by measuring its volume.

Ipatiev et al. (39) and Akers et al. (4) collected the hydrocarbon on activated charcoal. Prausnitz and Benson (62) passed the gas-phase sample through a refrigerated condenser. The remaining gas was passed through a wet-test meter. Correction was made for residual hydrocarbon vapor. Dean and Tooke (20), Krichevskii et al. (44, 45), and Peter and Reinhartz (57) cooled the trap with dry ice-acetone baths to remove the hydrocarbon in the solid phase.

Present Method

The last method mentioned above was chosen as being the simplest and most accurate method available. Equilibrium samples were passed through dry ice-acetone traps, freezing out the hydrocarbon. The traps were weighed before and after sampling. The hydrogen volume was measured at a known temperature and pressure to determine its amount.

Experimental Data

The available literature data for binary mixtures of the materials under consideration are summarized in Table II. Not included in this list are the low pressure solubility for hydrogen in these solvents, which can be found in Seidell and Linke (48). Silver (76) obtained data for ternary and quaternary mixtures of hydrogen with n-hexane, cyclohexane, and benzene at 100 and 200 °F and at 1000 and 2000 psia.

With one exception, the data taken prior to 1957 were only for the solubility of hydrogen in the liquid phase, although Krichevskii and Efremova (44) did determine liquid densities as well. The data of Ipatiev _et al_. (39) include vapor compositions, but their work was at pressures so high that extrapolation to low pressures is difficult. The latest data on cyclohexane (45) and benzene (17) were found after initiation of this work. The range of the available data and the limitations of the apparatus were considered in selecting the temperatures used in the present work.

TABLE II

HYDROGEN-HYDROCARBON BINARY VAPOR-LIQUID EQUILIBRIUM DATA

Hydrocarbon	Pressure Range, psia	Temperatures,* °F	Type of Data	Reference
n-Hexane	500-1700	77	p-T-x	25
	15-2200	95.4	p-T-x	74
	500-10,000	40-460 (40)	p-V-T-x-y**	54
Cyclohexane	670-4500	77, 302, 464	p-T-x	38
	1000-2500	77	p-t-x	25
	15-2000	95.4	p-T-x	74
	750-10,000	68, 104, 140	p-V-T-x-y***	45
Benzene	380-4600	77, 104, 212	p-T-x	40
	750-4500	77, 212, 302 392, 464	p-T-x	38
	15-2200	95.4, 162.7	p-T-x	74
	3500-42,000	77, 122, 158, 212, 302	p-T-x-y	39
	725-7150	77	p-V-T-x***	44
	280-2500	320-500 (18)	p-V-T-x-y**	17

*Where the temperature interval is constant, the temperature limits are listed, followed by the interval in parentheses. Otherwise, individual temperatures are shown.

**Liquid and vapor densities measured.

***Liquid densities only measured.

CHAPTER III

THEORY

The experimental method of obtaining vapor-liquid equilibrium data has always been the direct method. That is, the phases were equilibrated and P-T-x-y data were measured. A second method for obtaining phase-equilibrium data--termed by Dodge (22) the "thermodynamic method"--is possible. This method involves the measurement of volumetric data for the individual phases. The second method is seldom used for determining equilibrium conditions, but is used in the thermodynamic testing of data, and in the correlation of experimental data. Before these subjects can be explored in detail, it will be necessary to present the basic thermodynamic equations of phase equilibria.

Fundamental Relations

The criterion for equilibrium in any isolated system follows directly from the second law of thermodynamics.

$$dS = 0 \quad \text{at constant } U \text{ and } V, \qquad \text{(III-1)}$$

where dS = change in entropy of the system,

U = internal energy of the system,

V = volume of the system.

Gibbs (27) showed that an equivalent criterion is that

$$dU = 0 \quad \text{at constant } S \text{ and } V. \qquad \text{(III-2)}$$

For an open phase composed of a homogeneous mixture of N components,

$$dU = TdS - PdV + \sum_{i=1}^{N} \mu_i dn_i, \qquad \text{(III-3)}$$

where T = absolute temperature in the phase,

P = absolute pressure in the phase,

n_i = number of moles of component i in the phase,

μ_i = chemical potential of component i.

$$\mu_i = \left(\frac{\partial U}{\partial n_i}\right)_{S,V,n_j} \qquad \text{(III-4)}$$

Gibbs deduced two important results from Equations III-2 and III-3. The first result is that the necessary and sufficient conditions for equilibrium in an isolated heterogeneous system are

$$T' = T'' = T''' = \ldots, \qquad \text{(III-5)}$$

$$P' = P'' = P''' = \ldots, \qquad \text{(III-6)}$$

$$\text{and } \mu_i' = \mu_i'' = \mu_i''' = \ldots \quad \text{(for all i).} \qquad \text{(III-7)}$$

The primes refer to different phases.

The second result deduced by Gibbs was the phase rule,

$$D = N - \Phi + 2, \qquad \text{(III-8)}$$

where D = degrees of freedom, or the number of independent intensive thermodynamic variables,

Φ = number of phases in the system

Gibbs also defined the potential function

$$F = U - TS + PV, \tag{III-8}$$

where F = the Gibbs free energy,

and showed that

$$\mu_i = \left(\frac{\partial F}{\partial n_i}\right)_{P,T,n_j} \tag{III-9}$$

The Gibbs free energy, F, is convenient for use in phase equilibrium work because of the particular combination of variables. Differentiation of Equation III-8 at constant temperature yields, eventually, for a pure component,

$$\left(\frac{\partial F}{\partial P}\right)_T = V. \tag{III-10}$$

Integration of Equation III-10 at constant temperature yields

$$F - F^o = \int_{P^o}^{P} VdP. \tag{III-11}$$

It can be shown (22) that

$$\mu_i - \mu_i^o = \int_{P^o}^{P} \bar{V}_i dP, \tag{III-12}$$

where $\bar{V}_i$ = partial molal volume of
component i.

The above relations are essentially all that are needed for work in phase equilibria. Their use turns out to be awkward in some applications. For this reason, Lewis (22) defined the fugacity.

$$\mu_i - \mu_i^o = RT \ln \frac{\overline{f}_i}{f_i^o} \qquad \text{(III-13)}$$

where $\overline{f}_i$ = fugacity of component i in a mixture at T and P,

f_i^o = fugacity of pure i at T and P^o.

The definition of fugacity is completed by the following relation.

$$\lim_{P^o \to 0} \left(\frac{f_i^o}{y_i P^o} \right) = 1 \qquad \text{(III-14)}$$

where y_i = mole fraction of component i in the gas mixture.

Equations III-7 and III-13 yield, for phase equilibrium,

$$\overline{f}_i' = \overline{f}_i'' = \overline{f}_i''' = \ldots \quad \text{(for all i).} \qquad \text{(III-15)}$$

Fugacities are evaluated by means of the equation

$$RT \ln \overline{f}_i = \int_0^P (\overline{V}_i - \frac{RT}{P})dP + RT \ln Py_i, \qquad \text{(III-16)}$$

which can be derived from Equations III-12 and III-13. Fugacities at different pressures are related as shown in the following equation.

$$RT \ln \frac{(\bar{f}_i)_2}{(\bar{f}_i)_1} = \int_{P_1}^{P_2} \bar{V}_i \, dP \qquad \text{(III-17)}$$

Equations III-12 through III-17 apply at constant temperature. Although these equations are written for mixtures, they apply to the case of pure components. For pure components, $y_i = 1$ and $\bar{V}_i = \underline{V}_i$, the pure component molal volume.

Several auxiliary functions have been defined for convenience; these are the activity coefficient, γ_i, the mixture fugacity coefficient, ϕ_i, and the pure component fugacity coefficient, ν_i.

$$\gamma_i = \frac{\bar{f}_i}{x_i f_i^o} \qquad \text{(III-18)}$$

$$\phi_i = \frac{\bar{f}_i}{Py_i} \qquad \text{(III-19)}$$

$$\nu_i = \frac{f_i}{P} \qquad \text{(III-20)}$$

where x_i = mole fraction of component i in the liquid phase (y_i is used if a gas mixture is considered),

f_i^o = fugacity of component i in the "standard state,"

f_i = fugacity of component i at T and P.

Experimental Applications

The experimental method in which equilibrium P-T-x-y data are measured is an application of Equations III-5 and III-6 (which are intuitively true). In this method, the relation between x_i and y_i is sought directly. The experimental information is not sufficient, however, to calculate chemical potentials. From the theoretical standpoint, there is no assurance that equilibrium is actually being observed.

In the general case, the Gibbs free energy must be known as a function of temperature, pressure, and composition in order to calculate chemical potentials (see Equation III-9). At constant temperature, volume must be known as a function of pressure and composition in order to calculate chemical potentials (see Equation III-12). The latter case forms the basis for the thermodynamic method of investigating phase equilibria. In this method, the volumes of the separate phases are determined at constant temperature for different compositions and pressures. Chemical potentials may then be evaluated by use of Equation III-12.

The determination of equilibrium compositions will be a trial-and-error procedure in the thermodynamic method. Consider the case of binary vapor-liquid equilibrium, for example. Compositions x_i and y_i for one component are assumed for the two phases at pressure P. Interpolation of the chemical potential data in each phase for these compositions, at pressure P, gives the thermodynamic potential in each phase. If the proper choice of x_i and y_i has been made, the chemical potentials in the two phases will be equal to each other.

The thermodynamic method is not actually applied to vapor-liquid equilibria in the experimental sense implied here. The reason is that the experimental data required for the calculation of the chemical potential in the liquid phase are not available. Benedict et al. (7) have used the thermodynamic method, but used an equation of state to describe the volumetric behavior of both phases. The use of the equation was justified by comparison with experimental vapor-liquid equilibria data. The experimental thermodynamic method was used by Adams (1) in a study of solid-liquid equilibria.

Other problems are encountered with the thermodynamic method, even where it may be used. The identity of the equilibrium phases may have to be established by independent means. The amount of data required is large, and the processing of the data tedious. The P-V data may be fitted to analytical relations to facilitate processing of the data.

In principle, a second thermodynamic method can be proposed, based on enthalpy data taken at constant pressure for the separate phases. The method itself is perhaps of little practical value, but the principle is invoked in thermodynamic consistency tests, as indicated below.

Thermodynamic Consistency Tests

The direct and thermodynamic experimental methods described above could, in theory, be used to check each other. However, Ibl and Dodge (37), among others, have shown that the explicit evaluation of the chemical potential is not necessary to check the consistency of volumetric and equilibrium data. Relations of the type that they derived are referred to as thermodynamic consistency tests. Perhaps the most convenient equations for testing thermodynamic consistency were presented by Adler *et al*. (2). The integrated equation derived by Adler *et al*. for binary mixtures at constant temperature is

$$\int x_1 \, d\ln K_1 + \int x_2 \, d\ln K_2 = \int \left[z^L + \bar{z}_1^V y_1 \left(\frac{1}{K_2} - \frac{1}{K_1} \right) - \frac{z^V}{K_2} \right] d\ln P, \tag{III-21}$$

where $K_i = y_i/x_i$,

$z = P\underline{V}/RT$.

In this case, the volumes of the saturated liquid and vapor mixtures are required, as well as the volumes of superheated vapor mixtures. The latter are needed in order to calculate $\bar{z}_1^V$, which is given by

$$\bar{z}_1^V = \frac{P\bar{V}_1^V}{RT} = \frac{P}{RT} \left(\frac{\partial V}{\partial n_1} \right)_{P,T,n_2} \tag{III-22}$$

Equation III-21 is preferable to other constant-temperature forms of thermodynamic consistency tests because it relates the experimental data, whereas other forms use derived variables, such as the liquid-phase activity coefficient. In addition, Equation III-21 can be used where one component is a gas--the condition of interest in this study.

Methods have been presented for checking the thermodynamic consistency of equilibrium and volumetric data that use approximations for the volumetric data, or what is equivalent, for fugacity or activity coefficient data. These methods have been used in some instances with no apparent realization that they were, in fact, approximations. Because of this fact, Ibl and Dodge (37) presented rigorous relations and indicated where approximations might be used. For <u>rigorous</u> testing, volumetric data are required for constant-temperature data, and heat-of-mixing data for constant-pressure data.

Gautreaux and Coates (26) stated that a rigorous thermodynamic consistency check based only on P-T-x-y data could be made at one condition, that of infinite dilution. Even in this case pure-component liquid and vapor volumes are needed. These authors presented equations for the case of infinite dilution which are applicable to gases dissolved in liquids. The isothermal form for a binary mixture is

$$(K_1)_{x_1 = 0} = 1 - \left(\frac{\partial P}{\partial x_1}\right)\left(\frac{\underline{V}_2^V}{RT} - \frac{\underline{V}_2^L}{RT}\right), \qquad \text{(III-23)}$$

where all terms are evaluated at conditions corresponding to $x_1 = 0$.

A plot of total pressure as a function of gas solubility is used to find the slope term. The right-hand side of Equation III-23 can then be compared with the extrapolated K value for the solute gas.

Prausnitz and Keeler (65) have suggested a constant-temperature thermodynamic consistency test that can be applied to gas-liquid equilibria at moderate pressures. These authors do not point out in what sense the test is a thermodynamic consistency check. Actually, the use of their method involves certain assumptions. But granting these assumptions, the method is a consistency check in the sense used here. This method is discussed in detail in Appendix H.

Correlation of Experimental Data

The correlation of experimental vapor-liquid equilibrium data may be based on the thermodynamic method of determining equilibrium data. Thus, if equations of state relating volume to pressure and composition at constant temperature are available for liquid and vapor mixtures, the equilibrium compositions may be calculated. This basic method was, in fact, used by Benedict, Webb, and Rubin (7). The same eight-constant equation of state was used to calculate the mixture fugacity in both phases.

Other correlation methods using this general approach have been proposed. Two of these methods will be described below, but some points common to these methods will be discussed first.

K Values

Commonly-used methods of correlating vapor-liquid equilibrium data involve the use of the component distribution coefficient, or vapor-liquid equilibrium ratio,

$$K_i = y_i/x_i. \tag{III-24}$$

Application of the Gibbs phase rule to a two-component system shows that the composition of the equilibrium phases is invariant if system temperature and pressure are specified. Thus, we may regard the K value of Equation III-24 as a function of temperature and pressure. It is obvious, however, that the K value is also a function of the identity of the component in question and of the identity of the second component present. We can express the latter dependence by saying that the K value is also a function of the solvent.

$$K_i = K_i\ (T,\ P,\ \text{component identity, solvent}) \tag{III-25}$$

Application of the phase rule to a N-component two-phase system shows that the specification of temperature and pressure still leaves N - 2 variables, or relations between variables, to be specified for the system to be invariant. For any one temperature and pressure, the K value of a given component is thus a function of the composition of the equilibrium phases. The "solvent" referred to in Equation III-25 is now a mixture of variable composition.

The K value can be expressed in various forms, depending on the combination of Equation III-24 with Equations III-18 through III-20. For the particular case of vapor-liquid equilibrium, the following equations can be derived easily.

$$K_i = \gamma_i^L \nu_i^L / \phi_i^V \tag{III-26}$$

$$K_i = \gamma_i^L \nu_i^L / \gamma_i^V \nu_i^V \tag{III-27}$$

Standard States

Some caution must be exercised in the use of Equations III-26 and III-27. Whenever an activity coefficient is used, the standard state used for f_i^o must be stated clearly. In this work the standard state will always be the pure component at the temperature and pressure of the mixture.

The use of the pure-component standard state has been criticized because it is a hypothetical state for the case of a heavy component in the vapor phase and for a light component in the liquid phase. The standard state fugacity cannot be calculated, for instance, by Equation III-16, because pure component volumetric data do not exist past the limits imposed by the vapor-pressure curve.

Other standard states used are (a) the component in the liquid solution at infinite dilution and (b) the pure component at 1 atm pressure. These latter standard states appear to have no general advantage over the pure-component standard state, since they also may be hypothetical. Furthermore, the use of the pure component standard state permits comparison of activity coefficients of a given solute in different solvents. Prausnitz (61) has discussed the problem of hypothetical standard states in some detail.

Equations of State

The use of the thermodynamic method for correlating vapor-liquid equilibrium data depends on the availability of suitable equations of state, or else tabulations of volumetric data. The Benedict-Webb-Rubin equation seems to be satisfactory for light hydrocarbons and certain gases. Other equations are satisfactory in limited circumstances. No single equation seems to be available that can be applied generally to the correlation problem. Usually, only gas- or vapor-phase equations are used, the liquid being treated separately in some way.

Empirical or semi-empirical equations of state are of two types, depending on the method of evaluating the constants. In generalized equations, the constants are evaluated from critical properties. In the other type, the constants are found by fitting the equation to experimental data.

One weakness of empirical equations of state lies in their use with mixtures. Arbitrary mixture combination rules must be used for the evaluation of the constants used in the equations. Total mixture properties may be estimated with some confidence, provided that the equation is being used in its range of applicability. The estimation of partial properties, such as component fugacities in mixtures, depends directly on the arbitrary mixing rules. Derived partial properties may, therefore, be only approximate.

Barr-David (6) cites a further difficulty, as follows:

> This method of calculation of fugacities of components of a binary solution can never be strictly applied in the case of vapor-liquid equilibrium, since each component is necessarily stable in only one phase when pure at the temperature and pressure of the solution. It is still considered valid to combine constants even though one component does not exist as a vapor under the conditions. Little work has been done to test the validity of this extrapolation.

Barr-David evaluated the various methods used in the past for estimating mixture fugacities, including the well-known Lewis-and-Randall rule.

The virial equation of state (34), which has its basis in statistical mechanics, appears to avoid some of these problems. The virial equation is

$$P\underline{V} \,/\, RT = 1 + \frac{B}{\underline{V}} + \frac{C}{\underline{V}^2} + \frac{D}{\underline{V}^3} + \ldots \qquad \text{(III-28)}$$

The constants in the virial equation, called the "virial coefficients," are given for mixtures by

$$B = \sum_{i=1}^{N} \sum_{j=1}^{N} y_i y_j B_{ij}, \qquad \text{(III-29)}$$

$$C = \sum_{i=1}^{N} \sum_{j=1}^{N} \sum_{k=1}^{N} y_i y_i y_k C_{ijk}, \qquad \text{(III-30)}$$

etc.

The second virial coefficient, B, represents interactions between pairs of molecules; the third virial coefficient, C, represents interactions between three molecules; etc. All of the coefficients are functions of temperature only.

Barr-David's criticism of empirical equations of state does not seem to apply to the virial equation. While it is true that one component may not exist as a pure vapor under the conditions of the mixture, the interactions of its molecules in the vapor mixture should be accounted for by the virial coefficients.

In principle, virial coefficients can be calculated from intermolecular potential functions. The actual situation is that virial coefficients derived from volumetric data are used to test various models of intermolecular potential. The second virial coefficient is not extremely sensitive to the potential function used; fair estimates of it are obtained from very crude models. The third and higher coefficients are much more sensitive to the potential used.

The use of the virial equation of state depends, then, on the availability of the virial coefficients. Pure component second virial coefficients ($i = j$) are available, or can be estimated with some confidence, for many substances. The cross-coefficients usually must be estimated using empirical combination rules, which reduces the value of equation. Third and higher coefficients are relatively scarce.

Use of the virial equation of state is limited to moderate pressures, since the series diverges at about the liquid density (34). In spite of its limitations, the virial equation seems to be the best general equation presently available, since it is based in theory.

Chao and Seader (12) used the Redlich-Kwong equation of state (68) in their work. The equation was developed originally for gases and cannot be expected to be accurate below the critical temperature. The R-K equation is a generalized two-constant equation of the van der Waals form; it was used by Chao and Seader outside its intended range of applicability because of its relative simplicity.

Hoffman et al. (35,36) and Edmister et al. (24) used the Black equation of state (9). The Black equation is applicable to both vapors and gases, but is limited to relatively low pressures.

The above comments are admittedly critical. Emphasis seems necessary because of the intimate relationship between volumetric data and phase-equilibrium data. Successful correlation would seem to require good volumetric data. The use of hypothetical standard states complicates correlation, but does not necessarily justify the use of approximate equations of state.

Regular Solution Correlations

Scatchard (75) and Hildebrand and Wood (32) derived the following relation for the liquid activity coefficient of components in regular solutions.

$$\ln \gamma_i^L = \frac{\underline{V}_i^L}{RT} (\delta_i - \delta_{mix})^2 \qquad \text{(III-31)}$$

$$\text{where } \delta_i = \left(\frac{\Delta E_i^{vap}}{\underline{V}_i^L} \right)^{1/2}, \qquad \text{(III-32)}$$

ΔE_i^{vap} = energy of vaporization from the liquid to the ideal gas,

$$\delta_{mix} = \frac{\sum_{j=1}^{N} x_j \underline{V}_j^L \delta_j}{\sum_{j=1}^{N} x_j \underline{V}_j^L}, \tag{III-33}$$

A regular solution is one in which there is no volume change on mixing and in which the entropy of mixing is ideal.

Prausnitz, Edmister, and Chao (64), and Chao and Seader (12) have used Equations III-26 and III-31 to correlate K-values for hydrocarbons and hydrogen. The mixture vapor fugacity coefficient, ϕ_i^V, is evaluated by use of the Redlich-Kwong equation of state. For light components, the pure liquid state is hypothetical; the terms $\underline{V}_i^L$, δ_i, and ν_i^L cannot be evaluated directly. Values of $\underline{V}_i^L$ were assigned arbitrarily from partial molar volume data. Equilibrium data for the light component in several solvents were then used to back-calculate consistent values of δ_i and ν_i^L. Chao and Seader generalized the liquid fugacity coefficients by use of the Pitzer et al. (58) corresponding states treatment.

$$\log \nu^L = \log \nu^{(o)} + \omega \log \nu^{(1)} \tag{III-34}$$

where $\nu^{(o)}$ and $\nu^{(1)}$ are functions of T_r and P_r

and ω = the acentric factor = $-(\log_{10} p_r)_{T_r=0.7} - 1.0$.

p_r = reduced vapor pressure.

These authors also simplified the correlation by neglecting the effect of temperature on $\underline{V}_i^L$ and δ_i.

The final form of the above correlation, as presented by Chao and

Seader, represents K-values for paraffinic, naphthenic, and aromatic hydrocarbons and for hydrogen in binary and multicomponent mixtures with reasonably good accuracy. The correlation has the advantage that it is analytical in form and thus may be used conveniently with digital computers. Conversely, the correlation is difficult to use for hand calculations because of the lengthy trial-and-error calculations required in process calculations. The Chao-Seader method is described in Appendix J.

Additional comments should be made about the above correlation of Chao and Seader. One of the properties of a regular solution is the ideal entropy of mixing. When components of widely different molecular size are mixed, the entropy of mixing is not ideal. Hildebrand and Scott (31) showed how correction could be made for non-ideal entropy of mixing in binary mixtures. Silver (76) extended this entropy correction to multicomponent mixtures. Silver showed that better agreement resulted between experimental K-values for hydrogen in benzene-cyclohexane-n-hexane-hydrogen mixtures and K-values calculated by the Chao-Seader method when the entropy correction was made.

A more serious criticism of the Chao-Seader correlation from the theoretical standpoint involves the use of the Scatchard-Hildebrand equation (Equation III-31) for light components, such as methane and hydrogen. A regular solution is one for which there is no volume change on mixing of the pure components. The mixing of a gaseous pure component with a liquid component obviously involves a large volume change. Also, the definition of the solubility parameter, δ_i, cannot be applied to the gaseous component. Prausnitz, Edmister, and Chao (64) recognized the above situation, pointing out that they considered the use of Equation III-32 as semi-empirical for gases. Use of the equation was justified from the practical standpoint. One should recognize, however, that the δ and ν^L values obtained for gases are correlating parameters and not rigorous thermodynamic functions. Use of these δ and ν^L values in any other correlation should be made only with their origin in mind.

Prausnitz (59) has shown how correction can be made for large volume changes on mixing. A three-step process is proposed. The first step is the isothermal compression of the pure gas from the equilibrium partial pressure to the "isometric mixing pressure," at which pressure the pure gas molar volume is equal to its liquid partial molar volume. The second step involves mixing the gas and liquid at constant volume, pressure, and temperature. The Scatchard-Hildebrand equation is applied to the second step. The final step is the isothermal expansion of the solution to the equilibrium total pressure. Prausnitz used the above steps, plus the Lewis-and-Randall rule, to derive expressions for the prediction of solubility of gases in liquids at low pressures. There does not appear to be any way in which this procedure can be used to modify the basic Chao-Seader method because the Lewis-and-Randall rule is used.

Ideal K-Value Correlations

The correlation of K-values by use of the ideal K-value has been proposed by Hoffman et al. (35,36), among others. Notice that in Equation III-27 the ratio ν_i^L/ν_i^V depends only on pure component properties, while γ_i^V and γ_i^L correct for mixture effects. The ratio ν_i^L/ν_i^V is denoted as K^{ideal} and accounts for deviations from ideality due to the effect of pressure. In the special case where the components form ideal mixtures in both the vapor and liquid phases, the K-value and the ideal K-value are identical. If the Lewis-and-Randall rule is applicable for the gas phase, then $\gamma_i^V = 1$, and

$$K = \gamma_i^L K^{ideal} \tag{III-35}$$

The ideal K-value is difficult to evaluate because of the hypothetical standard states mentioned above. In cases where the hypothetical state is not far removed from the actual state, ν^L or ν^V might be evaluated by extrapolation. For vapor-liquid equilibria involving components differing widely in volatility, such extrapolation is not possible. The light component may be above its critical temperature, in which case the liquid phase is hypothetical at any pressure. The heavy component will exist in the vapor phase at pressures far exceeding the vapor pressure at that temperature.

Hoffman et al. suggested a procedure for evaluating ideal K-values that is outlined below. Constant-temperature equilibrium data were treated. The first step was the evaluation of γ^V for the light component (component 1) by an equation of state. The equation of state was used to calculate Φ_1^V and ν_1^V. But

$$\gamma_i^V = \frac{\Phi_i^V}{\nu_i^V} \, . \tag{III-36}$$

Values of γ_1^V were obtained by Equation III-36 for various values of equilibrium pressure. Note that the equation of state cannot be used to evaluate γ^V for the heavy component (component 2) because the pure vapor is a hypothetical state.

Hoffman et al. fitted the van Laar equation to the light-component vapor activity coefficients.

$$\ln \gamma_1^V = \frac{a_1}{(1 + \frac{a_1 y_1}{a_2 y_2})^2} \qquad \text{(III-37a)}$$

The values of the van Laar equation constants, a_1 and a_2, so obtained were used to predict the heavy-component vapor activity coefficients, γ_2^V, from the van Laar equation for the second component.

$$\ln \gamma_2^V = \frac{a_2}{(1 + \frac{a_2 y_2}{a_1 y_1})^2} \qquad \text{(III-37b)}$$

The equation of state was then used to calculate ϕ_2^V, and ν_2^V was calculated by Equation III-36.

It may be noted in passing that Robinson and Gilliland (71) have shown that the Scatchard-Hildebrand equation is of the same form as the van Laar equation. In the use shown here, the constants of the van Laar equation are derived by curve-fitting activity coefficient data, rather than by calculation from theoretical considerations.

Values of ν_2^L can be evaluated by any of several methods; Hoffman et al. used the correlation of Lydersen et al. (49). Ideal K-values were then calculated by the defining equation.

$$K_i^{\text{ideal}} = \frac{\nu_i^L}{\nu_i^V} \qquad \text{(III-38)}$$

The light component was handled in a similar manner. The equation of state was used to calculate ϕ_2^V. Since the two phases are in equilibrium,

$$\bar{f}_2^L = \bar{f}_2^V = \phi_2^V P y_2. \qquad \text{(III-39)}$$

Values of ν_2^L were obtained as above. Then the heavy-component liquid activity coefficients were calculated by

$$\gamma_2^L = \frac{\bar{f}_2^L}{x_2 P \nu_2^L} \qquad \text{(III-40)}$$

The van Laar equation was used to correlate the γ_2^L values, and thus to predict γ_1^L values. The γ_1^L values were used with equation-of-state ϕ_1^V values to obtain ν_1^L as shown in the following equations.

$$\bar{f}_1^L = \bar{f}_1^V = \phi_1^V P y_1 \qquad \text{(III-41)}$$

$$\nu_1^L = \frac{\bar{f}_1^L}{P x_1 \gamma_1^L} \qquad \text{(III-42)}$$

The equation of state was used to obtain ν_1^V. Ideal K-values were then evaluated for the light component.

Edmister <u>et al</u>. (24) used a similar procedure to evaluate heavy-component ideal K-values. The main modification was in the evaluation of γ_2^V. The van Laar equation is a particular solution of the constant-temperature constant-pressure form of the Gibbs-Duhem equation

$$x_1 \frac{d\ln\gamma_1}{dx_1} = x_2 \frac{d\ln\gamma_2}{dx_2} \qquad \text{(III-43)}$$

For this reason, Edmister et al. simply used graphical integration of Equation III-43 to obtain γ_2^V.

Both the above procedures involve an approximation, because isothermal vapor-liquid equilibrium data are not constant-pressure data. The rigorous relation for constant temperature (37) is

$$x_1 \frac{d\ln\gamma_1}{dx_1} = x_2 \frac{d\ln\gamma_2}{dx_2} + \frac{\underline{V}^E}{RT} \frac{dP}{dx_1} \qquad \text{(III-44)}$$

Thus, both procedures neglect the right-hand term of Equation III-44. Where one component is above its critical temperature, the excess volume term cannot be evaluated rigorously.

After satisfactory values of the ideal K-values are obtained, several problems remain. The ideal K-values must be generalized or correlated in some manner. Expressions must be developed for the activity coefficients in both phases. Stuckey (78) has correlated ideal K-values by use of the 3-parameter corresponding-states principle, using T_r, P_r, and the acentric factor, ω. The liquid-phase activity coefficient can be estimated by the Scatchard-Hildebrand equation for non-polar mixtures. The correlation of vapor-phase activity coefficients is the biggest difficulty; no theoretical approach analogous to regular solution theory is presently available.

The use of ideal K-values with activity coefficients has strong appeal, in spite of the difficulties outlined above. The contributions of pressure and composition to non-ideality are separated. As theoretical methods are developed to predict activity coefficients, they may be incorporated in such a correlation. The correlation is potentially useful even where mixtures are polar or where other unusual solution behavior occurs.

CHAPTER IV

EXPERIMENTAL APPARATUS

The equilibrium cell used in this work was a dynamic cell, as previously mentioned. Details of the cell and supporting apparatus are given below. The materials used in the study are also described.

Apparatus

A schematic diagram of the experimental apparatus is shown in Figure 2. For convenience of description the equipment is divided into four sections: (1) feed, (2) pressure regulation and measurement, (3) equilibrium cell and thermostat, and (4) sampling and analysis. Each of the above sections is discussed separately.

Feed Section

Hydrogen was fed from a supply cylinder through a gauge block, drying tube, and needle valve to the gas compressor. The capillary tubing and fittings in this section were 316 stainless steel, with a maximum allowable working pressure of 15,000 psi. The drying tube was an Autoclave Engineers Co. 30 cc MD test tube reactor packed with silica gel. The maximum working pressure of the drying tube is 10,000 psi.

Hydrocarbons were fed from a glass cylinder, through a short copper adapter to a needle valve, and then through stainless-steel

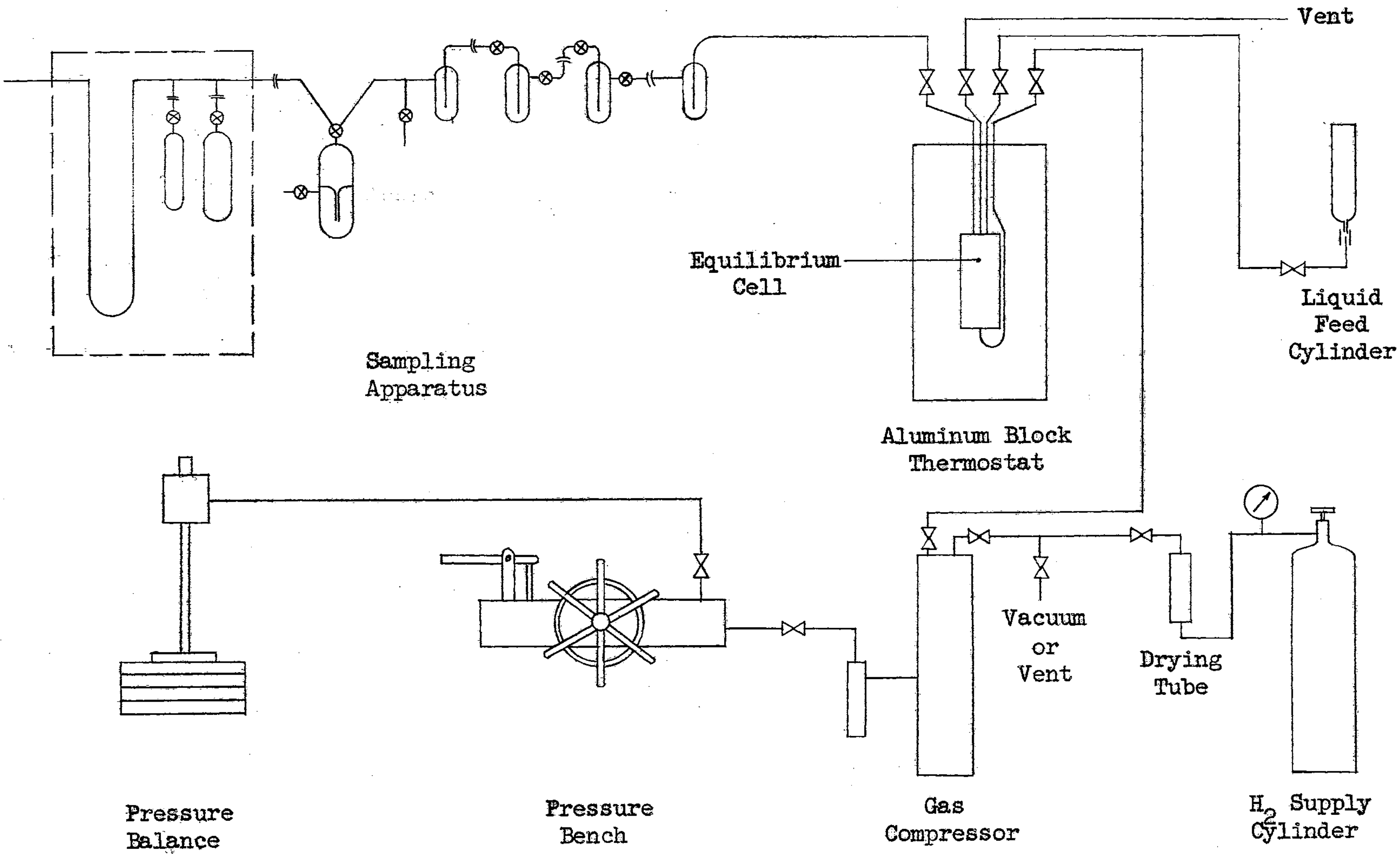

Figure 2

Schematic Diagram of Equilibrium Apparatus capillary tubing to the equilibrium cell. The glass-to-copper joint was sealed by a Teflon sleeve, except for early benzene-hydrogen runs, when a Tygon sleeve was used.

Pressure Regulation and Measurement Section

Pressure regulation and measurement were accomplished by use of a Michels pressure balance in conjunction with a gas compressor. A pressure bench was used to obtain and maintain pressure in the system. The balance, bench, compressor, equilibrium cell and aluminum block thermostat were all manufactured by W. C. t'Hart and Zn, Instrumenten- and Apparaten-fabriek N.V., Rotterdam.

Michels Pressure Balance. The Michels pressure balance (50) is a dead-weight tester distinguished by the use of a differential piston. The piston-cylinder, or measuring cylinder, is pictured in Figure 3.

The entire balance is shown in Figure 4. The differential piston, A, is connected to weight axle B by a nut and half-ring joint, C. The weight axle has a guide pin, D, under the base weight, E. The guide pin is inserted in bronze bearing F and is lubricated by oil from reservoir G. Top axle H is screwed onto the differential piston. Position indicator I and weight pan J are mounted on the top axle. All the above parts rotate during the operation of the balance.

A rotating clutch, K, around the top axle is used to lower the driving mechanism, L, which in turn contacts a claw on the piston, rotating the axle at about 71 rpm. Rotation of the axle, combined with a controlled oil leak between the piston and cylinder, reduces friction to a minimum. Vertical movement of the shaft is measured

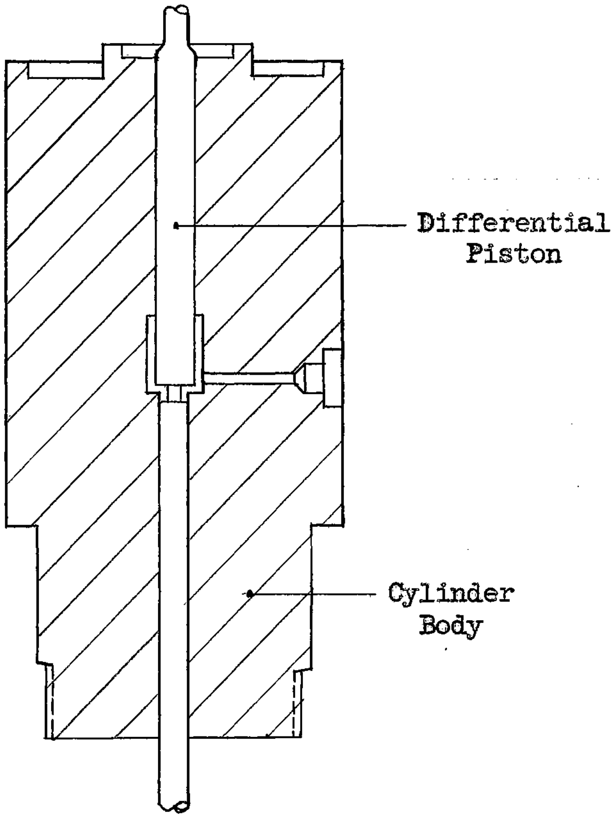

Figure 3

Sectional View of
Measuring Cylinder

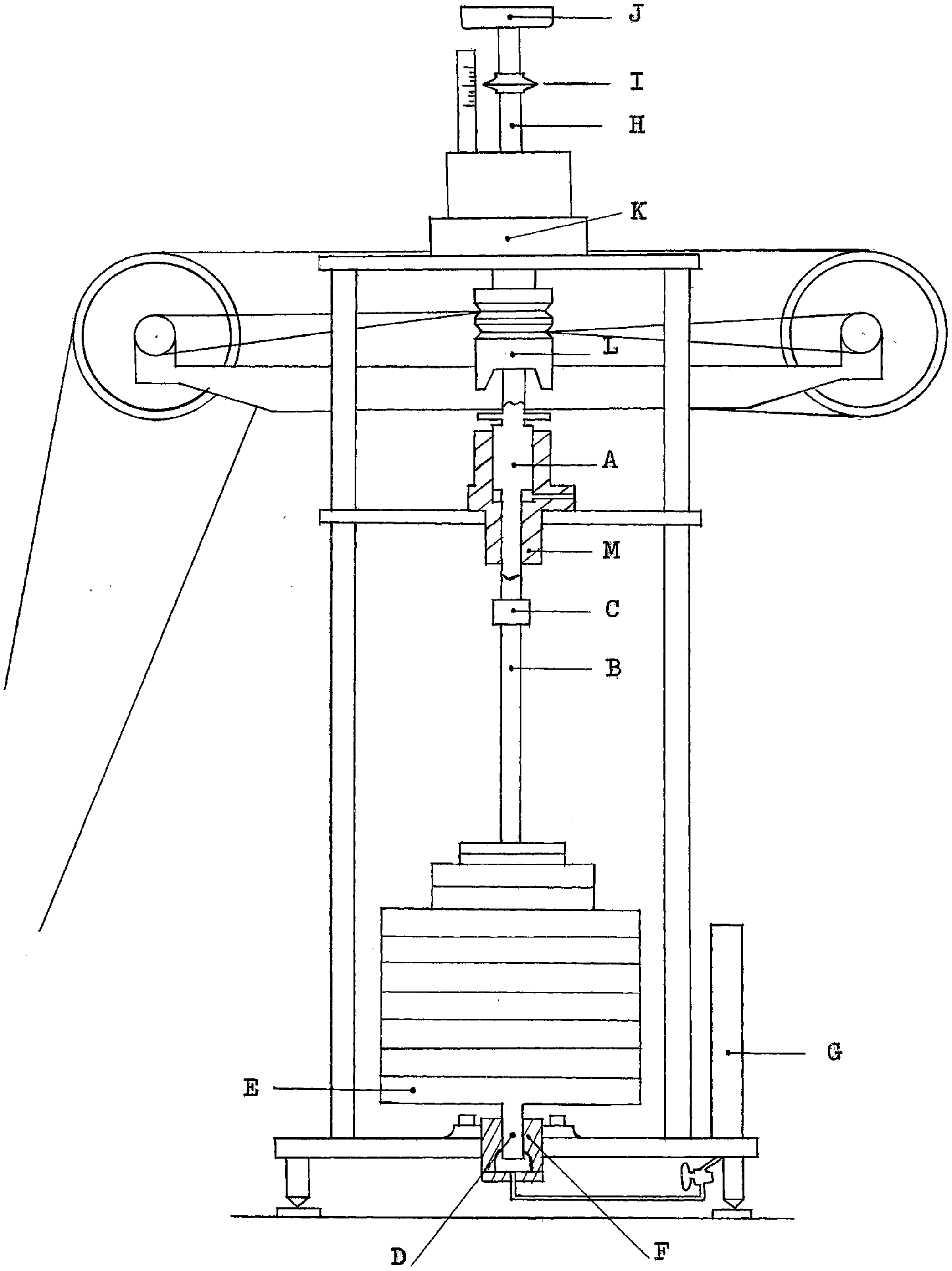

Figure 4

Michels Pressure Balance

by indicator I. The driving mechanism is rotated by a General Electric 1/3-HP motor through a system of leather belts.

Pressure is obtained by pumping oil into cylinder M, lifting piston A and all other rotating parts. Large weights (1 to 25 Kg) are loaded on base weight E. Small weights (less than 1 Kg) are placed in weight pan J.

The maximum allowable pressure for the pressure balance is 3,000 atm. In practice, a set of nine piston-cylinders is used to cover the entire pressure range. The balance used in this study was equipped with six of the piston-cylinders and could be used to measure pressures from 3 to 1,000 atm. The calibration of the balance and piston-cylinders is described in Appendix A. The balance is claimed to be accurate to approximately 1 part in 10,000 and to have a precision of 1 part in 100,000.

Pressure Bench. Figure 5 is a diagram of the pressure bench. A hand pump is provided for pumping oil from the oil reservoir into the system. A screw press provides fine control of the system volume. Appropriate capillary tubing and valves permit pumping oil to the balance and/or the gas compressor. Drain lines are provided for removing oil from the system. The oil used was a special petroleum oil having good viscosity-pressure properties. The maximum allowable operating pressure for the pressure bench is 3,000 atm.

Gas Compressor. The gas compressor is shown in section in Figure 6. Oil from the pressure bench flows into the upper end of the lower compartment, on top of mercury. The mercury, in turn, flows upward through the center tube into the upper compartment, where the gas is

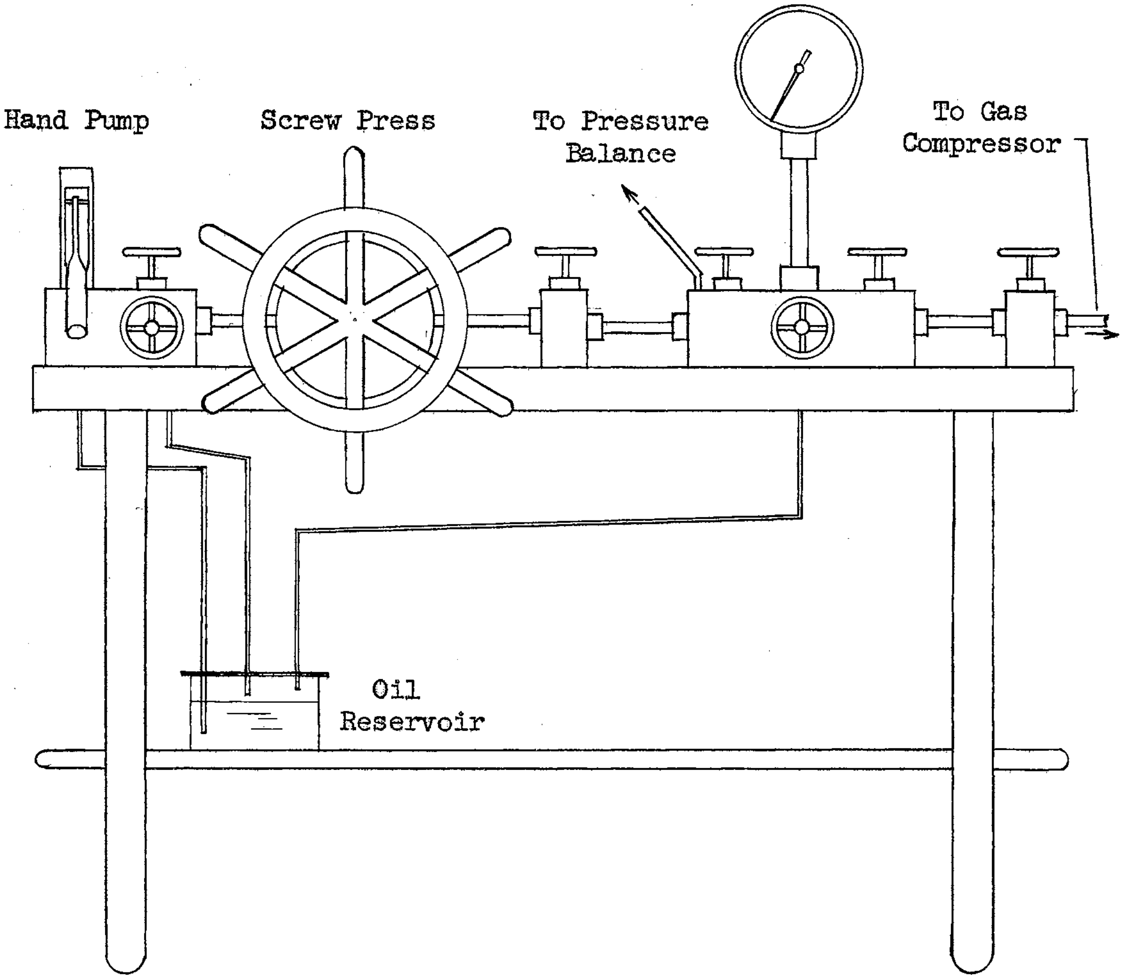

Figure 5

Pressure Bench

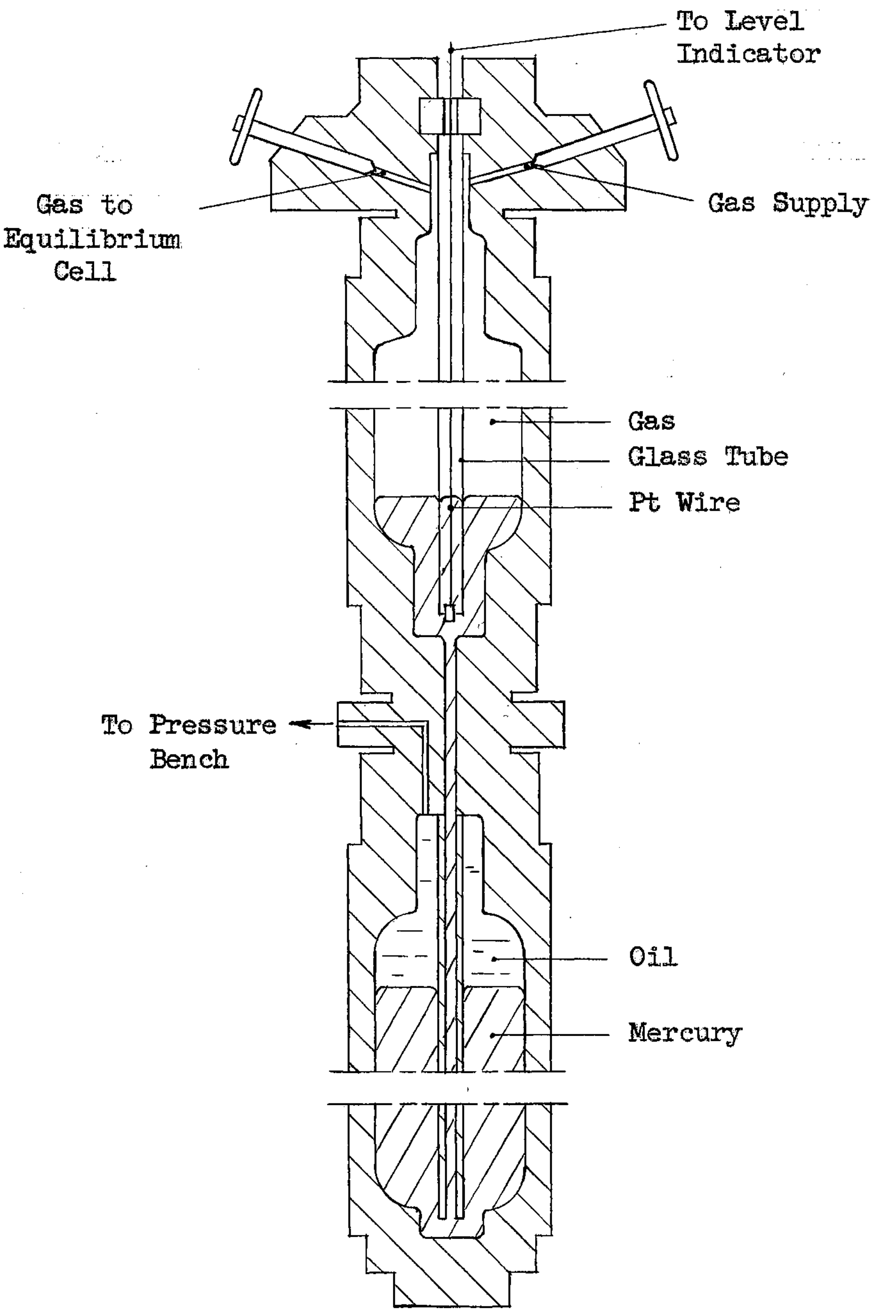

Figure 6

Gas Compressor

confined. A catch-pot is provided in the oil line in case mercury should accidently flow back into this line. Gas inlet and outlet valves are located at the upper end of the compressor.

The position of the mercury meniscus in the upper compartment is measured by means of a bridge circuit. One leg of the bridge circuit is a platinum wire extending the length of the upper compartment. The calibration of the actual mercury levels in the compartments as a function of level indicator reading is described in Appendix B.

The capacity of the gas compressor is 500 cc and the maximum allowable operating pressure is 1500 atm.

Equilibrium Cell and Thermostat Section

The equilibrium cell is shown in Figure 7. Gas flows into the cell through valve A. The gas stream is broken up into small streams by approximately 0.05-mm deep groves in cone E. Further intimate contact of gas and liquid in the cell is provided by a packed section of fiber-glass cloth. The fiber-glass cloth is compressed between two perforated steel discs.

Liquid feed enters through valve B. Vapor and liquid samples are removed through valves C and D, respectively. All capillary lines are 0.6 mm ID.

The total internal capacity of the cell is about 150 cc. The maximum allowable operating pressure is 1,000 atm. The cell and its component parts are constructed primarily of stainless steel of the composition indicated below.

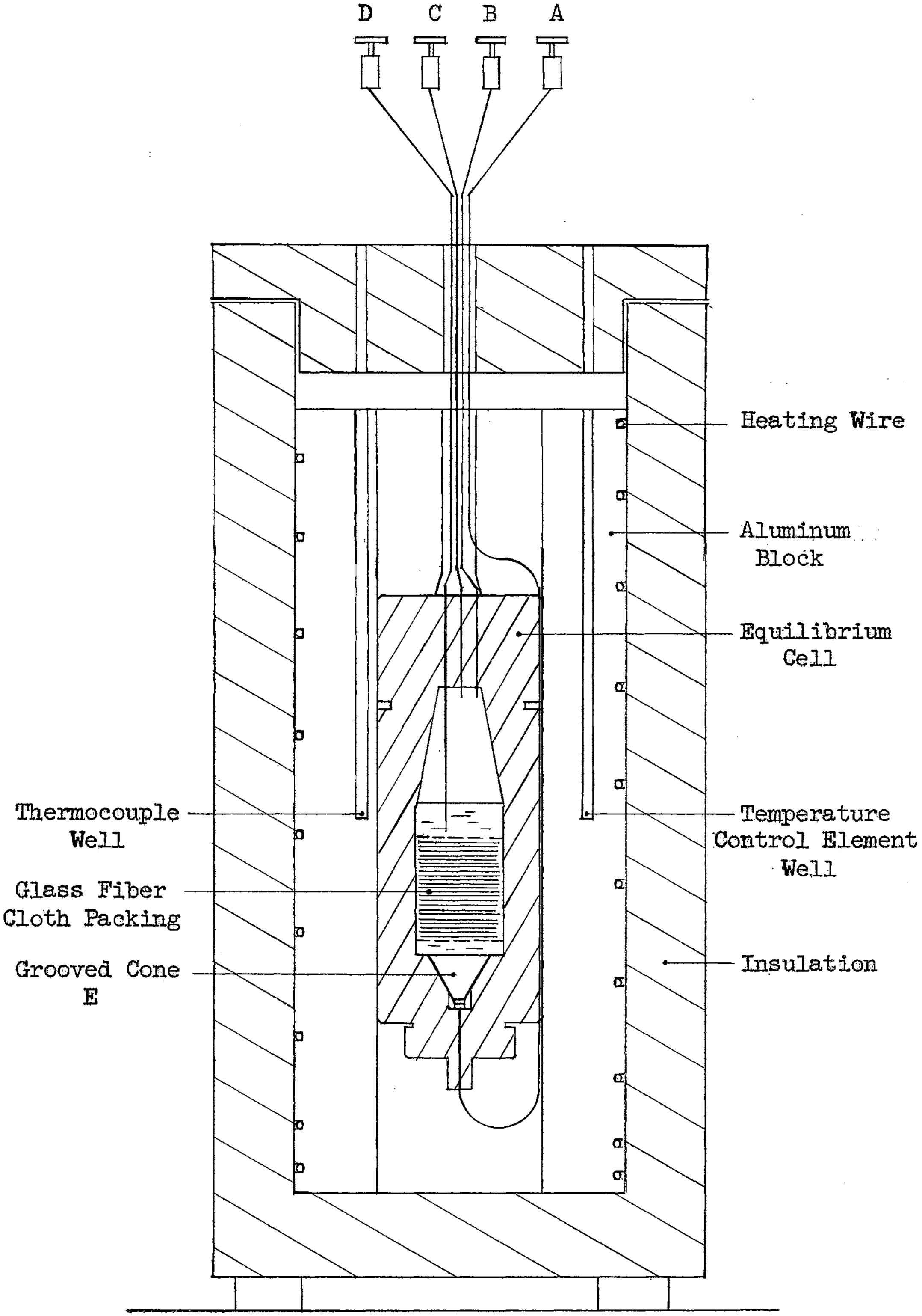

Figure 7

Equilibrium Cell and
Temperature Bath

Component	Weight per cent
Cr	16.0
C	0.35
Mo	1.0

The equilibrium cell was contained in an aluminum block that served as a constant temperature bath. The block is mounted in an insulating jacket packed with expanded mica. The aluminum block is heated by nichrome heating wires located in grooves around the outside of the block. The grooves are spaced more closely near the ends of the block to reduce heat leakage out of the ends. Two 1/2-inch diameter wells are provided for temperature measurement and control sensing elements. Plate 1 is a photograph of the thermostat and equilibrium cell.

Temperature was measured by use of a chromel-constantan thermocouple in conjunction with a Leeds and Northrup Type K-3 potentiometer and 2430-C galvanometer. The thermocouple was calibrated in place by comparison with a platinum resistance thermometer (Appendix C).

Temperature control was effected with a Hallikainen Model 1253A Thermotrol controller. The sensing element was a resistance thermometer.

Sampling and Analysis Section

The method of analysis used in this study was that of passing the sample through cold traps, freezing out the hydrocarbon, and finally measuring the volume of gas remaining. Figure 8 is a diagram of the sampling and analysis apparatus.

A steel capillary was attached to the appropriate sampling valve. A brass adapter was silver-soldered to the free end of the

Plate I

Aluminum Block Thermostat and Equilibrium Cell

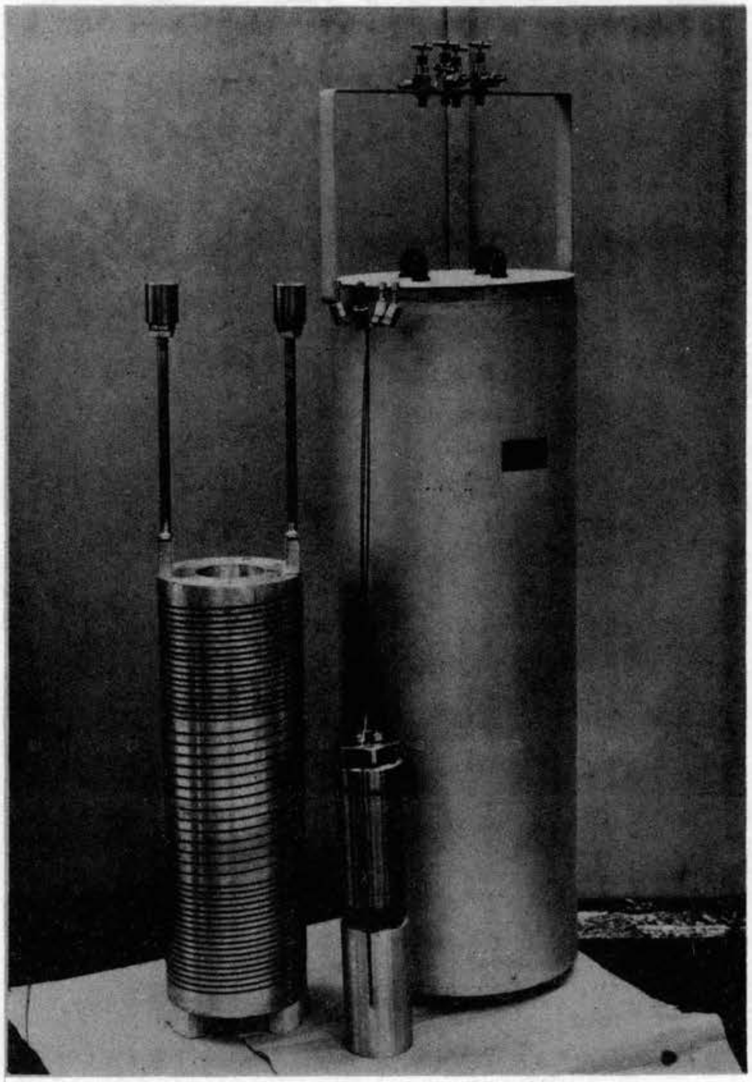

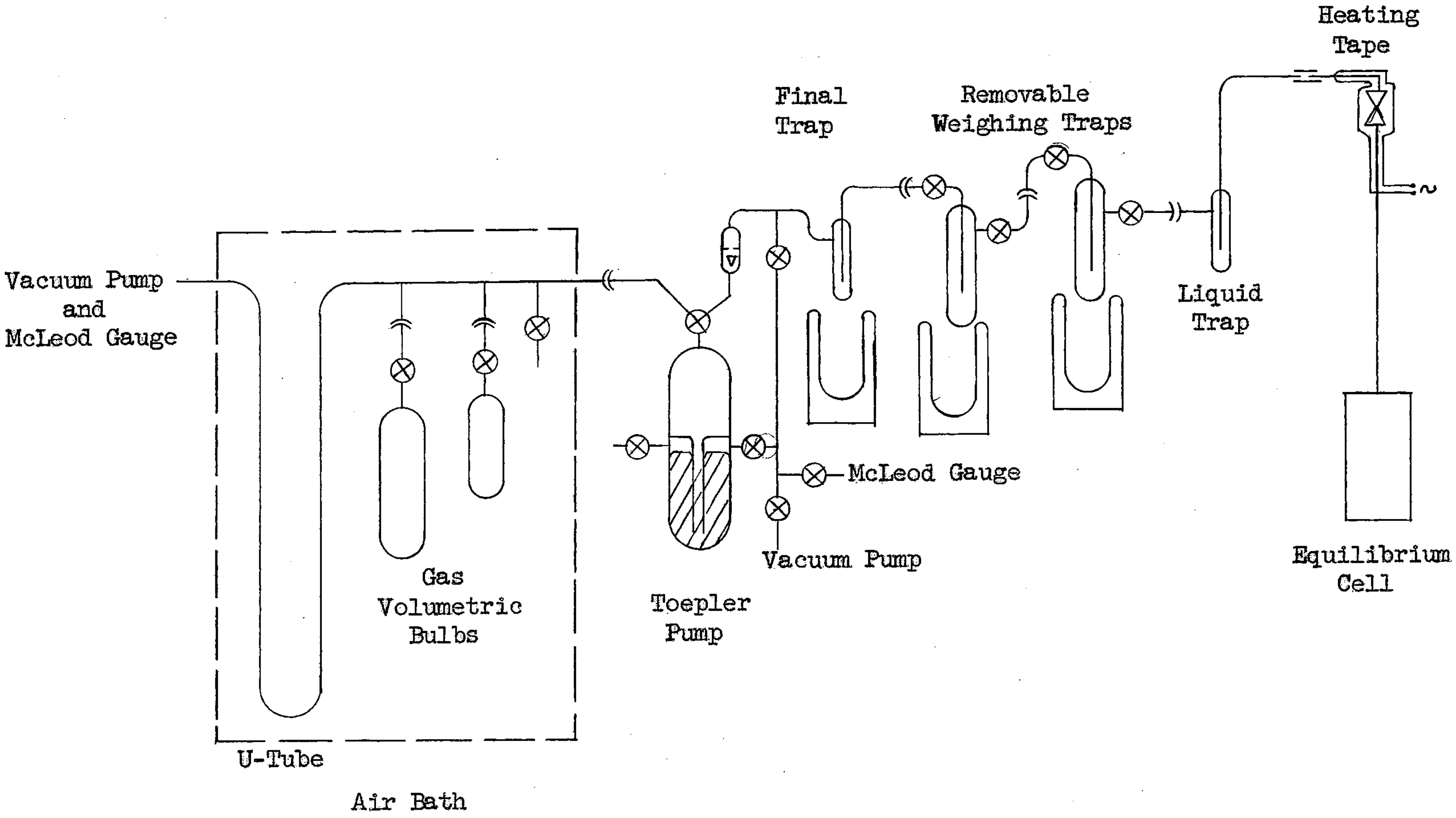

Figure 8

Sampling and Analysis System

capillary. The adapter was connected to the glass sampling apparatus through a short piece of closely-fitting polyethylene tubing. The joint was wrapped with electrical tape and then coated with shellac. The remainder of the sampling and analysis system was glass. During collecting of gas samples, the steel capillary portion of the sampling system that was not enclosed in the temperature bath was wrapped with flexible heating tape.

The first trap in the sampling system was a liquid catch trap and was not cooled. The second and third traps were removable weighing traps. The weighing traps were connected to each other, and to the remainder of the sampling apparatus, by 12/5 ball-and-socket joints. The final trap was mounted permanently in the apparatus and was used to freeze out minute traces of hydrocarbon from the gas stream. The weighing and final traps were immersed in dry ice-acetone baths. A Voland and Sons Model No. 220 analytical balance was used to weigh the sample traps.

The Toepler pump was used to transfer gas from the trap side of the apparatus to the volumetric side. The volumetric side of the apparatus consisted of a capillary to which was attached a mercury manometer and two side arms with 7/1 ball-and-socket joints. Volumetric bulbs of 25 cc, 500 cc, 1 liter, 2 liter, and 4 liter nominal capacity were attached to the side arms. The particular bulbs used depended on the type of sample (liquid- or vapor-phase) and the temperature and pressure in the equilibrium cell. All parts of the volumetric side were calibrated for volume (see Appendix D) and were enclosed in a constant-temperature air bath.

Side tubes were provided for evacuation of the sampling apparatus. Pressure was measured by use of a small McLeod gauge, except for the vacuum side of the U-tube manometer, which was attached directly to a large McLeod gauge.

The constant temperature air bath was a wooden box approximately 2 1/2 ft. wide, 4 ft. high, and 1 1/2 ft. deep. The outside was covered with corrugated cardboard and painted with aluminum paint. Air was circulated by a fan. Mounting boards were provided for the glass equipment enclosed in the air bath. A small door allowed access to the interior for changing the volumetric bulbs. An optically-flat glass window, 6 in. x 30 in., was located in front of the U-tube manometer. The temperature sensing element in the air bath was a mercury-contact switch. An electronic relay was used to control the temperature by on-off control. Heat was supplied by one or more light bulbs located under a false bottom in the lower part of the box. A fluorescent tube provided interior lighting.

The height of the mercury in both legs of the U-tube manometer was measured with a Gaertner M911 cathetometer placed directly in front of the air-bath window. The cathetometer scale is of Type 416 stainless steel and has a temperature coefficient of linear expansion of $9.9 \times 10^{-6}\ {}^{o}C^{-1}$. The scale was standardized at 20 °C.

Materials

The hydrocarbons used in this study were Phillips Petroleum Company Research-Grade hydrocarbons. The stated purities were as follows:

Benzene	99.93 mole per cent minimum
Cyclohexane	99.94

The purity of these materials was checked by gas chromatography, using a 4-ft. column of tricresylphosphate on crushed firebrick at a temperature of 100 °C. The chromatographs showed no significant impurities. The hydrocarbons were dried over calcium chloride before introducing them to the equilibrium cell.

The hydrogen first used was Mathieson Electrolytic Grade with a stated purity of 99.8 mole per cent minimum. This hydrogen, used in Runs 1 through 21, was analyzed by mass spectroscopy by the Continental Oil Company, Ponca City, Oklahoma. The mass spectrograph showed 99.74 mole per cent hydrogen. Runs 21 through 54 were made using a second bottle of hydrogen, which was Extra-Dry Grade and also had a stated purity of 99.8 mole per cent minimum.

CHAPTER V

EXPERIMENTAL PROCEDURE

The experimental procedure can be broken down into three parts: (1) feeding of components, (2) equilibration, and (3) sampling. Each of these three parts will be discussed separately and the experimental data presented. Preliminary calibrations are discussed separately in appendices, as noted in Chapter IV.

Feeding of Components

The general method used in the experimental work consisted of making a series of runs at the same temperature, beginning at a pressure of about 100 psia and increasing the pressure in increments to 10,000 psia. The first step in any series of runs was to evacuate completely the equilibrium cell and gas compressor. Before evacuation, any residual pressure in the system was relieved by venting hydrogen and hydrocarbon to a ventilated hood.

The gas compressor, hydrogen feed line, and the line from the gas compressor to the equilibrium cell were evacuated first. A Cenco Hyvac pump was connected to the evacuation tap in the gas feed line and the compressor was evacuated until the pressure on a portable McLeod gauge remained below 0.025 mm Hg for about one-half hour. The evacuation was stopped and hydrogen was added from the cylinder to flush the system. The evacuation procedure was repeated. Hydrogen was then introduced to the compressor to a pressure of about 100 psia.

The vacuum pump was then connected to the equilibrium cell via the sampling outlet line. A cold trap was connected between the pump and the McLeod gauge to prevent hydrocarbon vapors from entering the vacuum pump. The cell and sampling and inlet lines were evacuated from 12 to 24 hours in order to remove residual hydrocarbon from the cell. At the end of this period, the pressure indicated on the McLeod gauge remained at less than 0.01 mm Hg for several hours. A few cc of the hydrocarbon to be used were then admitted to the cell to flush it. The evacuation was continued for several hours.

Following the cell evacuation procedure, approximately 90 cc of hydrocarbon were introduced to the cell by the atmospheric plus gravity head feed pressure. The hydrocarbon in the cell was degassed by further evacuation of the cell. During the initial phase of the degassing operation, the McLeod gauge generally indicated about 1 mm Hg pressure. After a few minutes the indicated pressure fell to less than 0.025 mm Hg. The degassing procedure was stopped after 30 to 40 minutes, during which time a few cc of hydrocarbon distilled over into the cold trap. Hydrogen was bled immediately into the cell to pressure it and prevent the possibility of air leakage prior to making a run.

Equilibration

The first step in making a run was to heat the cell to operating temperature and allow the temperature to stabilize. This procedure took about 2 hours. The Hallikainen Thermotrol coarse and fine controls were adjusted to obtain the proper temperature. The temperature was noted periodically by means of the thermocouple-potentiometer hookup.

During temperature equilibration the pressure regulation and measuring system was prepared for operation. The proper measuring cylinder was placed in the pressure balance, if necessary. As noted in Chapter IV, 6 measuring cylinders were needed to cover the range of pressure from 3 to 1000 atm. The cylinders not in use were stored in special containers filled with pressure balance oil.

After the measuring cylinder was mounted, weights were placed on the balance to obtain the desired pressure. The balance was connected to the pressure bench. The hand pump was used to inject oil and lift the piston and all rotating parts to operating height. The weights were set in rotation and the gauge pressure on the pressure bench was noted. The pressure balance was then shut down and isolated from the pressure bench.

The bench pressure was again raised and the valve to the gas compressor opened. The pressure gauge then indicated the pressure of the hydrogen in the compressor. Two courses of action were possible. If sufficient hydrogen were in the compressor, the pressure was raised to the operating level by pumping oil into the gas compressor. Alternatively, additional hydrogen was added to the compressor from the feed cylinder. The compressor pressure was then adjusted to the desired level by adding or removing oil at the pressure bench. The gauge reading was matched with that obtained with the pressure balance on line.

The gas compressor was isolated and the pressure balance again opened to the pressure bench and set in operation. The valve to the gas compressor was opened carefully. During this step the level of the pressure balance piston was maintained by adding oil to the system or backing out the screw press. The pressure regulation and measurement system was then cross-floated and ready for operation.

At low operating pressures (up to 3000 psia), hydrogen was added to the equilibrium cell by opening the valve to the cell slightly. As the hydrogen began to flow into the cell, the pressure balance piston began to fall slowly. The hand pump was used to introduce oil and thus maintain the level of the piston. After 2 to 10 minutes the addition of hydrogen was virtually complete and the gas-inlet valve to the cell was opened completely. The system was allowed to equilibrate by maintaining the pressure on the cell. At these lower pressures the pressure regulation and maintenance section could be shut down, isolating the cell at pressure, after an hour or two. Reconnecting the cell to pressure after a few hours showed little or no change in pressure, as indicated by the fact that the pressure balance piston level did not change appreciably when the valve to the cell was reopened.

At high operating pressures (3000 to 10,000 psia) the pressuring procedure was modified. The reason for this modification was that the hydrogen feed-cylinder pressure of 1500-1700 psig prevented the addition of sufficient hydrogen to the compressor to fill the equilibrium cell in one loading. Before the pressure balance and gas compressor were cross-floated, the compressor and bench were used to fill the cell to a pressure just below the operating level.

In this preliminary loading, the gas compressor was opened to the pressure bench and filled with hydrogen at cylinder pressure.

The feed valve was closed and the hydrogen was compressed by pumping oil into the system. The valve to the cell was then opened and hydrogen pumped in. This procedure was repeated until the pressure in the cell was just below the desired operating pressure. The gas compressor was refilled and cross-floated with the balance at full operating pressure. The pressure in the cell was then raised to the operating level by the procedure used in the low-pressure runs.

In the high pressure runs the pressure balance remained on line to the cell throughout the run. Very minute leaks, which gave no apparent trouble at low pressures, did appear at high pressures. These leaks were extremely small and did not make maintaining the pressure difficult with the balance on line. The equilibrium cell, gas compressor, and all lines and valves were checked carefully for leaks at 10,000 psia, but these tiny leaks were never eliminated completely.

During the equilibration period, several preliminary measurements were made. The cell temperature was checked periodically, as before. The barometric pressure was read, using the U-tube manometer in the sample apparatus. A calibrated barometer was not available. The use of the U-tube manometer was considered to be more accurate than the use of an uncalibrated barometer because no corrections for capillarity, scale expansion, or residual vacuum were necessary for the manometer (see reference 30). The temperature of the manometer was taken to be that in the air bath. The pressure on the vacuum side was measured with the McLeod gauge to insure that it was negligible. Room temperature was noted periodically during the equilibration period. The pressure balance measuring cylinder and weights were recorded.

Preparations for sampling were made next. The sample traps were cleaned, regreased, and evacuated. The ball-joint connections were cleaned carefully, using a light solvent, and the tare weights of the traps were determined. The weighing procedure consisted of repeating the weighings, without opening the Voland balance case, until consecutive readings were the same.

Appropriate gas volumetric bulbs were connected to the volumetric side of the sampling apparatus. The volumetric side, up to the 3-way cock on the Toepler pump was evacuated and checked for leaks. At the same time, the Toepler pump was prepared for operation by filling the upper portion with mercury. The air bath operating temperature was established during this period.

Sampling

Preparations for sampling were completed during the final part of the equilibration period. Heating tape was applied to the steel portion of the sampling line and the sampling valve, after the line had been connected to the liquid or gas sampling valve. For gas samples, the tape was wrapped around the portion of gas sampling capillary that extended out of the aluminum block bath insulation. Asbestos rope was wrapped around the heating tape and heat applied by means of a Variac.

About one-half to one hour before the actual sample was withdrawn, the sample capillary was purged. The sample line was connected to the vacuum pump, with intervening cold trap. Then the sample valve was opened slightly to purge the line. During purging the screw press or hand pump on the pressure bench was used to maintain the pressure balance piston at its operating height.

After the purging procedure, the sample trap ball-joint connections were greased and the traps put in place. The trap side of the sampling apparatus was then evacuated and checked for leaks. The portable McLeod gauge was used in the leak-testing procedure. With properly-lubricated stopcocks and ball-joints, the leak rate of the glass apparatus was less than 0.1 mm Hg per hour.

The procedure for gas sampling was necessarily more elaborate than that for liquid sampling. Each type of sampling is discussed separately below. In either case, dry ice--acetone baths in small Dewar flasks were applied to the two sample traps and the final catch trap just prior to withdrawing the sample. At sampling time the gas compressor level, pressure balance oil level, and pressure-bench gauge pressure were recorded.

Liquid Samples

Liquid samples were withdrawn in approximately one second by opening the liquid sampling valve slightly. At higher pressures the screw press was used to maintain the balance piston at operating level during sampling. For liquid samples, the 3-way cock on the Toepler pump was turned so as to isolate the volumetric side of the sampling apparatus from the trapside.

Any liquid in the sample was caught in the liquid trap. If the partial pressure of the hydrocarbon exceeded its vapor pressure, liquid remained in the liquid trap until the first expansion to the volumetric side. Otherwise, the hydrocarbon passed immediately to the sample traps in the vapor phase. The heating tape on the sample capillary and valve was used to prevent the accumulation of solid or liquid hydrocarbon in these parts and to facilitate evaporation into the traps.

The hydrogen in the sample was transferred to the volumetric side by means of the Toepler pump. Vacuum was applied to the lower compartment of the pump to pull down the mercury level in the upper portion. The 3-way cock was turned to allow hydrogen to expand from the trap side into the upper compartment. Vacuum was applied again to the lower compartment to allow the entire upper compartment to be filled with hydrogen. The 3-way cock was closed and atmospheric air was bled slowly into the lower compartment. The 3-way cock was turned to allow the hydrogen to pass into the volumetric side. The upper compartment and 3-way cock passage were filled with mercury to displace the hydrogen.

The Toepler pump transfer was repeated until the level of the mercury in the U-tube manometer in the volumetric side did not change on successive pumpings. Seven or eight transfers were sufficient to transfer virtually all of the hydrogen. Calculations showed that this number of transfers reduced the hydrogen pressure on the trap side to a negligible level.

Next the dry ice--acetone bath was removed from the final trap, and the latter trap was warmed quickly to distill any residual hydrocarbon back into the second sample trap. There was seldom an observable quantity of hydrocarbon in the final trap. The trap was used as a precaution to prevent passage of hydrocarbon into the volumetric side. The greatest part of the hydrocarbon was collected in the first sample trap. Both cyclohexane and benzene are in the solid phase at dry ice--acetone temperature.

The sample trap cocks were closed, the traps removed, and the ball-joint connections cleaned carefully. The traps were allowed to warm to room temperature and were weighed.

The hydrogen gas in the volumetric side was allowed to attain air bath temperature, as indicated by constancy of the mercury levels in the U-tube manometer. One-half hour was sufficient for temperature equilibration of the hydrogen in the air bath. The vacuum side of the U-tube manometer was evacuated to less than 0.02 mm Hg, as indicated by the McLeod gauge mounted on this side. The U-tube mercury levels and the height of a reference mark on the manometer were recorded, along with the size of the attached volumetric bulbs and the position (open or closed) of their stopcocks.

At low equilibrium-cell pressures, only a small quantity of hydrogen was dissolved in the hydrocarbon. In these runs, volumetric bulbs were attached but the cocks were not opened. This procedure allowed obtaining the smallest possible sample volume and thus, the largest pressure reading. At intermediate cell pressures, sufficient hydrogen was obtained to allow opening the 25 cc volumetric bulb. At the highest pressures, enough hydrogen was dissolved that the transfer of hydrogen had to be made in two batches. After the volume and pressure of the first portion were measured, the volumetric side was evacuated. The remainder of the hydrogen was transferred and its pressure and volume determined.

Gas Samples

Gas samples were withdrawn over a time period of from 15 minutes to 3 hours, depending on the equilibrium cell pressure and the allowable sampling rate. The 3-way cock on the Toepler pump was opened to interconnect the volumetric and trap sides when gas samples were withdrawn. The rate of sampling was regulated on the basis of the change in U-tube manometer level as a function of time. The U-tube level-time readings were recorded.

During gas sample withdrawal the pressure balance piston fell continuously. The piston level was maintained within ± 3 mm of the reference level either by pumping oil into the system or by turning in the screw press. At the same time, the level in the gas compressor rose slowly as hydrogen was fed to the equilibrium cell. The rise in mercury level caused a pressure reduction in the hydrogen gas because of the increased mercury head between the balance and the gas. To counteract this decrease in pressure, small weights were periodically added to the weight pan on the balance. During the sampling period a record was kept of the weights added and of the corresponding gas compressor level.

When sufficient gas sample was collected, the gas sampling valve was closed. The hydrogen was transferred and measured, and the traps were weighed, as for liquid samples. At higher equilibrium cell pressures a large volume of sample, at relatively high pressure (up to 740 mm Hg), had to be collected in order to obtain sufficient hydrocarbon in the sample traps. This procedure necessitated measuring the hydrogen in two batches because the Toepler pump would not transfer hydrogen against a pressure higher than about 400 mm Hg.

During the sampling period, the equilibrium cell and room temperature were monitored. After the sampling procedure was completed, the barometric pressure was determined again.

Experimental Results

Data were taken at eight pressures from 100 to 10,000 psia at temperatures of 150 and 250 °F for the binary mixtures hydrogen-benzene and hydrogen-cyclohexane. The temperatures were selected on the basis of the temperature range of available data (see Table II) and the limitations of the apparatus. Preliminary work showed that the combined characteristics of the aluminum block bath and temperature controller would not allow control of temperature to ± 0.1 °F below 150 °F. The type of steel used in the equilibrium cell precluded use with hydrogen at high pressures for temperatures above about 420 °F. The temperatures of 150 and 250 °F allowed checking against existing data for hydrogen-benzene and extension of data for both systems.

Pressure limitations involved operating characteristics rather than physical limitations on the apparatus. The maximum possible operating range of the present equipment is 45- 15,000 psia and is limited by the equilibrium cell and measuring cylinders available. At pressures below about 100 psia insufficient hydrogen is dissolved in the liquid phase for accurate analysis with the analytic procedure used here. At pressures above 10,000 psia another difficulty arises. Without auxiliary compression of the feed hydrogen, the volume remaining in the gas compressor at operating pressure is too small for convenient operation of the apparatus. This operator also noted that the operation of the pressure bench hand pump was extremely difficult at 10,000 psia. The particular values of pressure selected were based on approximately equal increments in the logarithm of the pressure.

The experimental results, in the form of p-T-x-y are listed in Tables III to VII. The raw experimental data are given in Appendix E. Calculation of the p-T-x-y data from the experimental data is illustrated in Appendix F.

A few preliminary runs were made at 280 and 320 °F. Runs 3A to 3I were the first runs made with the final sampling apparatus and were practice runs. Runs 3J to 3N were made to determine the effect of sampling rate on the gas composition. Runs 4 to 7 were comparisons with the data of Connolly.

The p-T-x-y data are plotted in Figures 9 to 12. The log-log plot was used for the p-y data for convenience. In Figures 9 and 10, the point $y = 1$ is plotted at the vapor pressure of the pure solvent. The solid circles in Figure 9 indicate data points that were discarded because of an error in sampling technique. The data are discussed in the following chapter.

TABLE III

EQUILIBRIUM DATA FOR HYDROGEN-BENZENE

AT 280 AND 320 °F

Run No.	Temp. Deg °F	Pressure psia	Mole fraction of Hydrogen in Liquid	Mole fraction of Benzene in Vapor
3A	280	1812	0.0697	---
3B	280	1812	0.0685	---
3D	280	1813	0.0607	---
3F	280	1813	0.0599	---
3G	280	1813	0.0614	---
3H	280	1813	0.0632	---
3I	280	1813	0.0632	---
3J	280	1813	---	0.0497
3K	280	1813	---	0.0540
3L	280	1812	---	0.0533
3M	280	1812	---	0.0519
3N	280	1812	---	0.0527
4	320	427.2	0.0144	---
4	320	427.0	---	0.292
5	320	601.8	0.0214	---
5	320	601.8	---	0.206
6	320	778.0	0.0291	---
6	320	778.0	---	0.167
7	320	1309	---	0.110
7	320	1309	0.506	---

TABLE IV

EQUILIBRIUM DATA FOR HYDROGEN-BENZENE
AT 150 °F

Run No.	Pressure, psia	Mole Fraction Hydrogen in Liquid	Mole Fraction Benzene in Vapor
8	76.3	0.00166	---
8	76.2	---	0.104
8	76.1	---	0.125
25	76.3	---	0.128
9	194.3	0.00443	---
9	194.2	---	0.0482
26	194.2	---	0.0500
10	503.1	0.0117	---
10	503.0	---	0.0203
27	502.9	---	0.0198
11	746.8	0.0174	---
12	1026	0.0238	---
12	1026	---	0.00984
12	1026	---	0.0111
28	1026	---	0.0113
13	1707	0.0389	---
13	1707	---	0.00517
13	1707	---	0.00705
21	1707	---	0.00850
21	1707	---	0.00843
21	1707	0.0389	---
14	2508	---	0.00614
14	2508	0.0536	---
14	2508	---	0.00596
22	2508	0.533	---
22	2508	---	0.00679
23	4000	0.0812	---
23	4000	---	0.00575
24	6998	0.131	---
24	6998	---	0.00497
35	9997	0.176	---
35	9997	---	0.00506
35	9997	0.180	---
35	9997	---	0.00443

TABLE V

EQUILIBRIUM DATA FOR HYDROGEN-BENZENE

AT 250 °F

Run No.	Pressure, psia	Mole Fraction Hydrogen in Liquid	Mole Fraction Benzene in Vapor
15	97.1	---	0.486
15	96.8	---	0.493
15	96.9	0.00186	---
29	96.9	---	0.493
16	201.0	0.00536	---
16	200.9	---	0.247
17	499.4	---	0.104
17	499.4	0.0153	---
18	1003	0.0321	---
18	1003	---	0.0557
30	1003	---	0.0571
19	1702	0.0541	---
19	1702	---	0.0379
31	1702	---	0.0383
20	2999	0.138	---
20	2999	0.0937	---
20	2999	---	0.0268
32	2999	---	0.0264
33	5995	0.167	---
33	5995	---	0.0208
34	9983	0.243	---
34	9983	---	0.0180

TABLE VI

EQUILIBRIUM DATA FOR HYDROGEN-CYCLOHEXANE

AT 150 °F

Run No.	Pressure, psia	Mole Fraction Hydrogen in Liquid	Mole Fraction Cyclohexane in Vapor
36	99.8	0.00362	---
36	99.8	---	0.0973
37	199.9	0.00670	---
37	199.9	0.00702	---
37	199.9	0.00710	---
37	199.9	0.00710	---
37	199.9	---	0.0477
46	501.8	0.0182	---
46	501.8	---	0.0227
53	501.5	---	0.0207
47	995.8	---	0.0120
47	995.8	0.0345	---
48	1694	0.0563	---
48	1694	---	0.00868
49	3002	---	0.00680
49	3002	0.102	---
50	5996	0.178	---
50	5996	---	0.00610
51	10013	---	0.00642
51	10013	0.262	---
54	10013	---	0.00685

TABLE VII

EQUILIBRIUM DATA FOR HYDROGEN-CYCLOHEXANE
AT 250 °F

Run No.	Pressure, psia	Mole Fraction Hydrogen in Liquid	Mole Fraction Cyclohexane in Vapor
39	101.3	0.00317	---
39	101.3	---	0.451
38	199.8	0.00780	---
38	199.9	0.00820	---
38	199.9	0.00796	---
38	199.8	0.00802	---
38	199.8	---	0.237
40	499.9	---	0.101
40	500.0	0.0225	---
41	999.8	0.0456	---
41	999.8	---	0.0565
42	1700	---	0.0377
42	1700	0.0774	---
43	3000	0.131	---
43	3000	---	0.0269
44	5996	---	0.0213
44	5996	0.236	---
45	9999	---	0.0188
45	9999	0.350	---

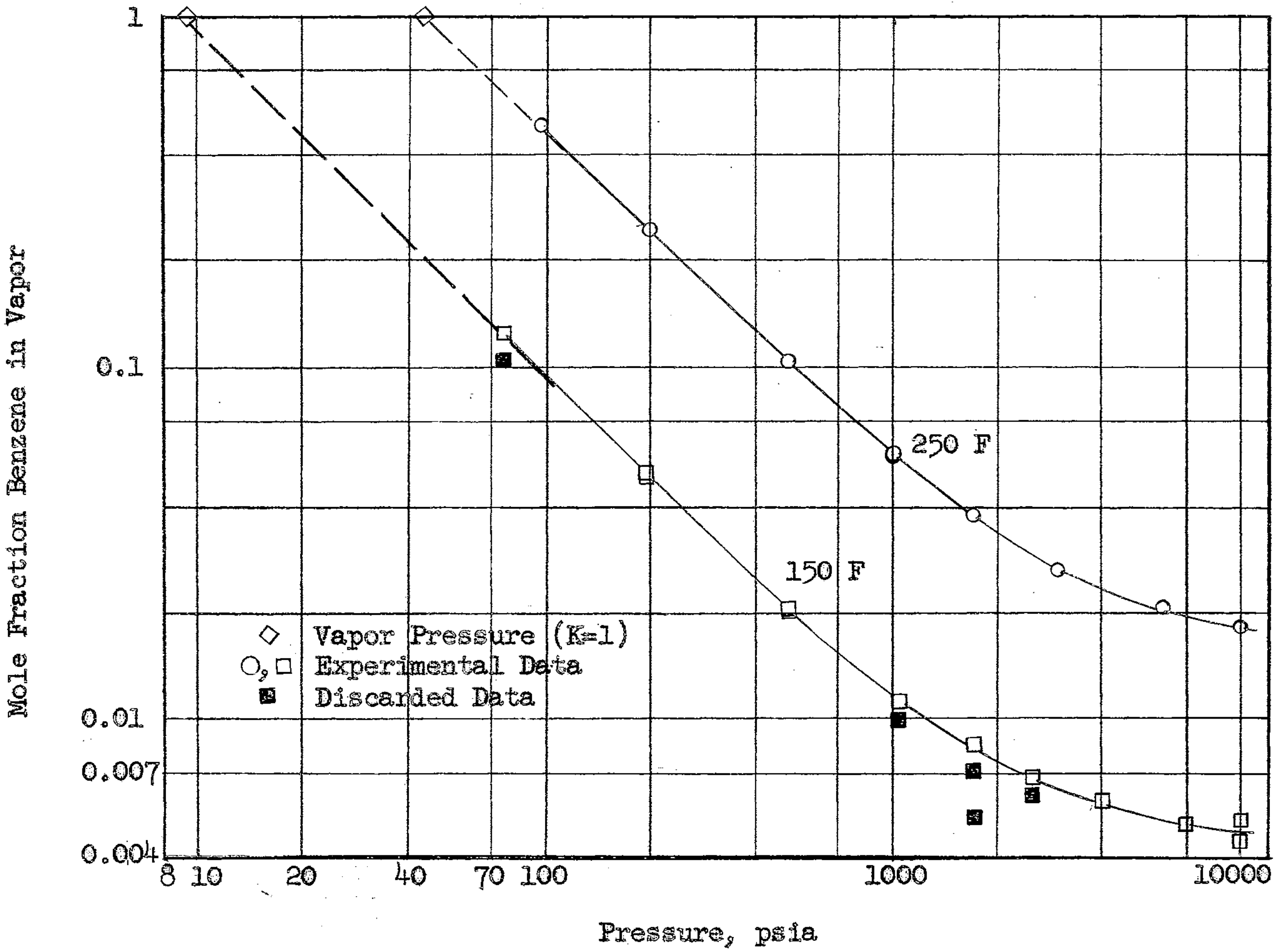

Solubili Figure 9

Solubility of Benzene in Hydrogen

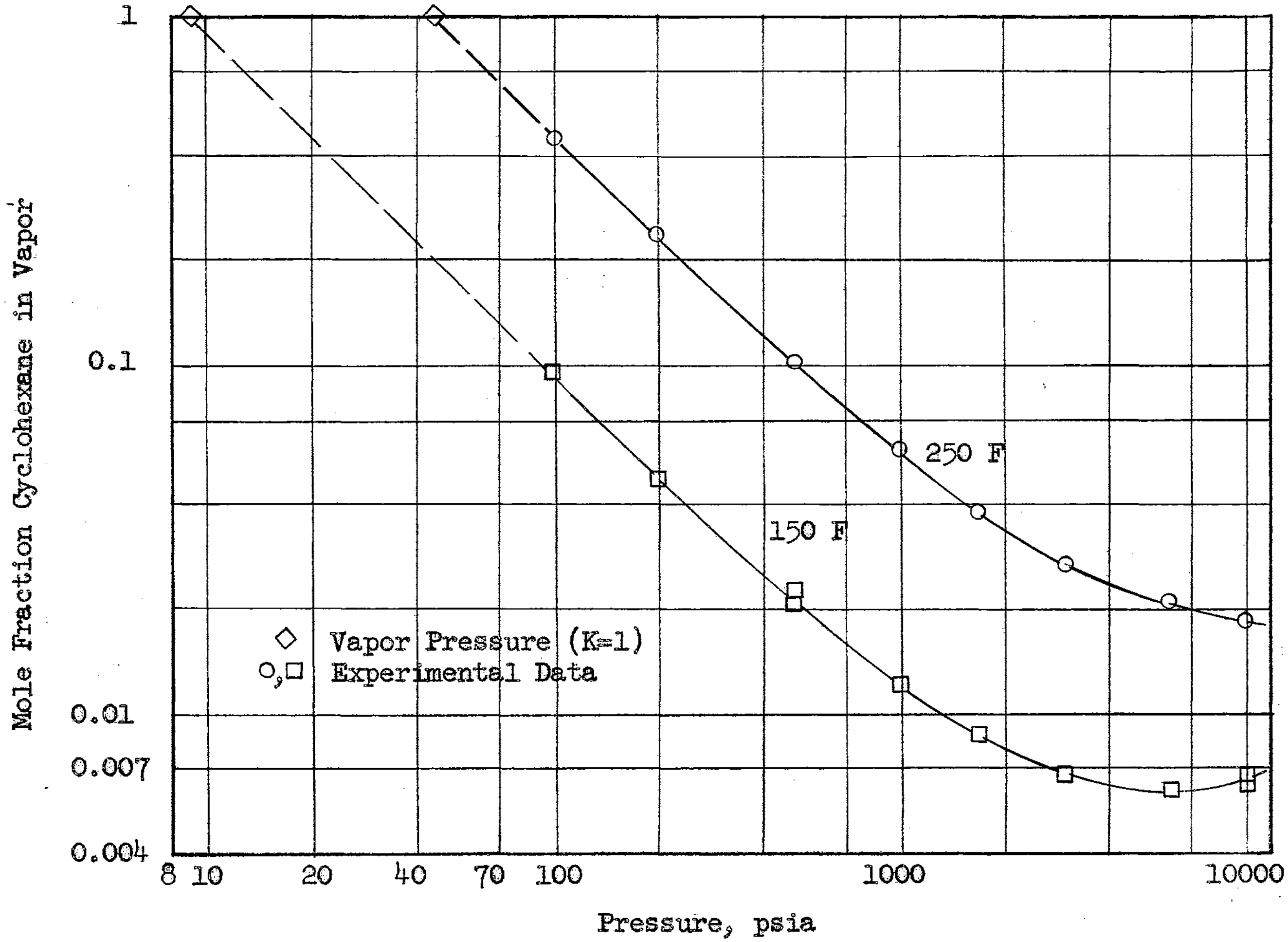

Figure 10

Solubility of Cyclohexane in Hydrogen

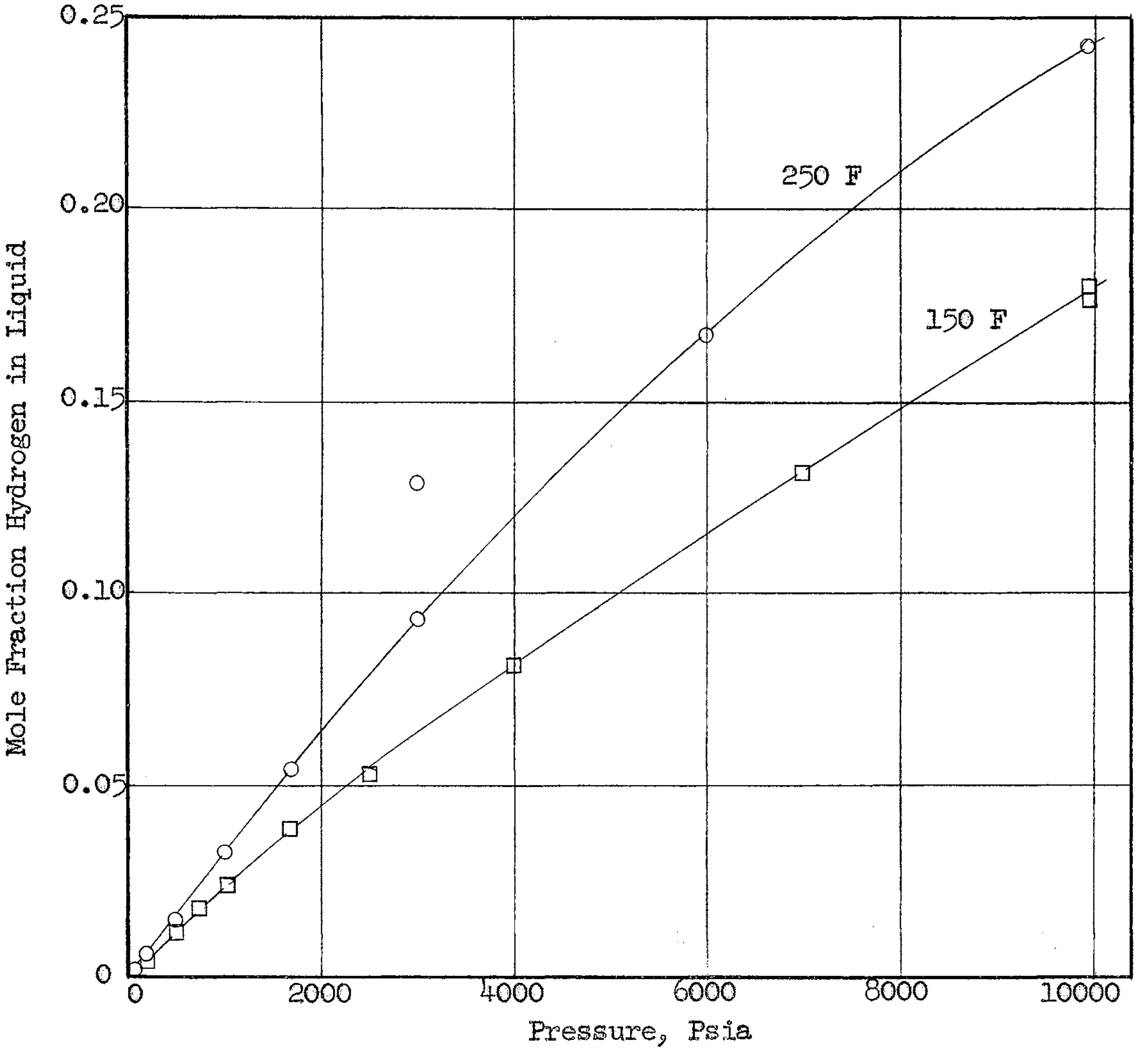

Figure 11

Solubility of Hydrogen in Benzene

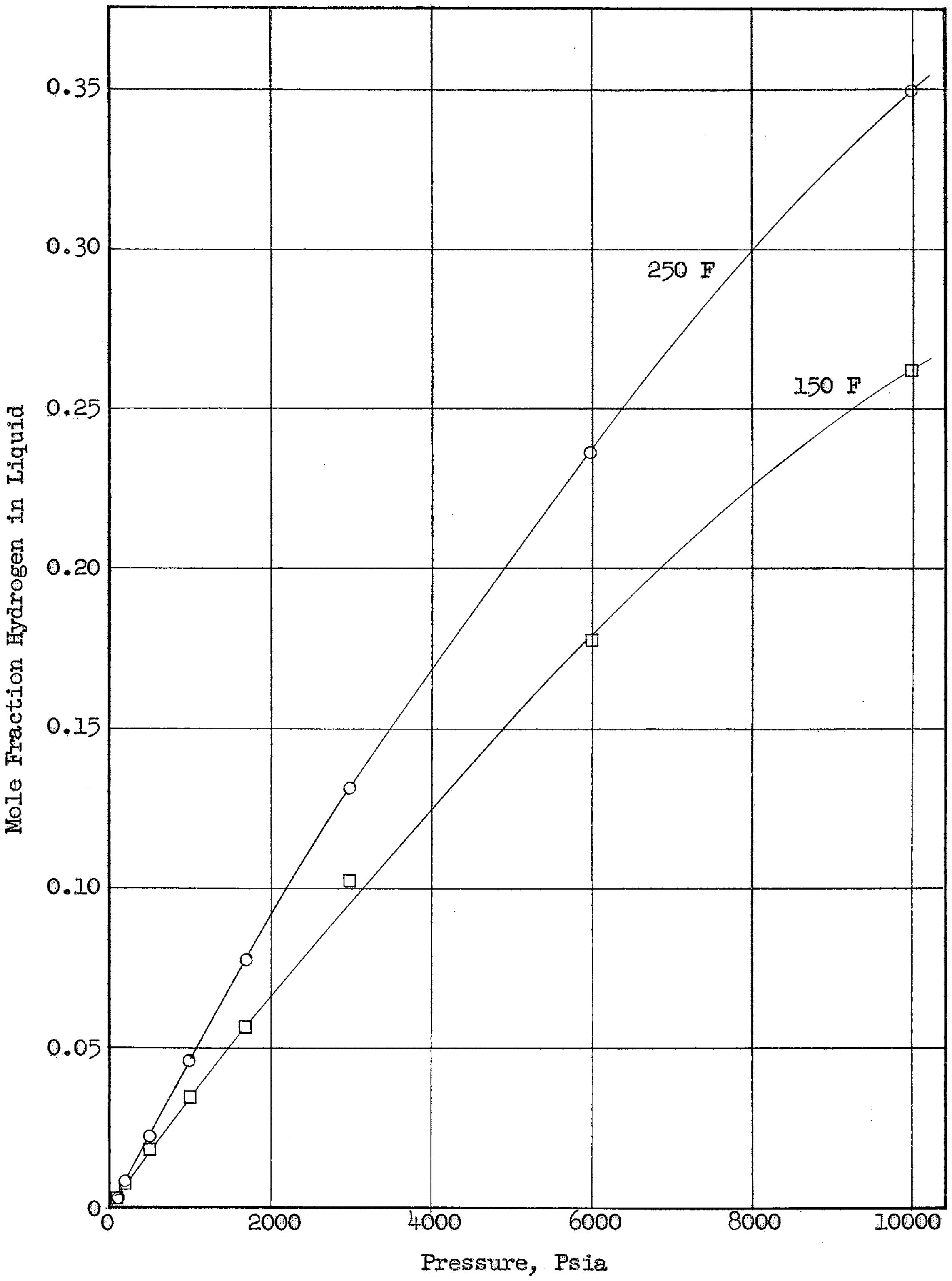

Figure 12

Solubility of Hydrogen in Cyclohexane

CHAPTER VI

DISCUSSION OF RESULTS

The experimental data obtained in this study are analyzed from two viewpoints in the discussion that follows. First, the sources and magnitude of various experimental errors are investigated; then thermodynamic consistency tests are applied. As a further guide in evaluating the data, comparisons were made with the available literature data. The final sections describe data correlation comparisons and correlation work.

Experimental Errors

In the discussion of experimental errors, it is necessary to differentiate between the concepts of precision and accuracy. Precision refers to the magnitude of the variation of observations in direct measurements. Accuracy refers to the magnitude of error between the observed and the actual (or true) behavior, irrespective of precision. Accuracy can only be determined by the agreement of measurements made by different methods and/or different observers. Thus, thermodynamic consistency tests and comparisons with other data were made to guide in establishing the accuracy of the data. The precision, or variability, of the data was studied by the method of propagation of errors and by comparing a few repetitions in measurements.

Precision

The method of propagation of errors (52) allows the estimation of error in a quantity from the errors in the directly-measured quantities from which it is derived. For instance, the quantity of hydrogen in the vapor and liquid samples was determined from measurements of the pressure, volume, and temperature of the hydrogen in the sample. The gas law was used to calculate the moles of hydrogen.

$$n = \frac{PV}{zRT} \tag{VI-1}$$

The method of propagation of errors shows that the variability in n is given by

$$\frac{\Delta n}{n} = \frac{\Delta P}{P} + \frac{\Delta V}{V} - \frac{\Delta T}{T} \tag{VI-2}$$

Ideally, the variability in P, V, and T should be determined by the methods of statistics. However, many replications of the same measurements are necessary for the application of statistical methods. Since replications were not made in any quantity, the maximum expected error was estimated from consideration of the variables involved.

The temperature in the air bath was measured with a mercury-in-glass thermometer that had been calibrated by comparison with a platinum resistance thermometer. The thermometer was placed at several locations in the bath to check for uniformity of temperature. This check showed agreement within 0.1 °F. The bath temperature was controlled to ±0.15 °F. The temperature in the gas sample was taken to be that in the bath. The maximum estimated error in the temperature was 0.25 °F. Then

$\Delta T/T = 0.25/546 = 0.0005$, or 0.05 per cent.

The U-tube manometer mercury levels were measured with a cathetometer that could be read to ±0.05 mm. Single repetitions of measurements indicated that observational errors rarely exceeded 0.05 mm Hg. Precautions against capillarity effects included the use of a clean 1/4-in. diameter U-tube filled with triple-distilled mercury. The maximum error in pressure measurement was estimated at 0.2 mm Hg. The relative error depended on the pressure of the particular sample.

Errors in the volume of the hydrogen sample were difficult to estimate. The precision of the volumetric calibrations appeared to be good. Reasonable estimates of the maximum error in the volumes of the various parts of the volumetric section are listed in Appendix D, Table D-I. The relative error in any one sample depended on the combination of volumetric bulbs used.

The quantity of hydrocarbon collected in the traps was determined by the difference in weights of the traps before and after sampling. Possible observational errors were those in the performance of the weighings, themselves, plus error in calibration of the weights, rider arm, and vernier. The latter errors would enter only when different weights or settings were used in the tare and gross weight determinations. Calculations showed that weighing errors due to arm correction and buoyancy were negligible.

Buoyancy changes could have occurred in Runs 2 to 34. Subsequent weighings were made with a "blank" trap to determine changes in buoyancy due to changes in ambient temperature, pressure, and humidity. The change in the blank weight was only 0 to 0.5 mg in 39 of 44 weighings. In the remaining 5 weighings, the blank weight changed by 0.8 to 1.9 mg.

It is likely that changes such as the latter could have occurred in Runs 2 to 34.

Operational errors could have occurred that would affect the weighings. The stopcock grease on the sample trap ball-joints was always carefully removed, and the traps wiped clean with a damp chamois. It is conceivable that in some cases the cleaning failed to remove some of the grease. The repeatability of the second trap weight in a number of cases indicated that cleaning was generally effective. This repeatability occurred in runs for which no hydrocarbon was observed in the second trap, so that little or no change in weight was expected.

A more serious possible source of operational error is that some hydrocarbon may have been absorbed in the grease on the first ball-joint in the trap system. In order to check this source of error, the following experiment was performed. Two traps were placed in their usual position in the sampling apparatus. The first contained benzene from a previous run, and the second was empty. A dry ice--acetone bath was placed on the first trap, and then the second trap and interconnecting arm were evacuated. The down stream cock was closed on the second trap, the dry ice--acetone bath was removed from the first trap, and the first trap was opened to the second, for 1/2 hour. The freezing bath was replaced on the first trap for 2 minutes, then both traps were closed.

Weights made before and after the above procedure showed a net loss of 3.4 mg. This loss was presumably due to absorption of benzene in the grease on the interconnecting ball-joint. A repeat of the same procedure, with 15 minutes contact time, showed a loss of 4.1 mg.

Consideration of the sampling procedure led to a second series of checks. In liquid samples the collection of benzene was usually very rapid because of the presence of the cold traps. In gas samples the collection of benzene was over a 15 minute to 2 hour period, but the partial pressure of the benzene was usually much less than its vapor pressure. Thus it seems unlikely that equilibrium between the stopcock grease and benzene would have occurred.

For the above reasons, three runs were made in which the traps were interconnected as before, but the benzene was distilled over into the second trap and frozen. A light bulb was used to speed the vaporization of benzene from the first trap. In these runs the net loss of weight was 1.0, 0, and 1.5 mg for 0.59, 0.15, and 0.55 g of benzene, respectively.

The conclusion reached was that some benzene probably was absorbed in the stopcock grease in the first ball-joint during sampling. However, the amount was probably small in comparison with the total sample collected.

A series of 30 weighings of the same 100 gram weight was performed over a period of several days to determine the systematic error in the weighing procedure. The results of these weighings were used to estimate the standard deviation of the 100 gram weight. The 99 per cent confidence limits for the weight were found to be ±0.3 mg. This variability was taken to be typical of the error in determination of the weight of objects on the balance.

Liquid-Phase Composition

The mole fraction of hydrogen in the liquid phase is given by

$$x_1 = \frac{n_1}{n_1 + n_2} \ . \qquad \text{(VI-3A)}$$

The error is given by

$$\frac{\Delta x_1}{x_1} = \frac{\Delta n_1}{n_1} - \frac{\Delta(n_1 + n_2)}{n_1 + n_2} \ . \qquad \text{(VI-4A)}$$

Error for the mole fraction of the hydrocarbon is given by a similar expression.

In liquid samples the moles of hydrocarbon, n_2, was never less than 4 times as great as the moles of hydrogen, n_1. Thus, errors in x_1 approach

$$\frac{\Delta x_1}{x_1} = \frac{\Delta n_1}{n_1} - \frac{\Delta n_2}{n_2} \ . \qquad \text{(VI-5)}$$

Similarly, errors in x_2 tend to cancel. For this reason the x_1 values are more in error and are analyzed here.

The weights of hydrocarbon collected in liquid-phase samples ranged from 0.23 to 2.3 g, and were usually greater than 0.4 g. It is considered unlikely that analysis error was greater than 4 mg. Errors in n_2 should be $\leq$ 1 per cent on this basis.

Estimation of the maximum error in n_1 follows from the discussion in previous paragraphs. The estimated maximum error in x_1 varies from about 2 1/2 per cent at low pressures to about 1 1/2 per cent at high pressures. The data in Tables III to VII may be inspected with the estimated errors in mind. Note again that these are analysis errors only, and have to do with precision.

Initial runs 3A to 3I have were made at 280 °F to develop the sampling and analysis technique. Runs 3A and 3B gave far different x_1 values than the remaining runs 3D to 3I. The latter 5 runs repeated to within ±2.7 per cent of the average.

In Runs 12 and 21 the values of x_1 at the same temperature and pressure were the same, 0.0389 in each case. The cell was purged and refilled between these runs. Runs 14 and 22 showed values of x_1 of 0.0536 and 0.0533, respectively. A repeat at 9997 psia and 150 °F in Run 35 gave values of 0.176 and 0.180.

These few repeats indicated that the variability in x_1 was probably within the error estimated, but the results of Run 35 indicated an increase in solubility with equilibration time. Because of this presumed time effect, a series of liquid samples were taken at different equilibration times in Runs 37 and 38. The results of these runs are shown in Figure 13.

In Runs 3 to 36 the criterion of equilibration was constancy of pressure in the equilibrium cell as a function of time. The indication of pressure constancy was the stability of the pressure balance piston level. In these runs it had been noted that virtually all of the addition of hydrogen gas to the cell was made in the first 5 minutes or so of operation. A small drop of piston level with time always occurred because of the controlled oil leakage around the piston. The pressure seemed quite stable, however, after only 1 to 2 hours. Samples were withdrawn in these runs after 1 1/2 to 5 hours equilibration. The data shown in Figure 13 indicate that longer equilibration times are probably needed, especially at 150 °F. In all subsequent runs, the equilibration time was at least 8 hours.

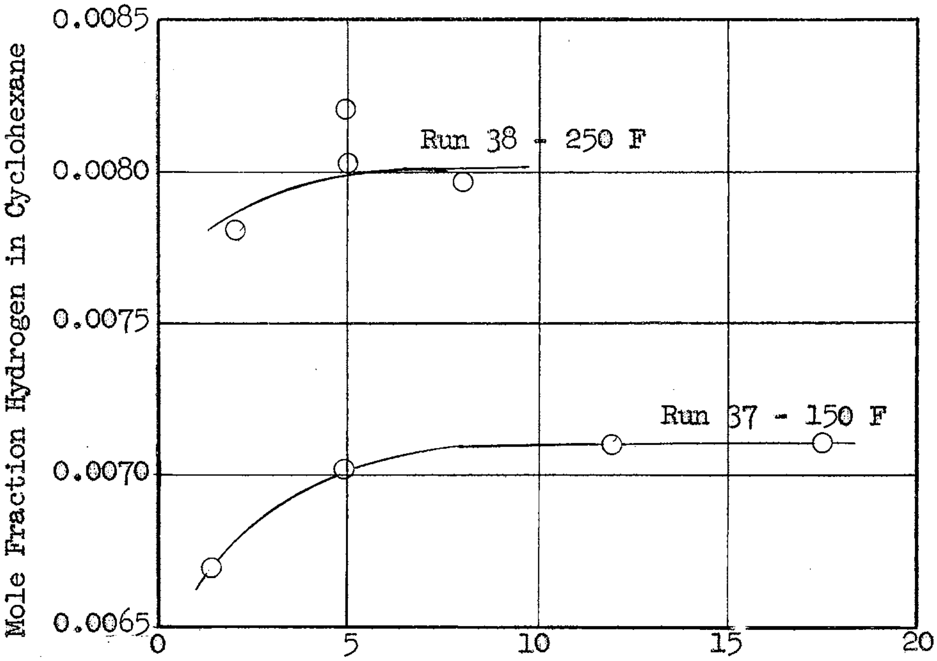

Figure 13

Liquid Sample Composition as a Function of
Equilibration Time

The repeatability of the liquid-phase hydrogen compositions appears to be within ±3 per cent. The possibility exists of an error in accuracy larger than 3 per cent due to insufficient equilibration time in Runs 3 to 36, particularly at 150 °F. This error would be present in the benzene data only.

The effect of errors in temperature and pressure measurements on the mole fraction of hydrogen in the liquid-phase are small. Typical values are shown in Table VIII.

TABLE VIII

EFFECT OF ERRORS IN TEMPERATURE AND PRESSURE ON THE SOLUBILITY OF HYDROGEN IN BENZENE LIQUID

Temperature °F	Pressure, psia	ΔT, °F	ΔP, psia	o/o Error in x_1
250	500	1	-	0.3
150	10,000	1	-	0.3
250	100	-	1	1.8
250	500	-	1	0.22
150	10,000	-	1	0.01

The thermocouples were calibrated in place against an NBS-calibrated platinum resistance thermometer. The error in calibration should not exceed 0.1 °F. Temperature profile measurements did show variations of 0.4 °F. between the centerline of the cell and the outside top of the cell. The temperature inside the cell should vary less. The aluminum block temperature was controlled to ±0.1 °F. Variation and error in the cell temperature should introduce negligible error in the liquid compositions in comparison to other sources of error.

Pressure was measured to within ±0.2 per cent in the worst case. Errors in pressure measurement should also introduce negligible error in the liquid compositions.

Liquid-phase compositions were obviously in error in Runs 20 and 49. The points were included because no reason for the error was known. In a few runs, failure to purge the sample line caused errors in liquid-phase compositions. These runs were discarded because of the known operational error.

Vapor-Phase Composition

The mole fraction of hydrocarbon in the vapor phase is given by

$$y_2 = \frac{n_2}{n_1 + n_2} . \qquad \text{(VI-3B)}$$

The error is given by

$$\frac{\Delta y_2}{y_2} = \frac{\Delta n_2}{n_2} - \frac{\Delta(n_1 + n_2)}{n_1 + n_2} \qquad \text{(VI-4B)}$$

The mole fraction of hydrocarbon varied widely, depending on the pressure. At pressures of 200 psia and greater, the ratio of n_1 to n_2 was more than 4 to 1. Thus, analysis error was more important for the hydrocarbon mole fraction in the vapor phase samples. The errors are, therefore, estimated for y_2 values.

The weight of hydrocarbon collected in the vapor samples ranged from .04 to 1.62 g. In most cases the weights were between 0.1 and 0.4 g. Analysis errors could have amounted to ±2 mg, so that the total analysis error in the gas-phase samples could have ranged from ±5 per cent down to about ±0.5 per cent.

Two sources of sampling error were investigated. The first of these was the effect of rate of withdrawal of vapor sample. Runs 3J to 3N were made at different sample withdrawal rates. The data are plotted in Figure 14. Excluding the one low point, the variability in the data is ±2 per cent. This variability is greater than might be expected from analysis error, but there does not seem to be any pronounced effect of sampling rate. The lowest practical sampling rate was used in all subsequent runs, and never exceeded 100 cc/min. at 1 atm. Prausnitz and Benson (62) in a similar study used sampling rates up to 570 cc/min.

A second sampling error was discovered after noticing that the vapor compositions of Runs 12 to 20 did not repeat well. At the time it was thought that the error was due to the very small amount of hydrocarbon collected. A 4-liter gas sample bulb was constructed and calibrated. Collection of larger samples seemed to improve the repeatability. Up to Run 21 the vapor sample line was heated by simply contacting the exposed portion with a heating tape. In Run 21 the tape and line were wrapped with asbestos to prevent heat loss and it was noticed that this increased the hydrocarbon composition substantially. In all subsequent runs the tape and line were wrapped and sufficient heating was provided to guarantee that the sample line was above bath temperature.

Use of the improved vapor-sampling line heating method in Runs 21, 22, and 25 through 32 showed that vapor compositions at 150 °F were severely affected by absence of proper heating. There seemed to be no effect of insufficient heating at 250 °F. The vapor composition data for Runs 12 through 14 were rejected as being incorrect due to insufficient heating. The results of all other repeat runs are shown in

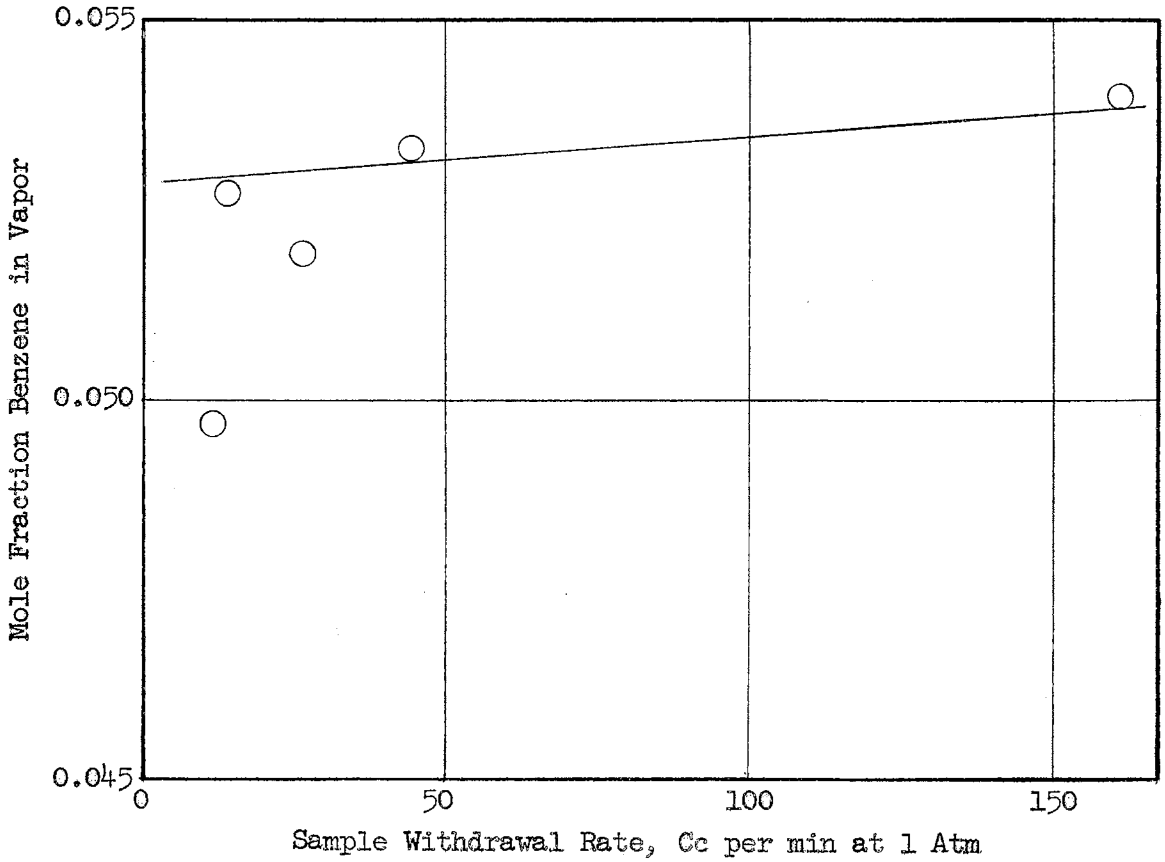

Figure 14

Effect of Sampling Rate on Vapor Composition

Table IX.

TABLE IX

COMPARISON OF REPEATED VAPOR SAMPLES FOR BENZENE AND HYDROGEN

Initial Run No.	Repeat Run No.	Initial y_2	Repeat y_2	o/o Difference based on Repeat
8	8	0.104	0.125	16.8
8	24	0.125	0.128	2.3
9	26	0.0482	0.0500	3.6
10	27	0.0203	0.0198	2.5
12	28	0.0111	0.0113	1.8
21	21	0.00850	0.00843	0.8
15	15	0.486	0.493	1.4
15	29	0.493	0.493	0
18	30	0.0557	0.0571	2.5
19	31	0.0379	0.0383	1.0
20	32	0.0268	0.0264	1.5
35	35	0.00506	0.00443	14.2

The repeatability of the gas-phase samples is within ±2 per cent of the average value, with two exceptions. Sampling errors probably reduce the accuracy of the data, particularly at the higher pressures, where the amount of hydrocarbon collected was small.

Errors in vapor composition due to errors in temperature and pressure measurement or control may be estimated by consideration of Table X. Errors in pressure measurement probably produced negligible errors in y_2. Errors in temperature measurement and control are more important, but it is estimated that errors in y_2 due to this source should be less than 0.5 per cent.

TABLE X

EFFECT OF ERRORS IN TEMPERATURE AND PRESSURE ON THE SOLUBILITY OF BENZENE IN HYDROGEN

Temperature, °F	Pressure, psia	ΔT, °F	ΔP, psia	o/o Error in y_2
150	75	-	0.1	0.1
250	100	-	0.1	0.1
150	200	-	0.2	0.1
250	200	-	0.2	0.1
150	10,000	-	10	0.1
250	10,000	-	10	0
150	200	0.3	-	0.6
250	200	0.3	-	0.4
150	1,000	0.3	-	0.5
250	1,000	0.3	-	0.4
150	10,000	0.3	-	0.5
250	10,000	0.3	-	0.5

Thermodynamic Consistency Tests

Three thermodynamic consistency tests were applied to the experimental data. Two of these methods required the use of K-values. For this reason, K-values were obtained from the x-y data. Since there were small differences in pressure between the x and y determinations in many cases, these data were adjusted to the same pressure. The x_1 values were adjusted by multiplying the difference in pressure by the slope of the x_1-P curves. Large plots similar to Figures 11 and 12 were used to determine the slopes. The corrections were negligible in most cases. The K-values thus calculated are given in Tables XI and XII.

Adler Test

The thermodynamic consistency test of Adler, et al. (2), was applied in a modified form. The integrand of the right-hand side of Equation

TABLE XI

HYDROGEN-BENZENE K-VALUES FROM x-y DATA

	Run No.	Pressure, psia	K_{BZ}	K_{H2}
T = 150 °F	8	76.27	0.105	540
	8	76.15	0.126	529
	25	76.39	0.128	525
	9	194.3	0.0484	215
	26	194.3	0.0502	214
	10	503.1	0.0205	83.4
	27	503.0	0.0200	83.6
	12	1026	0.0114	41.6
	28	1026	0.0116	41.5
	21	1707	0.00884	25.5
	21	1707	0.00877	25.5
	22	2508	0.00718	18.6
	23	4000	0.00626	12.2
	24	6998	0.00573	7.57
	35	9997	0.00614	5.64
	35	9997	0.00540	5.54
T = 250 °F	15	97.14	0.487	275
	15	96.90	0.494	272
	29	96.92	0.494	272
	16	201.0	0.249	140
	17	499.4	0.106	58.4
	18	1003	0.0590	29.4
	30	1003	0.0576	29.4
	19	1702	0.0401	17.8
	31	1702	0.0405	17.8
	20	2999	0.0295	10.4
	32	2999	0.0292	10.4
	33	5995	0.0250	5.86
	34	9983	0.0238	4.04

TABLE XII

HYDROGEN-CYCLOHEXANE K-VALUES FROM x-y DATA

	Run No.	Pressure, psia	K_{CH}	K_{H2}
T = 150 °F	36	99.83	0.0977	249
	37	199.9	0.0480	134
	46	501.9	0.0231	53.8
	53	501.6	0.0211	53.9
	47	995.9	0.0124	28.6
	48	1694	0.00920	17.6
	49	3002	0.00753	10.2*
	50	5996	0.00742	5.59
	51	10013	0.00869	3.80
	54	10013	0.00928	3.80
T = 250 °F	39	101.3	0.452	173
	38	199.9	0.239	95.2
	40	500.0	0.104	40.0
	41	999.9	0.0592	20.7
	42	1700	0.0409	12.4
	43	3000	0.0310	7.41
	44	5996	0.0279	4.15
	45	9999	0.0289	2.80

* Hydrogen x-value estimated from plot of data.

III-21 can be split into two terms.

$$\int\left[z^L + \bar{z}_1^V y_1\left(\frac{1}{K_2} - \frac{1}{K_1}\right) - \frac{z^V}{K_2}\right] d \ln P = \int\left(z^L - 1\right) d \ln P$$

$$+\int\left[1 + \bar{z}_1^V\ y_1\left(\frac{1}{K_2} - \frac{1}{K_1}\right) - \frac{z^V}{K_2}\right] d \ln P \qquad \text{(VI-6)}$$

If the gas phase is ideal, then $\bar{z}_1^V$ and z^V are equal to 1.0, and the second integral reduces to zero. The value of the integral thus represents the extent of deviation of the gas phase from ideal behavior. For convenience, the integrand of the right-hand term of Equation VI-6 will be called z'.

$$z' = 1 + \bar{z}_1^V\ y_1\left(\frac{1}{K_2} - \frac{1}{K_1}\right) - \frac{z^V}{K_2} \qquad \text{(VI-7)}$$

The integrals in Adler's relation may be integrated, for gas-liquid mixtures, between the vapor pressure of the solvent and any higher pressure. Thus Equation III-21 can be written

$$\int_{K_1(x_1 = 0)}^{K_1 = K_1} x_1 \, d \ln K_1 + \int_{K_2 = 1}^{K_2 = K_2} x_2 \, d \ln K_2$$

$$= \int_{P = p_2}^{P = P} (z^L - 1)\ d \ln P + \int_{P = p_2}^{P = P} z' \, d \ln P. \qquad \text{(VI-8)}$$

The evaluation of each term in Equation VI-8 is discussed below for hydrogen-benzene at 250 °F, for the pressure range p_2 = 44.67 psia to 2000 psia.

The evaluation of the first term in the left side of Equation VI-8 is shown in Figure 15. The value of K_1 at 44.67 psia was found by

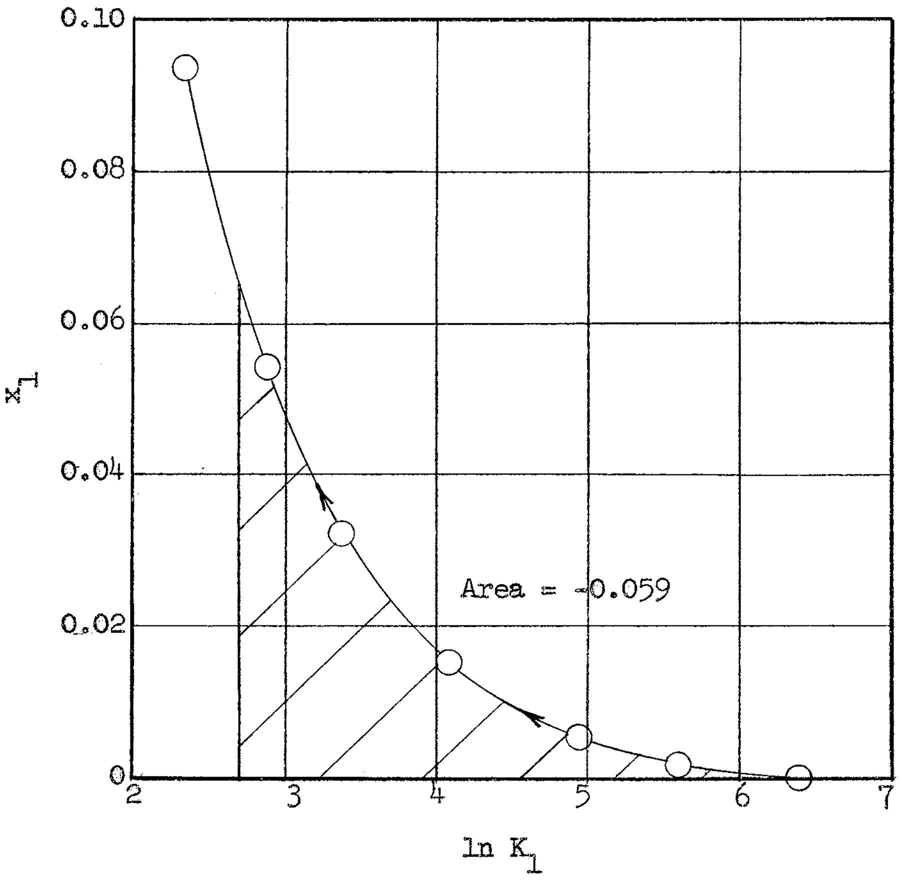

Figure 15

Evaluation of $\int x_1 \, d\ln K_1$ for Hydrogen-Benzene at 250 °F extrapolation of the hydrogen K-values. The accuracy of this extrapolation is not critical, as may be seen in Figure 15. The value of the integral is -0.059.

The evaluation of the second term in the left side of Equation VI-8 is shown in Figure 16. The value of this integral is -3.263. The left side of Equation VI-8 is thus equal to -3.322. Notice that the term involving x_1 is very small. In effect, Adler's test does not test the gas solubility data, but tests only the vapor-phase concentration of the hydrocarbon. This fact should be recognized when Adler's test is used for gas-liquid data.

The evaluation of the liquid compressibility term is shown in Figure 17. This term was evaluated in two ways to determine the importance of availability of liquid compressibility data. In the first method, the liquid volume was calculated by

$$\underline{V}^L = x_1 \bar{V}_1^L + x_2 \underline{V}_2^L \quad . \tag{VI-9}$$

Where $\bar{V}_1^L$ = partial molar volume of hydrogen in benzene (a constant value of 36 cc/g mole was used)

$\underline{V}_2^L$ = molar volume of pure benzene at its vapor pressure (101.7 cc/g mole)

The value of 36 cc/g mole for $\bar{V}_1^L$ was taken from Hildebrand and Scott (31), and is from low pressure measurements. The rather crude estimate of $\underline{V}^L$ of Equation VI-9 gave a value for the integral of -3.391.

Literature data for the compressibility of hydrogen and benzene equilibrium liquid mixtures at 77 °F (44) and 320 to 500 °F (16) were used to show that the liquid volume is given reasonably well by the following relation.

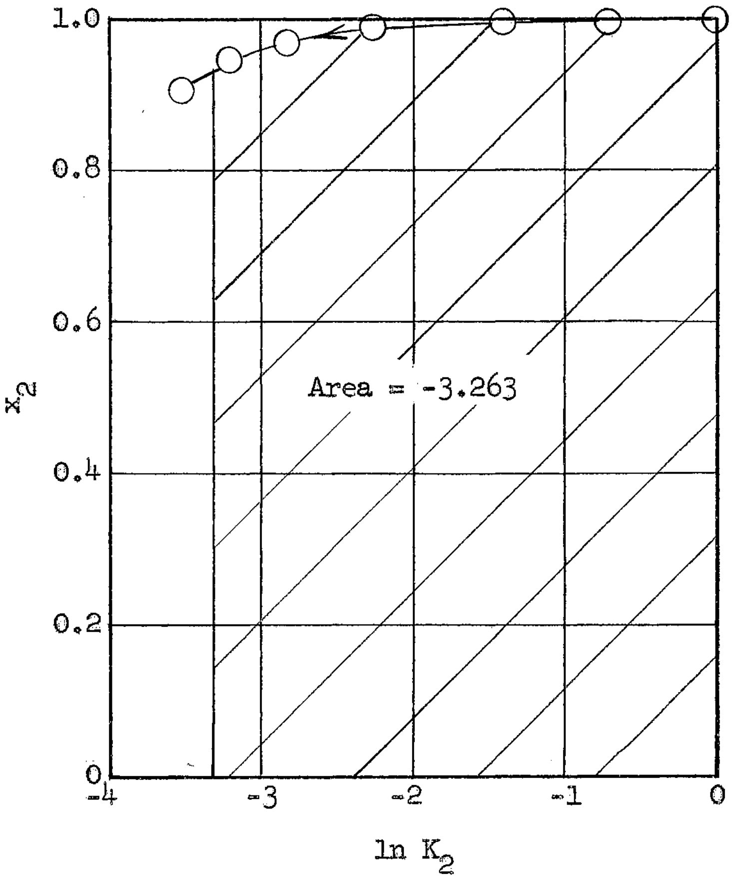

Figure 16

Evaluation of $\int x_2 \, d\ln K_2$ for Hydrogen-Benzene at 250 °F

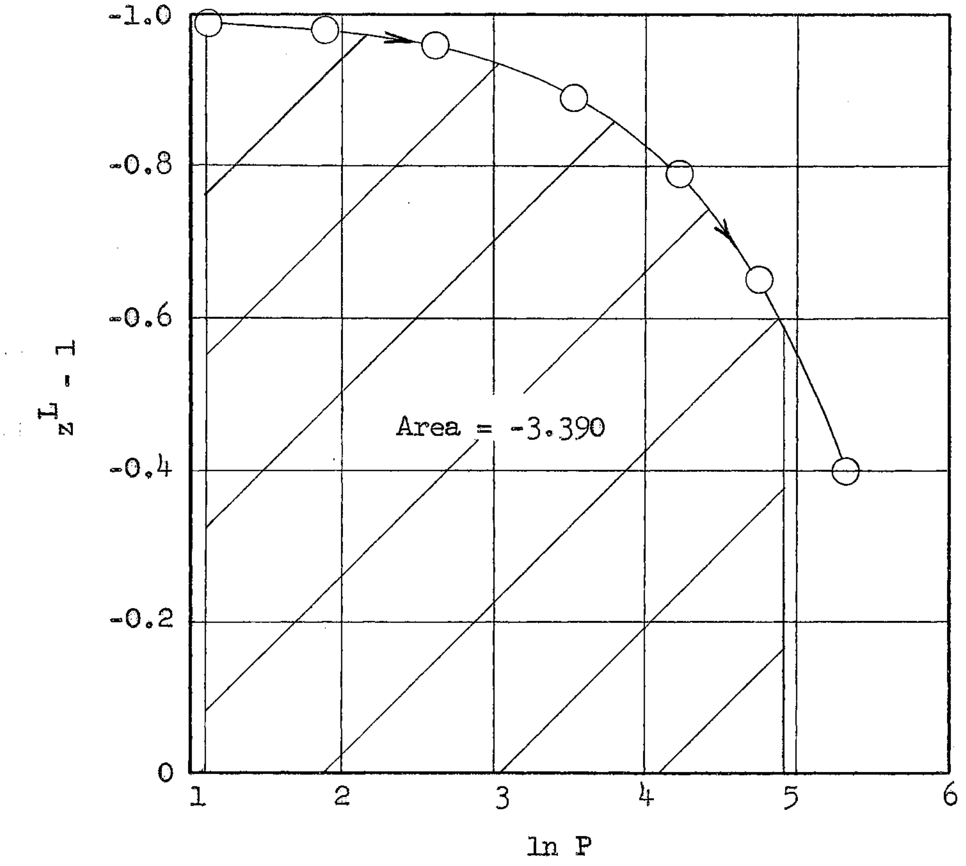

Figure 17

Evaluation of $\int (z^L - 1)\, d\ln P$ for Hydrogen-Benzene at 250 °F

$$\underline{V}^L = x_1 \bar{V}_1{}^* + \underline{V}_2^L \; (1 - \beta \, \Delta P) \, x_2 \; . \qquad \text{(VI-10)}$$

where $\bar{V}_1{}^*$ = partial molar volume of hydrogen in benzene at infinite dilution (61.9 cc/g mole)

$\underline{V}_2^L$ = molar volume of pure benzene at its vapor pressure (102.5 used here)

β = compressibility of liquid benzene (0.00021 atm^{-1})

ΔP = $P - p_2$

Values of $\bar{V}_1^*$ and $\underline{V}_2^L$ were given in the above references. The compressibility, β, was determined by fitting Equation VI-10 to the data. The parameters $\bar{V}_1^*$, $\underline{V}_2^L$, and β were then plotted against temperature and interpolated at 250 °F to obtain 61.9 cc/g mole, 102.5 cc/g mole, and 2.1×10^{-4} atm^{-1}, respectively.

The use of Equation VI-10 gave a value for the integral of -3.390, almost identical with the value estimated with Equation VI-9. A reasonable estimate for the liquid-phase molar volume appears to be satisfactory.

Combination of the terms in Equation VI-8 calculated thus far gives a difference of 0.068 between the right and left sides that must be accounted for by the gas-phase nonideality term--that is, if the data are consistent. The evaluation of this latter term requires gas-phase compressibility data. These data were not available, necessitating the use of an equation of state.

Prausnitz and Keeler (65) showed that the virial equation of state represents quite well the volumetric data for gas-vapor mixtures. Data for the system hydrogen-n-hexane were available from the literature (54). Several equations of state were used to calculate the compressibility factor for hydrogen-hexane equilibrium vapor mixtures. A typical comparison is shown in Figure 18. The virial equation is seen to approximate best the experimental data.

The z' term of Equation VI-7 can be rearranged to the following form:

$$z' = 1 + \frac{1}{K_2} (\bar{z}_1^V - z^V) - \bar{z}_1^V \quad . \qquad \text{(VI-11)}$$

This rearrangement is convenient for the evaluation of z', and it serves to point out the fact that K_1 does not actually appear in the right side of Adler's equation. It may be argued that K_2 and K_1 are directly related for binary mixtures, and that the absence of K_1 is illusory. However, K_1 is generally not affected much by errors in vapor compositions or K_2 by errors in liquid compositions, for gas-liquid equilibria. Thus, the z' term is almost entirely dependent on the vapor composition.

Equation VI-11 also shows that the evaluation of the vapor-phase compressibilities is quite important. The reciprocal of K_2 is generally rather large, and is multiplied by the rather small difference, $(\bar{z}_1^V - z^V)$. Errors in the compressibility terms are, therefore, exaggerated.

The evaluation of the z' integral term is shown in Figure 19. The value of the integral is 0.476. The right side of Equation VI-8 is, therefore, -2.914 and is different from the left side (-3.322) by 12.6 per cent, based on the left side. Adler's test would indicate that the experimental data for benzene-hydrogen at 250 °F are not consistent.

Since Adler's test obviously does not test the hydrogen solubility data, it was decided to determine the effect of varying the K_2 data. The latter amounts essentially to varying only the y_2 data,

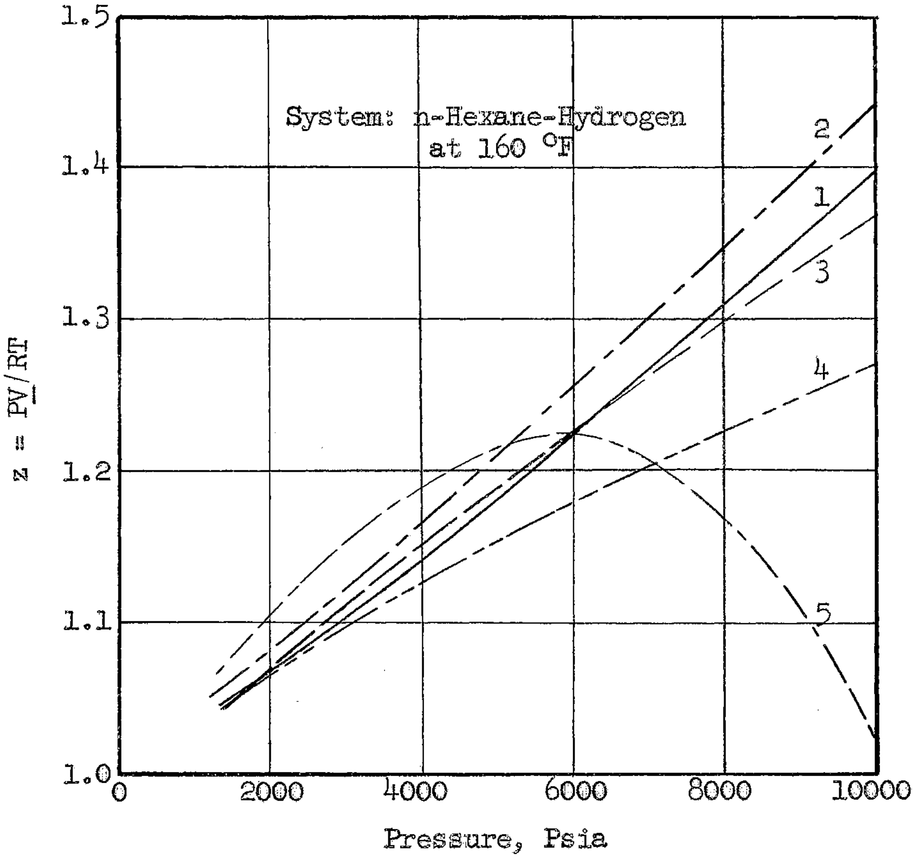

1 - Experimental Data
2 - Redlich-Kwong Equation
3 - Virial Equation with B and C
4 - Virial Equation with B Only
5 - Black Equation

Figure 18

Comparison of Compressibility for Equilibrium Vapor with Equations of State

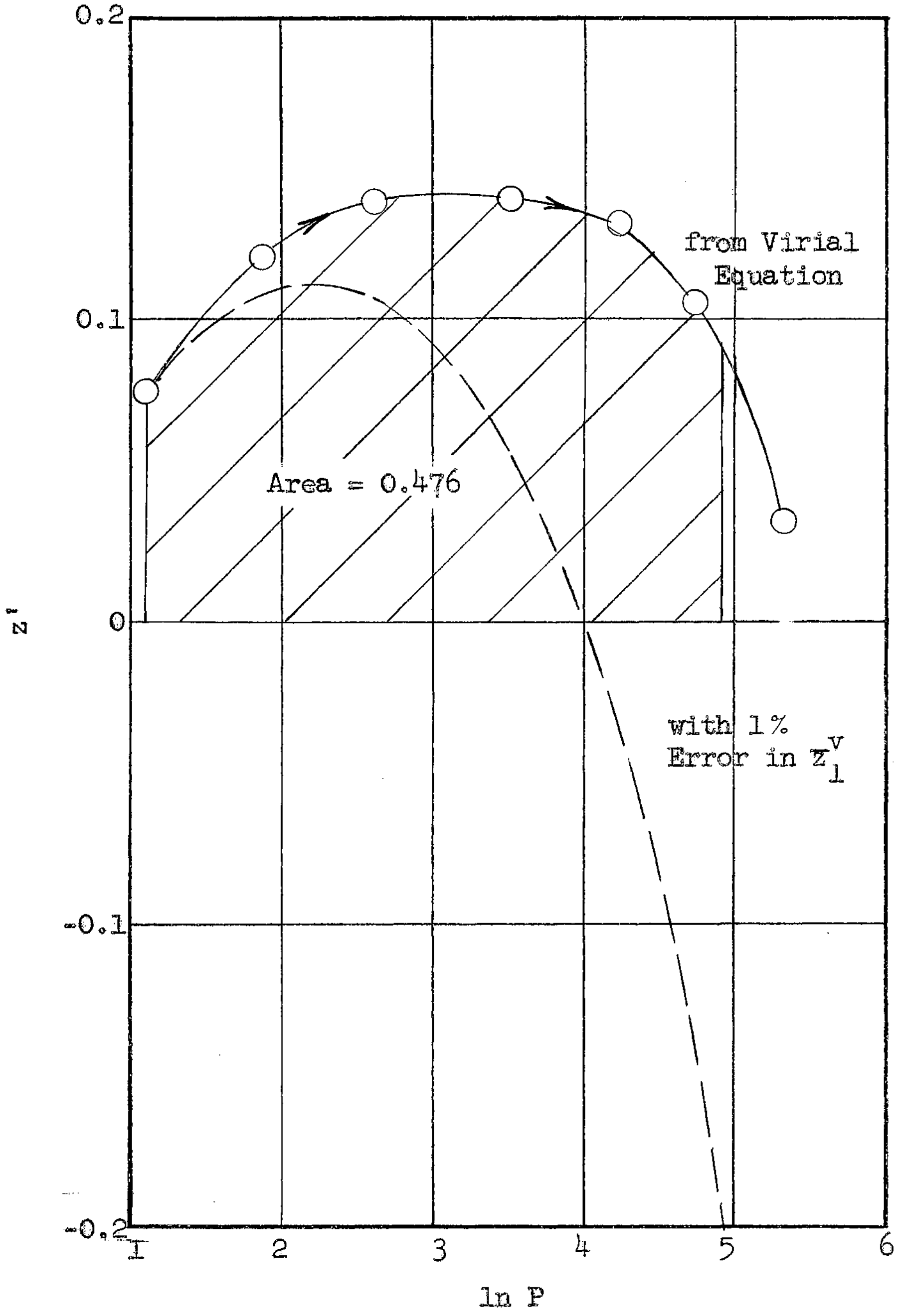

Figure 19

Evaluation of $\int z' \, d\ln P$ for Hydrogen-Benzene at 250 °F since x_2 is nearly 1.0. The y_2 data were increased 5 per cent and the integration repeated, yielding a value of -3.291 for the left side of Equation VI-8. The left side appears not to be affected much by errors in y_2.

The effect of $\bar{z}_1^v$ was also investigated. Suppose that $\bar{z}_1^v$ is in error by 1.0 per cent, while z^v is assumed correct. The dashed line in Figure 19 results, and the value of the integral of z' is now 0.092. Errors in the volumetric data appear to be important, as mentioned above. Even if experimental data were available, small errors could affect the value of the integral greatly.

Results similar to the above were obtained with the cyclohexane-hydrogen data at 250 °F. The Adler test indicates that experimental data are not consistent, but the results of the test cannot be accepted without reservation. The test appears to be insensitive to the K-data and over-sensitive to the compressibility data. The Adler test is probably most valuable when applied to systems of similar volatility at low pressures, particularly in the absence of good experimental vapor-phase compressibility data.

Prausnitz-Keeler Test

The consistency test of Prausnitz and Keeler consists of calculating interaction second virial coefficients (B_{12}) from isothermal P-x-y data and pure component second virial coefficients. Since B_{12} is a function of temperature only, and not of pressure or composition, values calculated for constant temperature should be the same, or at least show little variation. The calculational details for this method are given in Appendix H.

Interaction second virial coefficients were calculated from the data obtained in this work and from the data of Nichols <u>et al</u>. (54). The latter data were cross-plotted against temperature and interpolated on large charts to obtain hydrogen-n-hexane K values at 150 and 250 °F. The derived values of B_{12} are shown in Tables XIII, XIV, and XV. The values shown in these tables were calculated using terms including the third virial coefficients and liquid activity coefficients; the effect of including these terms is not large and is illustrated in Appendix H.

Consideration of the data in Tables XIII and XIV indicates that the derived B_{12} values are in reasonable agreement at pressures of 500 psia and higher, particularly at 250 °F. The marked deviation of the interaction coefficients at low pressures is not entirely due to inaccurate data. At low pressures the calculational procedure is extremely sensitive to small variations in y_2. For example, for benzene-hydrogen at 150 °F and 76.1 psia, values of y_2 of 0.125 and 0.128 yielded calculated B_{12} values of 9.6 and -77.8; a difference of only 2.4 per cent in the y_2 data produced interaction coefficients different by almost one order of magnitude.

In order to illustrate better the self-consistency of the experimental data, the calculational procedure was reversed. That is, average values of B_{12} were used to back-calculate values of y_2. In this calculation, the experimental values of x_2 were used. Since the x_1 values are small, x_2 values are close to 1.0. The Prausnitz-Keeler test, like the Adler test, does not really test the solubility data of the gas in the liquid. In obtaining average B_{12} values, only the data for high pressures were used. The back-calculated y_2 data are compared with the experimental y_2 data in Tables XVI and XVII.

TABLE XIII

SECOND VIRIAL INTERACTION COEFFICIENTS CALCULATED FROM BENZENE-HYDROGEN SOLUBILITY DATA

Temperature, °F	Pressure, psia	B_{12}, cc/g mole
150	76.2	602.9
	76.1	9.6
	76.3	- 77.8
	194.2	56.0
	194.2	15.3
	503.0	16.4
	502.9	26.7
	1026	11.2
	1026	7.6
	1707	- 3.5
	1707	- 2.5
	2508	- 0.9
250	97.1	- 15.2
	96.9	-110.6
	201.0	- 16.7
	499.4	12.7
	1003	15.9
	1003	10.3
	1702	10.5
	1702	9.1
	2999	9.4
	2999	10.4

TABLE XIV

SECOND VIRIAL INTERACTION COEFFICIENTS CALCULATED FROM CYCLOHEXANE-HYDROGEN SOLUBILITY DATA

Temperature, °F	Pressure, psia	B_{12}, cc/g mole
150	99.8	-36.0
	199.9	36.0
	501.8	-23.0
	501.3	14.6
	995.8	7.4
	1694	2.8
	3002	3.0
250	101.3	-15.7
	199.8	10.6
	499.9	18.1
	999.8	15.1
	1700	17.1
	3000	18.4

TABLE XV

SECOND VIRIAL INTERACTION COEFFICIENTS CALCULATED FROM N-HEXANE-HYDROGEN SOLUBILITY DATA

Temperature, °F	Pressure, psia	B_{12}, cc/g mole
150	500	- 8.9
	1000	3.9
	2000	7.6
	3000	3.0
250	500	27.0
	1000	24.6
	2000	20.3
	3000	19.1

TABLE XVI

COMPARISON OF CALCULATED AND EXPERIMENTAL SOLUBILITY OF BENZENE IN HYDROGEN

Temp., ^{o}F	B_{12}	Pressure, psia	y_2 calc'd	y_2 exp't
150	-0.2	76.2	0.125	0.104
		76.1	0.125	0.125
		76.3	0.125	0.128
		194.2	0.0507	0.0482
		194.2	0.0507	0.0500
		503.0	0.0211	0.0203
		502.9	0.0211	0.0198
		1026	0.0118	0.0111
		1026	0.0118	0.0113
		1707	0.00827	0.00850
		1707	0.00827	0.00843
		2508	0.00673	0.00679
250	9.9	97.1	0.484	0.486
		96.9	0.485	0.493
		201.0	0.243	0.247
		499.4	0.105	0.104
		1003	0.0572	0.0557
		1003	0.0572	0.0571
		1702	0.0381	0.0379
		1702	0.0381	0.0383
		2999	0.0266	0.0268
		2999	0.0266	0.0264

TABLE XVII

COMPARISON OF CALCULATED AND EXPERIMENTAL SOLUBILITY OF CYCLOHEXANE IN HYDROGEN

Temp., °F	B_{12}	Pressure, psia	y_2 calcd	y_2 exp't
150	4.3	99.8	0.0957	0.0973
		199.9	0.0491	0.0477
		501.8	0.0212	0.0207
		501.5	0.0212	0.0227
		995.8	0.0122	0.0120
		1694	0.00857	0.00868
		3002	0.00667	0.00680
250	17.2	101.3	0.449	0.451
		199.8	0.236	0.237
		499.9	0.101	0.101
		999.8	0.0560	0.0565
		1700	0.0377	0.0377
		3000	0.0274	0.0269

The B_{12} values derived from the experimental data cannot be compared rigorously against any standard other than additional experimental values. Generalized correlations of second virial coefficients based on the theorem of corresponding states are available. Comparison of derived B_{12} data with these correlations depends on the applicability of corresponding states theory and cannot be regarded as rigorous. General trends or gross errors probably can be determined by such comparisons.

A recent corresponding states correlation for interaction second virial coefficients is that of Prausnitz and Benson (63). The Prausnitz-Benson correlation is actually a modification of an earlier correlation (60) for pure components, in which the reduced second virial coefficient, $B/\underline{V}_c$, is given as a function of reduced temperature and the acentric factor, ω . The chief difficulty in the use of this type of correlation is the designation of the critical temperature of a mixture. Prausnitz and Benson suggested a method for predicting the critical temperature for mixtures of molecules differing widely in size, and thus applied corresponding states theory to interaction second virial coefficients.

Values of B_{12} were calculated for the mixtures studied here by the Prausnitz-Benson method. The calculation procedure is shown in Appendix K. The generalized B_{12} values are compared with the average values derived from the experimental data in Table XVIII. The agreement is not very good. Several comments may be made regarding this comparison. In the first place, critical volumes are not known with great certainty, and a correlation of the variable $B/\underline{V}_c$ reflects any error in the $\underline{V}_c$ values. Furthermore, the specification of mixture values of $\underline{V}_c$, ω, and T_c is arbitrary and may introduce error.

TABLE XVIII

COMPARISON OF DERIVED AND GENERALIZED VIRIAL COEFFICIENTS FOR HYDROGEN-6-CARBON HYDROCARBONS

Solvent	Temp., °F	Derived B_{12}	Generalized B_{12}
Bemzene	150	- 0.2	14.6
	250	9.9	26.0
Cyclohexane	150	4.3	26.1
	250	17.2	35.6
x-Hexane	150	4.8	43.9
	250	21.4	56.0

Perhaps a more fundamental problem is that the use of a corresponding states treatment for mixtures assumes tacitly that the theory also applies to the pure components. The three-parameter corresponding states treatment involving ω, the acentric factor, does apply to hydrocarbons, but was never intended for hydrogen. The correlations have been used with hydrogen in some cases by assigning fictitious values of T_c, $\underline{V}_c$, and ω, but such use may not always lead to reliable results.

Infinite Dilution Test

The consistency test of Gautreaux and Coates (26) is the only test considered here that tests the gas solubility data. The test also tests the y_2 data to a certain extent. The extrapolation of the light-component K data through the moderate- to low-pressure region involves passing through the region of greatest influence of y_2 on K_1.

The liquid molar volume data required in Equation III-24 were available from the literature (72). Vapor volumes were calculated from the virial equation of state. The slope term was evaluated from large plots of the experimental P-x_1 data. The K values for the solute gas were extrapolated to the vapor pressure of the solvent on large log-log plots, as shown for cyclohexane-hydrogen in Figure 20. The hydrogen K data were represented well at low pressures by straight lines on the log-log plots. The extrapolated and calculated values of K_1 at $x_1 = 0$ are listed in Table XIX.

TABLE XIX

INFINITE DILUTION CONSISTENCY TEST OF HYDROGEN K DATA

Solvent	Temp., °F	K_1, (extrapolated)	K_1 (Eq. III-24)	Per Cent Diff.*
Benzene	150	4200	4430	- 5.2
	250	600	607	- 1.2
Cyclohexane	150	2400	2870	-16.4
	250	395	423	- 6.6

* Based on calculated K_1

The agreement in Table XIX is not bad, considering the arbitrariness of the extrapolation procedure. The cyclohexane data show poorer agreement, which is interesting in view of the fact that these data were taken with longer equilibration times than the benzene data. To shift the K_1 lines upward would require lower x_1 or y_2 values.

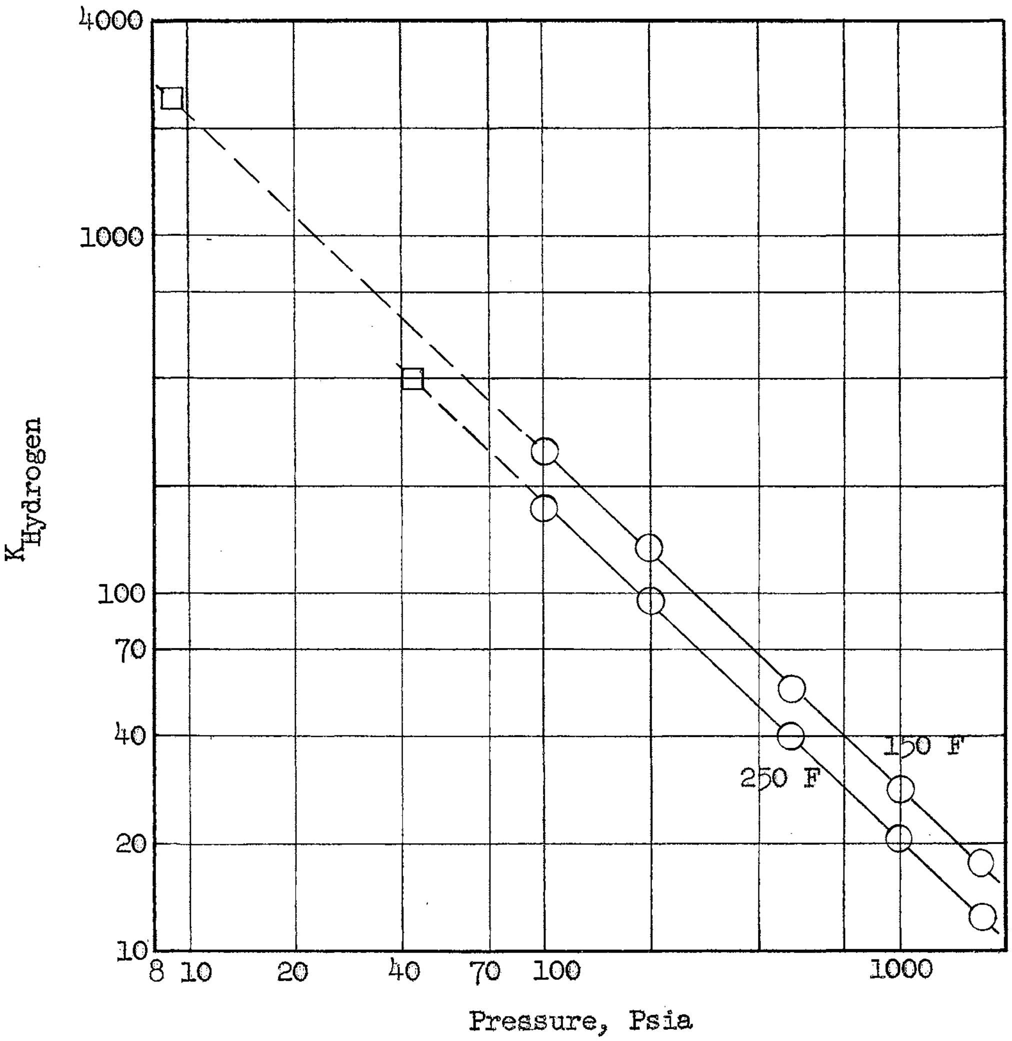

Figure 20

Extrapolation of K Values for Hydrogen in Cyclohexane

Data Comparisons

The available literature data are compared below with the experimental data of the present study. In order to make these comparisons, the literature data were plotted first as a function of pressure at constant temperature. Values were then read from these plots at convenient pressures.

Initial Comparison at 320 °F

Connolly (17) studied the hydrogen-benzene system at 320 to 500 °F, up to about 2300 psia, using the bubble- and dew-point method. The experimental part of Connolly's work was done very carefully, and the data appear to be very reliable. Connolly's data were tested by the Prausnitz-Keeler and infinite dilution tests, with good results in both cases.

Runs 4 through 7 were made at 320 °F in order to make a direct comparison with Connolly's work. Connolly's data were interpolated on large plots at the pressures of Runs 4 through 7. The comparison is shown in Table XX. The results appear to agree within the precision of the present data.

TABLE XX

COMPARISON OF BENZENE-HYDROGEN DATA AT 320 °F

Pressure, psia	K_{H2}	K_{H2}*	Per Cent Diff.**
427.2	49.3	50.3	-2.0
601.8	37.1	36.4	1.9
778.0	28.6	28.4	0.7
1309	17.6	17.3	1.7

TABLE XX (continued)

Pressure, psia	K_{BZ}	K_{BZ} *	Per Cent Diff.**
427.0	0.296	0.288	2.8
601.8	0.210	0.213	-1.4
778.0	0.172	0.172	0
1309	0.116	0.116	0

* Data of Connolly (17)
**Based on Connolly's data

Hydrogen-Benzene

Hydrogen solubilities in benzene at different temperatures are plotted in Figures 21 and 22. Inspection of these figures shows considerable scattering of the data. Connolly's data are smooth with respect to temperature and line up well with the data of the present work. Most of the earlier solubility data showed some scatter when plotted as a function of pressure at constant temperature. Figures 21 and 22 indicate similar scatter when the data are cross-plotted against temperature. This scatter, or lack of precision, seems to justify placing less confidence in the accuracy of these data.

The data of Ipatiev, et al. (39), for higher pressures, were smoother than other prior data, and cross-plot smoothly against temperature. The agreement of the latter data at 7000 and 10,000 psia with the present data is not perfect, but is gratifying when the difficulty of obtaining data at these pressures is considered.

The benzene data of Connolly and this work were compared by plotting the log of the benzene K values against reciprocal absolute temperature. The basis for this type of plot is the Clausius-Clapeyron equation. Paraffin hydrocarbon K values give almost straight lines when plotted in the above manner. Figure 23 shows good alignment of the

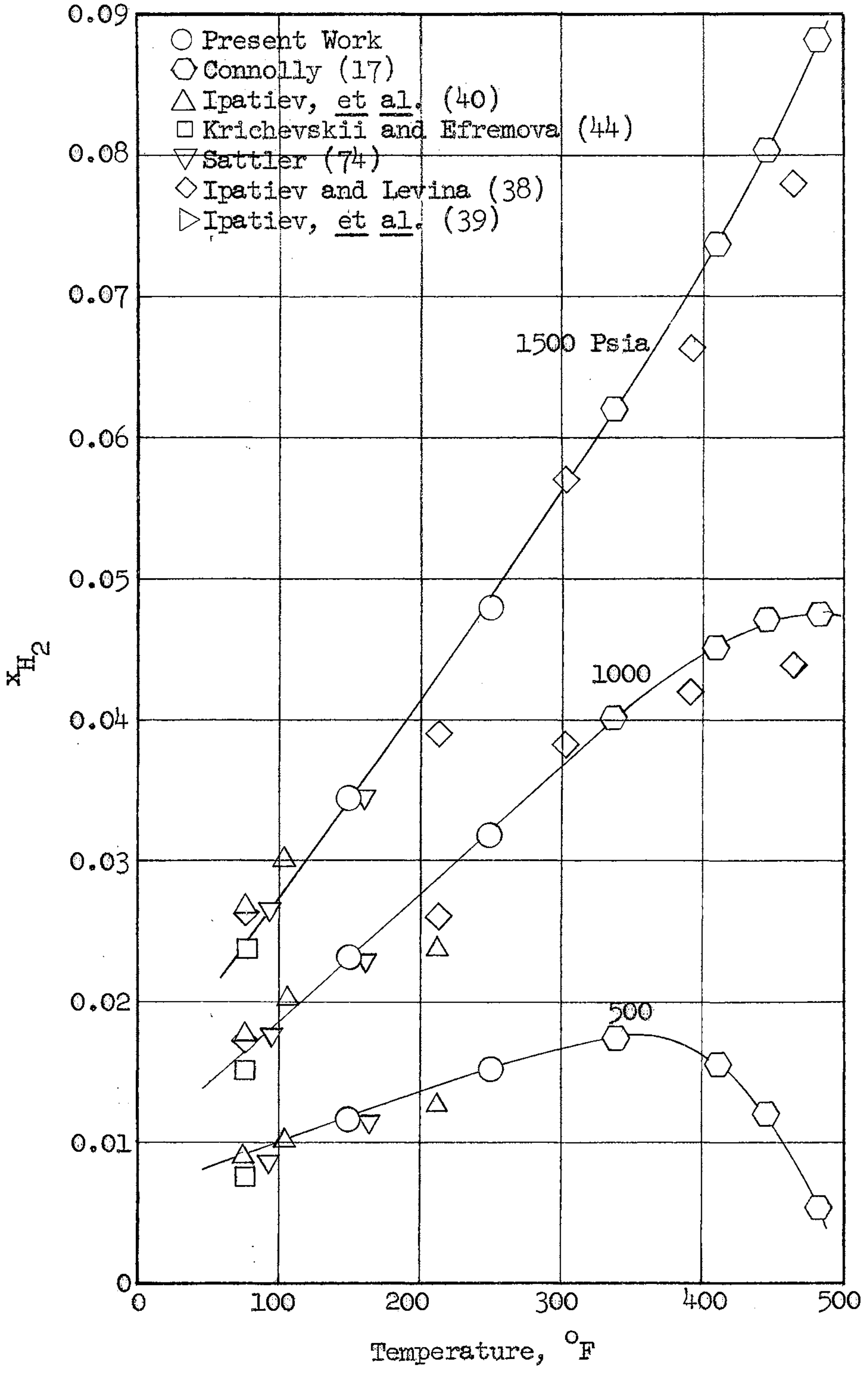

Figure 21

Comparison of Solubilities of Hydrogen in Benzene

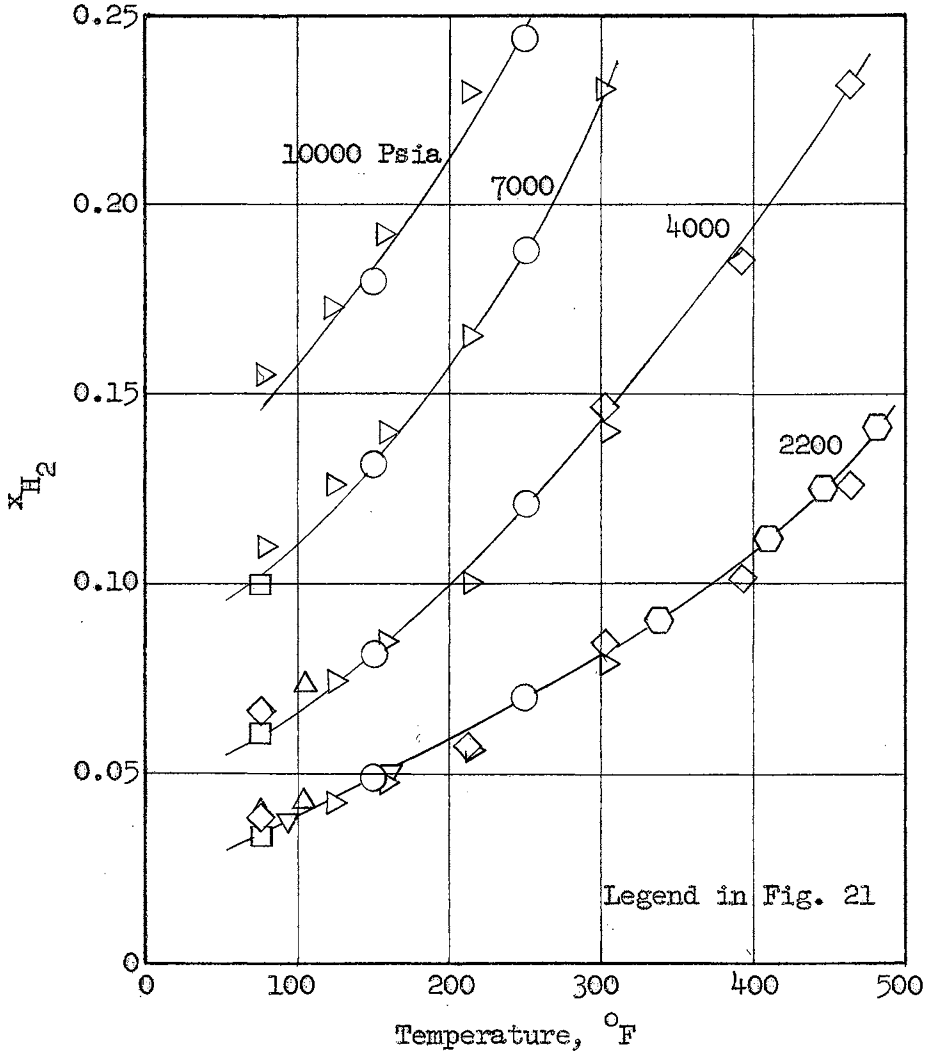

Figure 22

Comparison of Solubilities of Hydrogen in Benzene present data with Connolly's.

The only other previous vapor composition data were those of Ipatiev, et al. (39). The mole fraction of benzene in the vapor was plotted versus pressure on a log-log plot, Figure 24. The data show increasing divergence above 5000 psia. The presence of a consistent error in the high pressure benzene K data obtained in this work appears possible.

Hydrogen-Cyclohexane

The available solubility data for hydrogen in cyclohexane are plotted as a function of temperature in Figures 25 and 26. The consistency between the present data and that of Krichevskii and Sorina (45) is particularly evident, even at 10,000 psia.

Krichevskii and Sorina also obtained vapor compositions, which are compared with the present data in Figures 27 and 28. The low pressure 104 °F data of these authors were not consistent with the remainder of their own data, as is evident in Figure 27. This discrepancy disappeared at high pressures. The high pressure plots show a divergence between the present data and those of Krichevskii and Sorina above approximately 5000 psia. At lower pressures there is no apparent discrepancy.

Since the present vapor-phase compositions at high pressures seem to be low for both benzene and cyclohexane, the possibility of an error in these measurements must be considered. The dynamic method was used for all three studies involved in the comparisons at high pressure, the difference being in analysis method and amount of sample collected. Krichevskii and Sorina's data showed considerable

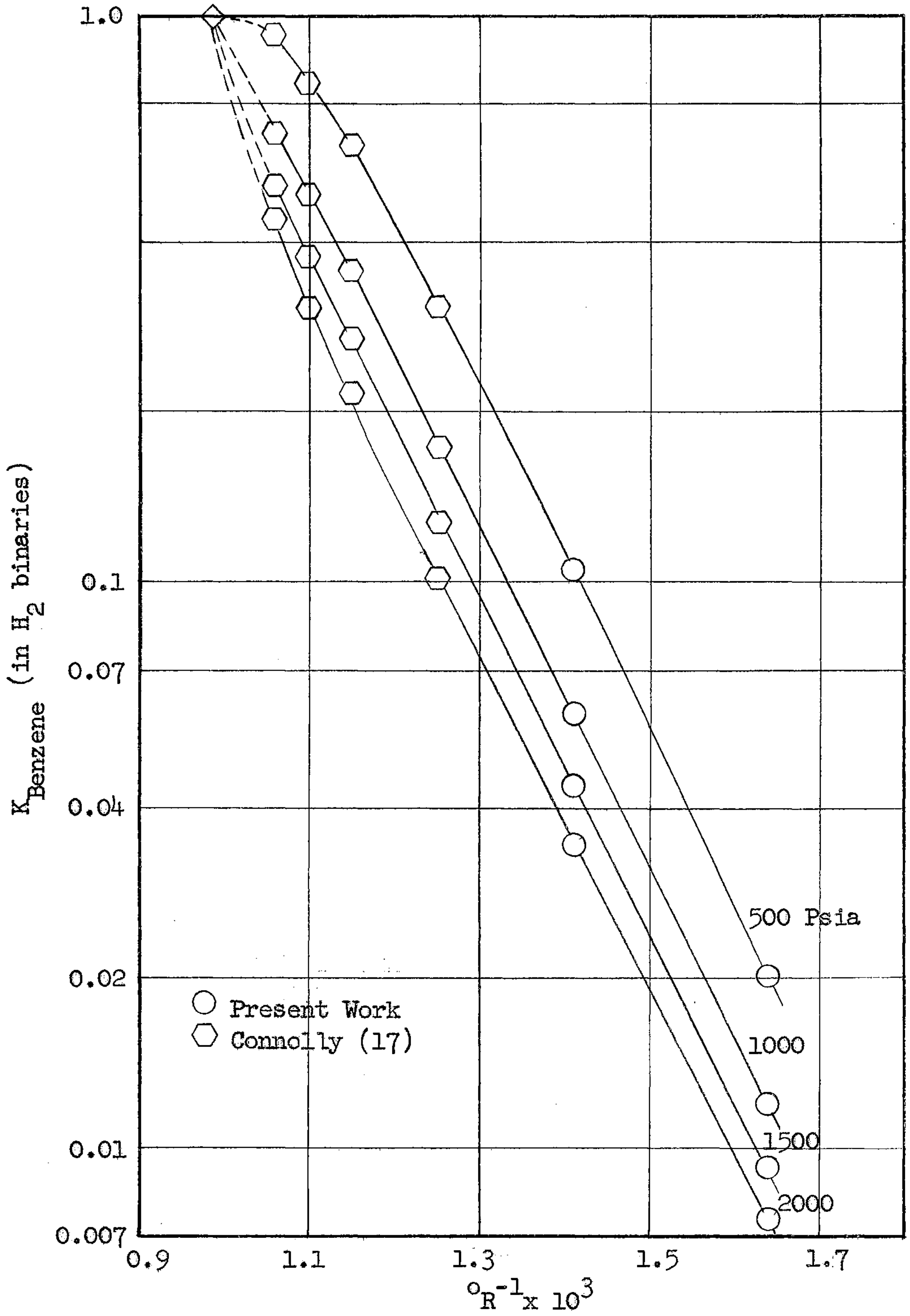

Figure 23

Comparison of Benzene K Values

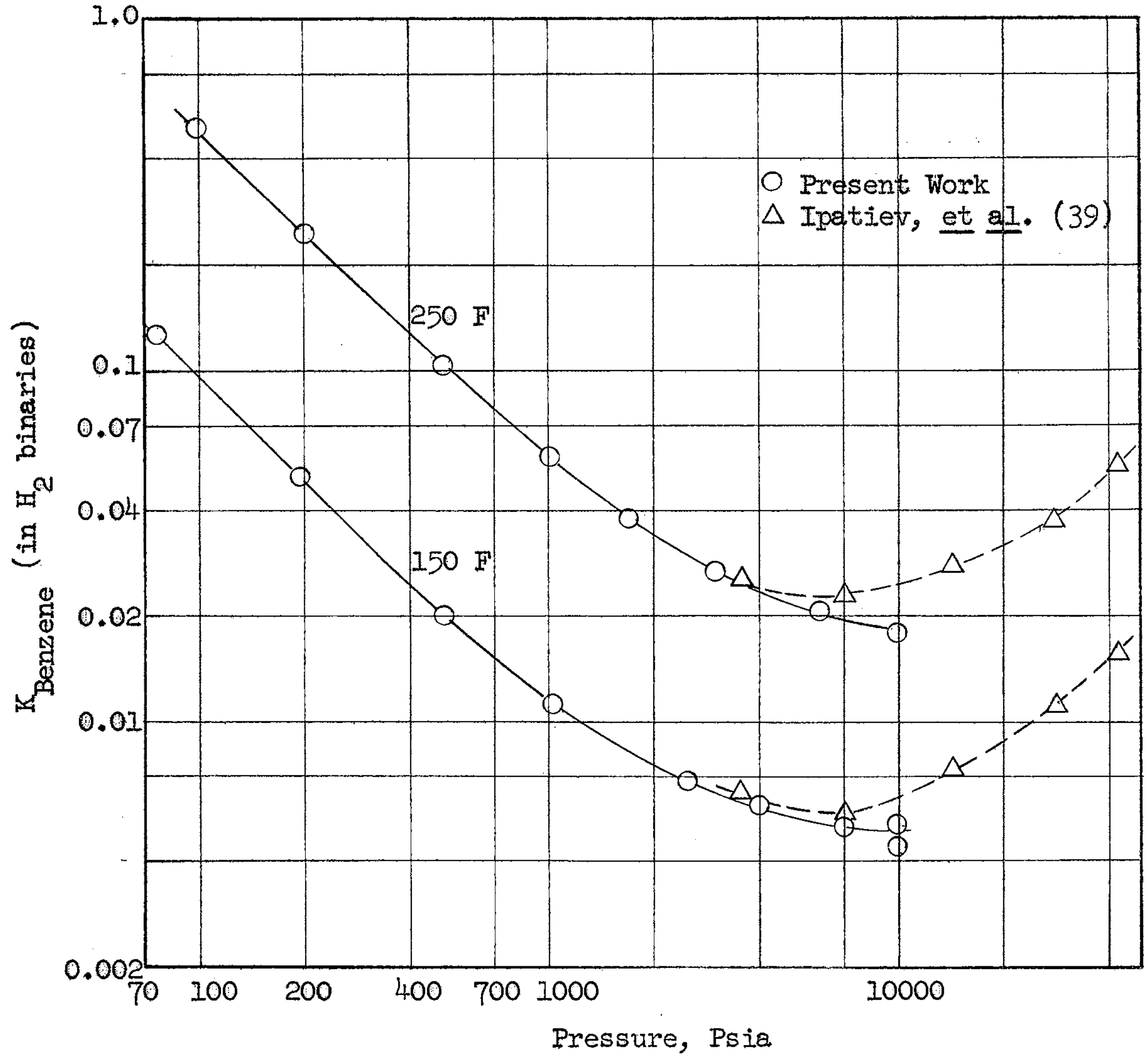

Figure 24

Comparison of Benzene Vapor Composition Data

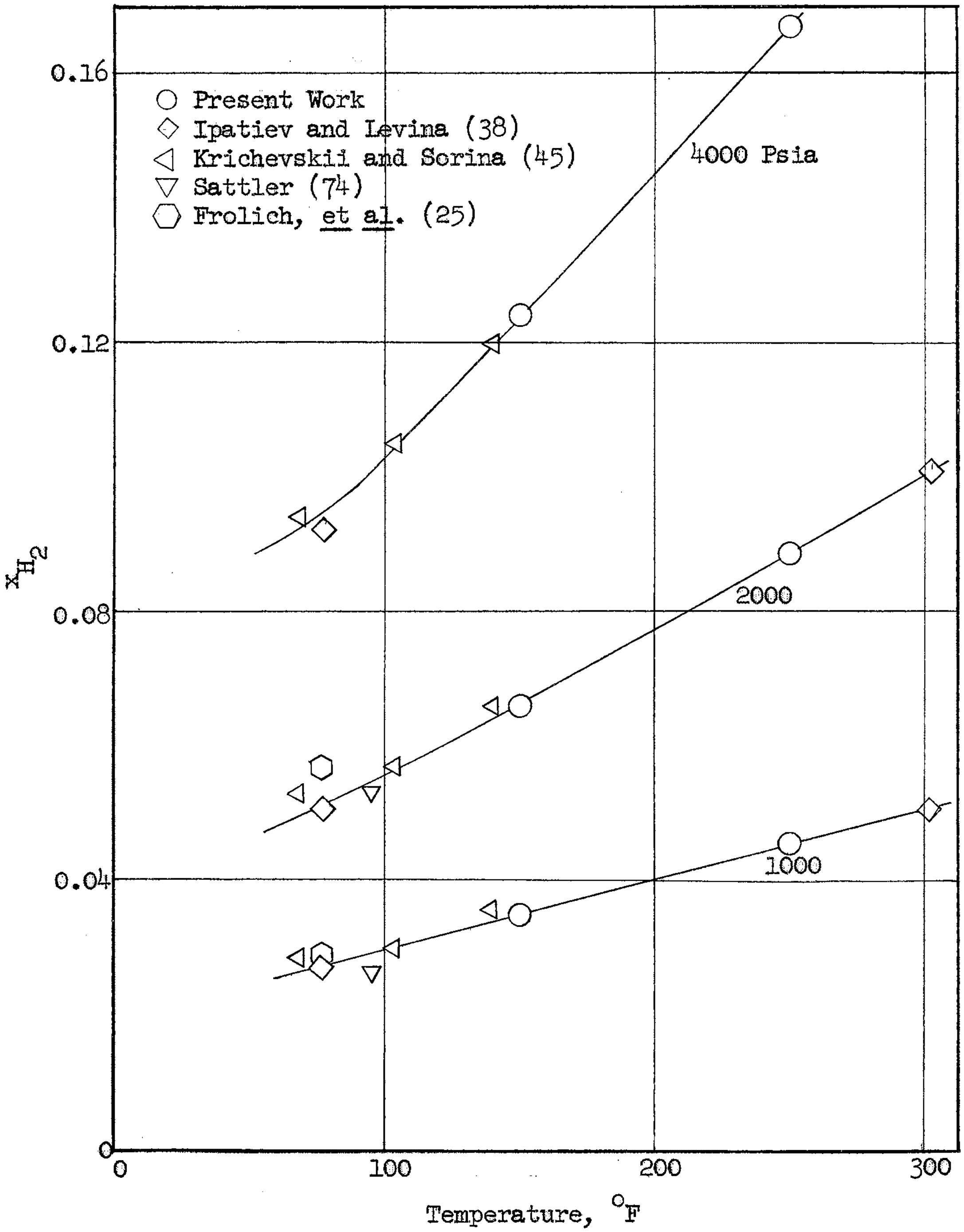

Figure 25

Comparison of Solubilities of Hydrogen in Cyclohexane

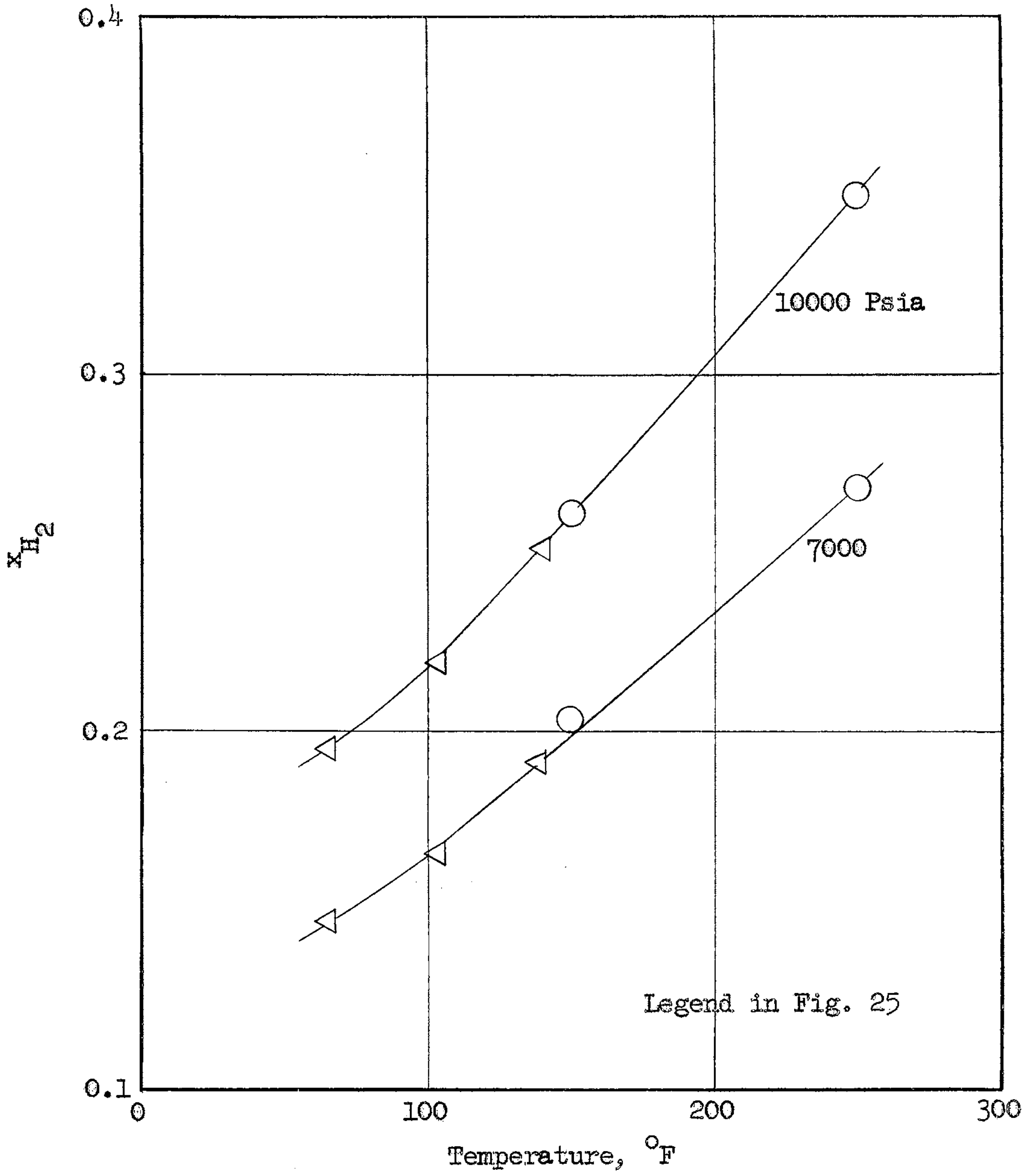

Figure 26

Comparison of Solubilities of Hydrogen in Cyclohexane

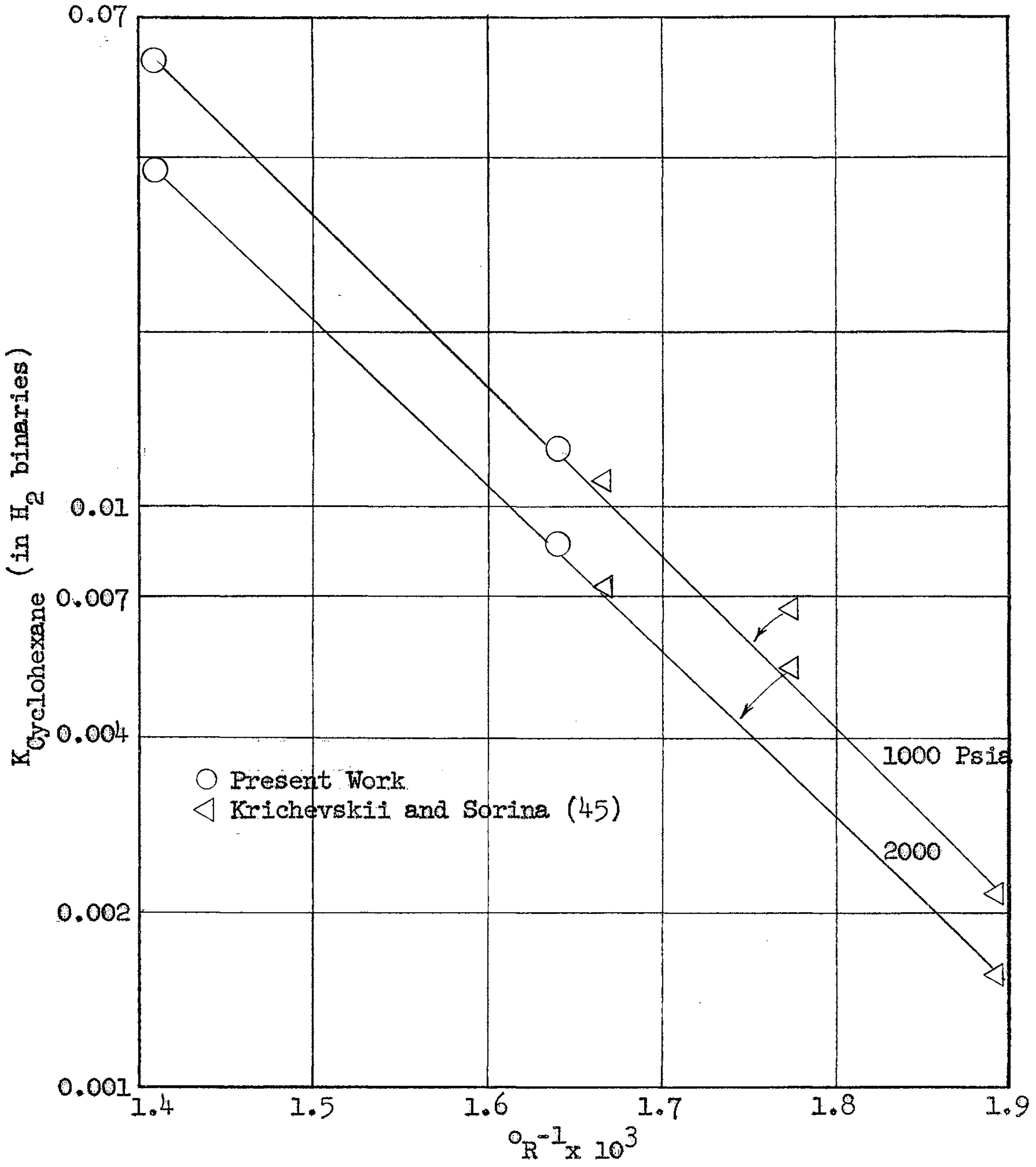

Figure 27

Comparison of Cyclohexane K Values

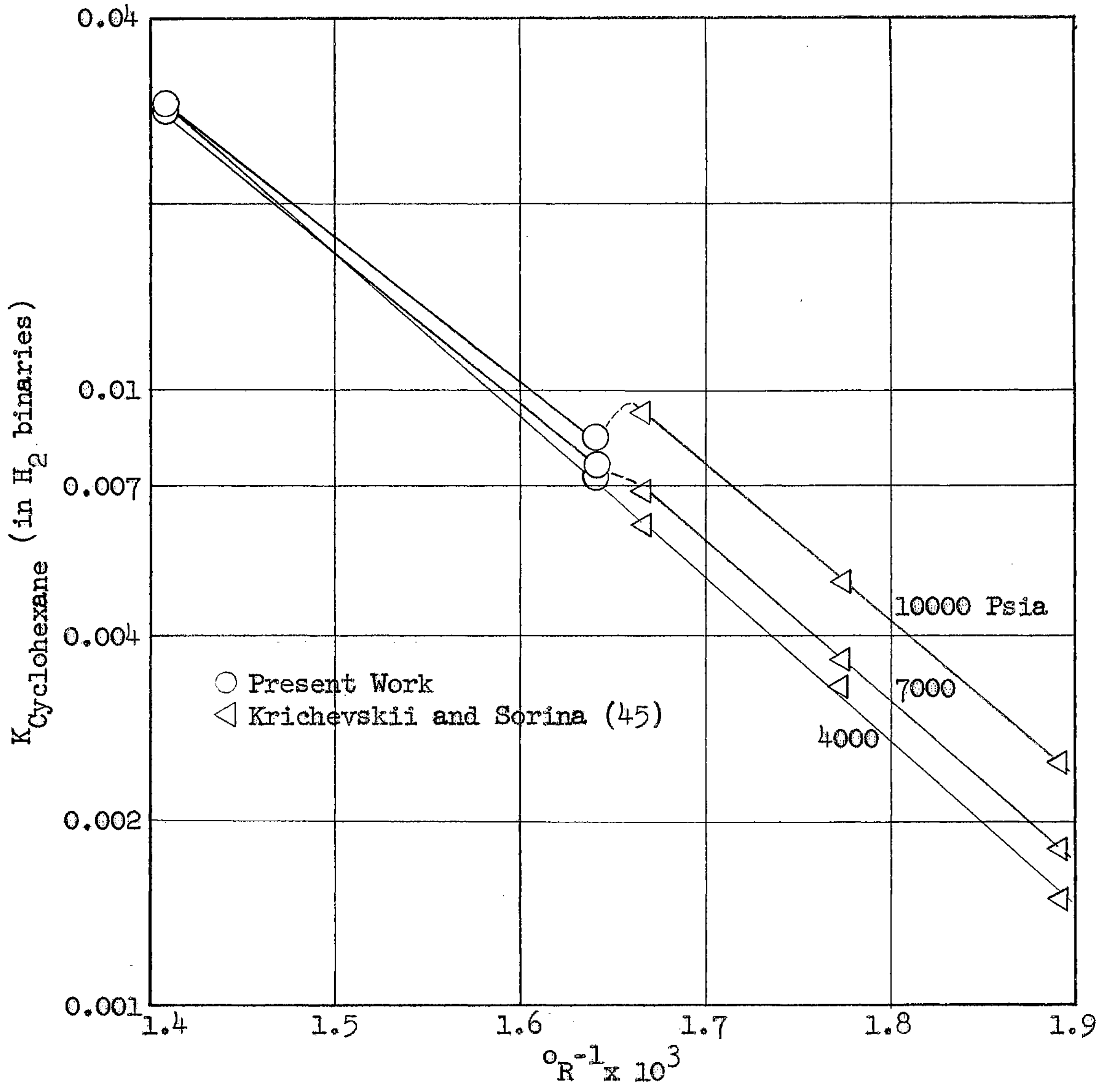

Figure 28

Comparison of Cyclohexane K Values

scatter at all pressures and could be in error. No definite conclusion may be drawn. The accurate determination of low vapor-phase hydrocarbon concentrations is difficult.

Correlation Work

The two types of correlations described in Chapter III were tried with the experimental data for the hydrogen-hydrocarbon binary mixtures considered in this work. The results are discussed below.

Regular Solution Correlations

The method of Chao and Seader (12) was applied to the experimental data for hydrogen with benzene, cyclohexane, and n-hexane. Comparisons of the calculated and experimental K-values for the hydrocarbons and hydrogen are presented in Tables XXI and XXII. All correlating parameters used were the same as in the original publication.

The average difference between calculated and experimental K-values for the hydrocarbons was 8.0 per cent. For hydrogen, the average difference was 14.3 per cent. Both of these are greater than the average differences claimed for the original correlation. However, the systems considered here are far from "normal," and larger differences might be expected.

As mentioned in Chapter III, an entropy correction can be made to the Scatchard-Hildebrand equation if the molal volumes of the components differ greatly. The corrected equation, as given by Hildebrand and Scott (31) is

TABLE XXI

COMPARISON OF CHAO-SEADER K VALUES WITH EXPERIMENTAL DATA FOR HYDROCARBONS WITH HYDROGEN

Solvent	Temp., °F	Pressure, psia	K Hydrocarbon Cal'd	K Hydrocarbon Expt.	o/o Diff.*
Benzene	150	76.39	.129	.128	0.8
		194.3	.0534	.0484	10.3
		503.1	.0235	.0205	14.6
		1026	.0139	.0116	19.8
		1707	.0103	.00884	17.0
	250	96.92	.461	.494	- 6.7
		201.0	.234	.249	- 6.0
		499.4	.106	.106	0
		1003	.0620	.0590	5.1
		1702	.0445	.0405	9.9
Cyclo-hexane	150	99.83	.0965	.0977	- 1.2
		199.9	.0508	.0480	5.8
		501.6	.0234	.0211	10.9
		995.9	.0145	.0124	16.9
		1694	.0107	.0092	16.3
	250	101.3	.412	.452	- 8.8
		199.9	.221	.239	- 7.5
		500.0	.101	.104	- 2.9
		999.9	.0612	.0592	3.4
		1700	.0447	.0409	9.3
n-Hexane	150	500	.0351	.0344	2.0
		1000	.0219	.0200	9.5
		2000	.0146	.0135	8.1
	250	500	.153	.150	2.0
		1000	.0939	.0871	7.8
		2000	.0629	.0590	6.6
				AVG.	± 8.0

* Based on experimental

TABLE XXII

COMPARISON OF CHAO-SEADER K VALUES WITH EXPERIMENTAL DATA FOR HYDROGEN

Solvent	Temp., °F	Pressure, psia	K Hydrogen Calc'd	K Hydrogen Expt	o/o Diff.*
Benzene	150	76.39	461	525	-12.2
		503.1	71.3	83.4	-14.5
		1026	35.6	41.5	-14.2
		2508	15.4	18.6	-17.2
		6998	6.58	7.57	-13.1
	250	96.92	233	272	-14.3
		499.4	46.7	58.4	-20.0
		1003	23.7	29.4	-19.4
		2999	8.4	10.4	-18.9
		5995	4.66	5.86	-20.5
Cyclohexane	150	99.83	219	249	-12.0
		501.6	44.2	53.9	-18.0
		995.9	22.7	28.6	-20.6
		3002	8.11	10.2	-20.5
		5996	4.56	5.59	-18.4
	250	101.3	147	173	-15.0
		500.0	30.9	40.0	-22.8
		999.9	15.8	20.7	-23.6
		3000	5.64	7.41	-23.9
		5996	3.12	4.15	-24.8
n-Hexane	150	500	30.3	29.3	3.4
		1000	15.5	15.6	- 0.6
		2000	8.07	8.45	- 4.5
		4000	4.38	4.66	- 6.0
		7000	2.83	2.83	0
	250	500	22.1	23.2	- 4.7
		1000	11.4	12.5	- 8.8
		2000	5.94	6.80	-12.6
		4000	3.23	3.75	-13.9
		7000	2.07	2.29	- 9.6
				AVG.	±14.3

* Based on experimental

$$\ln \gamma_1^L = \ln \frac{\overline{\Phi}_1}{x_1} + \overline{\Phi}_2 \; 1 - \frac{v_1^L}{v_2^L} + \frac{v_1^L}{RT} \; (\delta_i - \delta_{mix})^2, \qquad \text{(VI-12)}$$

$$\text{where } \Phi_1 = \frac{x_i \; v_i^L}{\sum_{j=1}^{2} (x_j \; v_j^L)}$$

Equation VI-12 was substituted for Equation III-31 in the Chao-Seader procedure. The K-values thus calculated for the hydrocarbons were hardly affected, while those for hydrogen showed even worse agreement with the experimental data than before. This result is not surprising in the light of the remarks of Chapter III. That is, the regular solution method is semi-empirical when applied to gas-liquid mixing.

The original Chao-Seader correlation embraced a very large amount of data, some 3000 points in all. If we confine our interest to the systems at hand, still retaining the basic framework of the Chao-Seader correlation, we can improve the agreement between the correlation and experimental data. This was done for the case of the hydrogen K-values. The results are shown in Table XXIII. Smoothed data were used in this work. The solubility parameter for hydrogen that produced the best fit of the data was 2.45, as compared with the Chao-Seader value of 3.25. Hypothetical liquid fugacity coefficients were obtained for hydrogen in this procedure and are listed in Table XXIV.

The range of data was limited to 2000 psia. The average difference between the computed and experimental hydrogen K values was lowered from 14.3 to 7.1 per cent. If the solubility parameter for cyclohexane were raised arbitrarily from the Chao-Seader value of 8.2 to a value of 8.4, the differences would have been reduced even further.

TABLE XXIII

RESULTS OF MODIFIED CHAO-SEADER CALCULATIONS FOR HYDROGEN

Solvent	Temp., °F	Pressure, psia	K_{H2} Calc'd	K_{H2} Expt	o/o Diff.*
Benzene	150	100	378	410	- 7.8
		500	87.1	84.0	3.7
		1000	45.8	42.3	8.3
		2000	24.2	22.4	8.0
	250	100	269	272	- 1.1
		500	59.5	58.0	2.6
		1000	31.2	29.6	5.4
		2000	16.1	15.1	6.6
Cyclohexane	150	100	218	249	-12.4
		500	50.5	54.5	- 7.3
		1000	20.5	28.6	- 7.3
		2000	15.0	15.0	- 6.7
	250	100	167	185	- 9.7
		500	37.6	40.0	- 6.0
		1000	19.5	20.7	- 5.8
		2000	10.1	10.7	- 5.6
n-Hexane	150	100	139	119	16.8
		500	31.9	29.3	8.9
		1000	16.8	15.6	7.7
		2000	8.90	8.45	5.3
	250	100	109	95.0	11.5
		500	25.1	23.2	8.2
		1000	13.3	12.5	6.4
		2000	6.86	6.80	0.9
				AVG.	±7.1

* Based on experimental

The basic Chao-Seader method correlates a wide variety of data fairly well. The above work for hydrogen binaries shows that limiting the data improves the correlation. It does not appear to be possible to retain both generality and high precision in this method.

TABLE XXIV

HYPOTHETICAL LIQUID FUGACITIES FOR HYDROGEN

Temp., °F	Pressure, psia	$\nu_{H_2}^{L}$ (Chao-Seader)	$\nu_{H_2}^{L}$ (Present Work)
150	100	71.2	48
	500	14.9	11.4
	1000	7.83	6.2
	2000	4.35	3.52
250	100	58.6	47
	500	12.2	10.5
	1000	6.44	5.7
	2000	3.58	3.15

Ideal K Value Correlation

The calculation of ideal K values for hydrogen was of particular interest in this work. The pure component liquid and vapor fugacities for pure hydrogen are functions of temperature and pressure only. Thus, the ideal K value for hydrogen should be the same in any solvent. It was hoped that ideal K values for hydrogen in the solvents benzene, cyclohexane, and n-hexane could be calculated by the procedure outlined in Chapter III. Several difficulties were encountered and the attempt was finally abandoned.

The first calculations were made using the Redlich-Kwong equation of state. Calculations for benzene-hydrogen at 250 °F gave liquid activity coefficients for benzene that were concave downward when plotted as ln γ_2^L vs. x_2. Gautreaux and Coates (26) have shown that $d\ln \gamma_2^L/dx_2$ must approach zero as x_2 approaches 1.0. The only way that the curve obtained could behave in this way is if there were a point of inflection at some value of x_2 less than 1.0. This behavior does not seem likely.

The virial equation of state was then used instead of the Redlich-Kwong equation. The derived liquid activity coefficients for the hydrocarbons showed a great deal of scatter and for some of the mixtures were never higher than 1.0. The cause of this behavior seemed to lie in the K values, although the fugacities calculated from the virial equation might be at fault. For gas-liquid equilibria at relatively low pressures, the mole fraction of the hydrocarbon is close to 1.0, and the liquid activity coefficients are also close to 1.0. Any slight error in composition influences greatly the liquid activity coefficients. Very precise values of γ_2^L are needed if an unambiguous fit is to be obtained for an equation such as the van Laar equation.

The only possible remedy seemed to be to smooth the K values carefully. Smoothing with the required precision cannot be done by hand. Curve-fitting the data would not be satisfactory either, because the mathematical model used for curve-fitting would automatically legislate the liquid activity coefficients. For the reasons outlined above, the ideal K value correlation method, at least in the form considered here, does not appear to be applicable to gas-liquid equilibria.

CHAPTER VII

CONCLUSIONS AND RECOMMENDATIONS

The subject matter of the present work has been the theoretical and experimental investigation of vapor-liquid equilibria. Experimental P-T-x-y data were obtained for the binary systems hydrogen-benzene and hydrogen-cyclohexane at temperatures of 150 and 250 °F, and at pressures from 76 to 10,000 psia. The equilibrium cell used was of the dynamic type.

The theoretical aspects of this thesis were primarily concerned with the evaluation and correlation of experimental vapor-liquid equilibrium data. Particular emphasis was made for the case of binary systems in which one component is a gas.

Major conclusions for the experimental part of the work are as follows:

1. The precision, or variability, of the experimental composition data is approximately ± 3 per cent.
2. The experimental data agree reasonably well with data of previous studies. The benzene-hydrogen data agree particularly well with the reliable data of Connolly at pressures up to 2200 psia. The concentration of hydrocarbon in the gas phase may be in error at pressures above 5000 psia, as indicated by comparison with the data of Ipatiev <u>et al</u>. and Krichevskii and Sorina.

3. The dynamic equilibrium cell used in this study is satisfactory for obtaining gas-liquid equilibria for binary mixtures. The main drawback of the experimental method is the long time required for equilibration at lower temperatures.
4. The use of the dynamic flow method for systems containing mixed liquids does not appear to be feasible, because the liquid-phase composition will change as the gas sample is removed. The method has been applied previously to the case in which a mixed gas is contacted with a single liquid component.

Major conclusions based on the theoretical part of the work are:

1. Rigorous thermodynamic consistency tests are just what the name implies, i.e., tests to determine the consistency between two different kinds of data. At constant temperature, volumetric data are compared with equilibrium concentration data. At constant pressure, calorimetric data are compared with equilibrium concentration data.
2. Presently-available equations of state are not entirely satisfactory because of arbitrary treatment required for mixtures. This problem is particularly important because of the close connection between volumetric and equilibrium data.
3. The thermodynamic consistency test in which isothermal K value data and compressibility data are compared (Adler's test) is of doubtful utility for gas-liquid systems. The method does not really test the liquid-phase concentration data and is

insensitive to changes in the vapor-phase concentration.

4. The present experimental data show fairly good self-consistency when tested by the method in which interaction second virial coefficients are calculated from equilibrium and pure component second virial coefficient data (Prausnitz-Keeler test). This consistency test also does not really test the liquid-phase concentration data.
5. The thermodynamic consistency test at infinite dilution indicates that the present experimental data are fairly reliable at low pressures.
6. Regular solution theory provides a convenient semi-empirical method of correlation for experimental gas-liquid equilibrium data.
7. The ideal K value method of correlating vapor-liquid equilibrium data does not appear to be applicable to the present data.

The following recommendations are made.

1. In future experimental work with the apparatus described here, several precautions should be observed:
    a. Adequate equilibration time should be provided.
    b. Vapor sample lines should be heated properly.
    c. Vapor samples should contain as much hydrocarbon as possible (by taking appropriately large samples).
    d. Absorption of hydrocarbon on stopcock grease should be eliminated.
    e. The temperature control should be improved and temperature gradients should be eliminated in the aluminum

block thermostat.

2. Equilibrium vapor and liquid densities should be determined if possible. Vapor densities will provide some basis for judging the applicability of equations of state.

LITERATURE CITED

1. Adams, L. H., "Equilibrium in Binary Systems Under Pressure. I. An Experimental and Thermodynamic Investigation of the System, NaCl-H_2O, at 25°C," J. Am. Chem. Soc. 53, 3769 (1931).

2. Adler, S. B., L. Friend, R. L. Pigford, and G. M. Rosselli, "Thermodynamic Consistency of Vapor-Liquid Equilibrium Data When One Component Is Above Its Critical Temperature," A. I. Ch. E. Journal 6, 104 (1960).

3. Akers, W. W., J. F. Burns, and W. R. Fairchild, "Low-Temperature Phase Equilibria," Ind. Eng. Chem. 46, 2531 (1954).

4. Akers, W. W., D. M. Kehn, and C. H. Kilgore, "Volumetric and Phase Behavior of Nitrogen-Hydrocarbon Systems," Ind. Eng. Chem. 46, 2536 (1954).

5. Aroyan, H. J., and D. L. Katz, "Low-Temperature Vapor-Liquid Equilibria in Hydrogen-n-Butane System," Ind. Eng. Chem. 43, 185 (1951).

6. Barr-David, F. H., "Vapor-Liquid Equilibrium at High Pressures. Systems: Ethanol-Water and 2-Propanol-Water," Ph. D. Thesis, Yale University (1956).

7. Benedict, M., G. B. Webb, and L. C. Rubin, "Fugacities and Liquid-Vapor Equilibria," Chem. Eng. Prog. 47, 449 (1951).

8. Bird, R. B., E. L. Spotz, and J. O. Hirschfelder, "The Third Virial Coefficient for Non-Polar Gases," J. Chem. Phys. 18, 1395 (1950).

9. Black, C., "Vapor Phase Imperfections in Vapor-Liquid Equilibria," Ind. Eng. Chem. 50, 391 (1958).

10. Blade, E., "Calibration of Weights," Ind. Eng. Chem., Anal. Ed. 11, 499 (1939).

11. Boomer, E. H., C. A. Johnson, and G. H. Argue, "Equilibria in Two-Phase Gas-Liquid Hydrocarbon Systems," Can. J. Research 16B, 319 (1938).

12. Chao, K. C., and J. D. Seader, "General Correlation of Vapor-Liquid Equilibria in Hydrocarbon Mixtures," A.I.Ch.E. Journal 7, 598 (1961).

13. Comings, E. W., High Pressure Technology, McGraw-Hill Book Co., Inc., New York (1956).

14. Condon, E. V., and H. Odishaw, Handbook of Physics, McGraw-Hill Book Co., Inc., New York (1958).

15. Connolly, J. F., "Hydrogen-Hydrocarbon Interaction Virial Coefficients," Notes for Applied Thermodynamics Conference, Oklahoma State University, Stillwater, Oklahoma (1961).

16. Connolly, J. F., "Partial-Molar Volumes and Thermodynamic Properties of Hydrogen in Liquid Hydrocarbon Solutions," Notes for Applied Thermodynamics Conference, Oklahoma State University, Stillwater, Oklahoma (1961).

17. Connolly, J. F., "Thermodynamic Properties of Hydrogen in Benzene Solutions," J. Chem. Phys. 36, 2897 (1962).

18. Connolly, J. F., and G. A. Kandalic, "Virial Coefficients and Intermolecular Forces of Hydrocarbons," Phys. Fluids 3, 463 (1960).

19. David, H. G., S. D. Hamann, and R. B. Thomas, "The Second Virial Coefficients of Some Cyclic Hydrocarbons," Australian J. Chem. 12, 309 (1959).

20. Dean, M. R., and J. W. Tooke, "Vapor-Liquid Equilibria in Three Hydrogen-Paraffin Systems," Ind. Eng. Chem. 38, 389 (1946).

21. Digest of Literature on Dielectrics, Vol. 25, National Academy of Science - National Research Council, Washington, D. C. (1961).

22. Dodge, B. F., Chemical Engineering Thermodynamics, McGraw-Hill Book Co., Inc., New York (1944).

23. Edmister, W. C., Applied Hydrocarbon Thermodynamics, Gulf Publishing Co., Houston, Texas (1961).

24. Edmister, W. C., R. E. Thompson, and A. N. Stuckey, "Method for Predicting Vapor-Liquid K-Values by Charts or Computers," Proceedings of the Forty-First Annual Convention of the Natural Gas Processors Association, 20 (1962).

25. Frolich, P. K., E. J. Tauch, J. J. Hogan, and A. A. Peer, "Solubility of Gases in Liquids at High Pressure," Ind. Eng. Chem. 23, 548 (1931).

26. Gautreaux, M. F., and J. Coates, "Activity Coefficients at Infinite Dilution," A.I.Ch.E. Journal 1, 496 (1955).

27. Gibbs, J. W., Collected Works, Vol. I, Longmans, Green, and Co., New York (1928).

28. Glanville, J. W., and B. H. Sage, "Volumetric Behavior of Benzene," *Ind. Eng. Chem.* *41*, 1272 (1949).

29. Granet, I., "Physical Properties of Hydrogen," *Petrol. Refiner* *33*, No. 5, 205 (1954).

30. Hala, E., J. Pick, V. Fried, and O. Vilim, *Vapor-Liquid Equilibrium*, Pergamon Press, New York (1958).

31. Hildebrand, J. H., and R. B. Scott, *Solubility of Nonelectrolytes*, Reinhold Publishing Corp., New York (1950).

32. Hildebrand, L. H., and S. E. Wood, "The Derivation of Equations for Regular Solutions," *J. Chem. Phys.* *1*, 817 (1933).

33. Hipkin, H., "Experimental Measurement of Vapor-Liquid Equilibria," Notes for Conference on Vapor-Liquid Phase Equilibria, Oklahoma State University, Stillwater, Oklahoma (1959).

34. Hirschfelder, J. O., C. F. Curtiss, and R. B. Bird, *Molecular Theory of Gases and Liquids*, John Wiley and Sons, Inc., New York (1954).

35. Hoffman, D. S., J. H. Weber, V. N. P. Rao, and J. R. Welker, "Vapor Phase Activity Coefficients and Standard State Hypothetical Vapor Fugacities," Paper Presented at Seventeenth Annual Oklahoma Tri-Sectional A.I.Ch.E. Meeting, Norman, Oklahoma (1962).

36. Hoffman, D. S., J. R. Welker, R. E. Felt, and J. H. Weber, "Liquid Phase Activity Coefficients and Standard State Hypothetical Liquid Fugacities for Hydrocarbons," *A.I.Ch.E. Journal* *8*, 508 (1962).

37. Ibl, N. V., and B. F. Dodge, "Note on the Duhem Equation," *Chem. Eng. Sci.* *2*, 120 (1953).

38. Ipatiev, V. V., and M. I. Levina, "Equilibrium between Liquids and Gases at High Pressures and Temperatures. I. Solubility of Hydrogen in Individual Hydrocarbons of the Aromatic and Naphthenic Series," *Zhur. Fiz. Khim.* *6*, 632 (1935).

39. Ipatiev, V. V., V. P. Teodorovitch, A. P. Brestkin, and V. S. Artemovich, "The Region of Ultrahigh Pressures. I. Equilibrium between Liquid and Vapor in the System Hydrogen-Benzene at Pressures up to 3000 Atm.," *Chem. Abstr.* *42*, 8610 (1948).

40. Ipatiev, V. V., V. P. Teodorovitch, and I. M. Levine, "Solubility of Hydrogen and Natural Gas in Oils at High Operating Temperature and Pressure," *Oil Gas J.* *32*, No. 20, 14 (1933).

41. Kay, W. B., "Liquid-Vapor Phase Equilibrium Relations in the Ethane-n-Heptane System," *Ind. Eng. Chem.* *30*, 459 (1938).

42. Kay, W. B., and G. M. Rambosek, "Liquid-Vapor Equilibrium Relations in Binary Systems: Propane-Hydrogen Sulfide Systems," *Ind. Eng. Chem. 45*, 221 (1953).

43. Keenan, J. H., and F. G. Keyes, *Thermodynamic Properties of Steam*, John Wiley and Sons, Inc., New York (1936).

44. Krichevskii, I. R., and G. D. Efremova, "Phase and Volume Relations in Liquid-Gas Systems at High Pressures," *Zhur. Fiz Khim. 22*, 1116 (1948).

45. Krichevskii, I. R., and G. A. Sorina, "Phase and Volume Relations in Liquid-Gas Systems at High Pressures. VI. The Cyclohexane-Hydrogen System," *Zhur. Fiz. Khim. 32*, 2080 (1958).

46. Leland, T. W., Jr., J. J. McKetta, Jr., and K. A. Kobe, "Phase Equilibria in 1-Butene-Water System and Correlation of Hydrocarbon-Water Solubility Data," *Ind. Eng. Chem. 47*, 1265 (1955).

47. Lindroos, A. E., and B. F. Dodge, "Phase Equilibria at High Pressures. The System: Nitrogen-Ammonia above 1000 Atmospheres." *Chem. Eng. Prog. Symp. Series 48*, 10 (1952).

48. Linke, W. F., *Solubilities of Inorganic and Metal Organic Compounds*," 4th Ed., Vol. 1, D. Van Nostrand Co., Inc., New York (1958).

49. Lydersen, A. L., R. A. Greenkorn, and O. A. Hougen, *Generalized Thermodynamic Properties of Pure Fluids*, Engineering Experiment Station, University of Wisconsin, Report No. 4 (1955).

50. Michels, A., "Accuracy and Sensitivity of a Pressure Balance with a So-Called Amagat Cylinder," *Ann. Physik (Series 4) 73*, 577 (1924).

51. Michels, A., G. F. Skelton, and E. M. L. Dumoulin, "Gas-Liquid Phase Equilibrium in the System Ammonia-Hydrogen-Nitrogen," *Physica 25*, 840 (1959).

52. Mickley, H. S., T. K. Sherwood, and C. E. Reed, *Applied Mathematics in Chemical Engineering*, McGraw-Hill Book Co., Inc., New York (1957).

53. Natural Gasoline Supply Men's Association, *Engineering Data Book*, 7th Ed., Tulsa, Oklahoma (1957).

54. Nichols, W. B., H. H. Reamer, and B. H. Sage, "Volumetric and Phase Behavior in the Hydrogen-Hexane System," *A.I.Ch.E. Journal 3*, 262 (1957).

55. Paauwe, J., Private Communication (1962).

56. Perry, J. H., Chemical Engineers Handbook, 2nd Ed., McGraw-Hill Book Co., Inc., New York (1940).

57. Peter, S., and K. Reinhartz, "Phase Equilibrium in the Systems H_2-n-Heptane, H_2-Methylcyclohexane, and H_2-2,2,4-Trimethylpentane at Elevated Pressures and Temperatures," Z. Physik. Chem. 24, 103 (1960).

58. Pitzer, K. S., et al., "The Volumetric and Thermodynamic Properties of Fluids," J. Am. Chem. Soc. 77, 3427 (1955).

59. Prausnitz, J. M., "Regular Solution Theory for Gas-Liquid Solutions," A.I.Ch.E. Journal 4, 269 (1958).

60. Prausnitz, J. M., "Fugacities in High-Pressure Equilibria and in Rate Processes," A.I.Ch.E. Journal 5, 3 (1959).

61. Prausnitz, J. M., "Hypothetical Standard States and the Thermodynamics of High-Pressure Phase Equilibria," A.I.Ch.E. Journal 6, 78 (1960).

62. Prausnitz, J. M., and P. R. Benson, "Solubility of Liquids in Compressed Hydrogen, Nitrogen, and Carbon Dioxide," A.I.Ch.E. Journal 5, 161 (1959).

63. Prausnitz, J. M., and P. R. Benson, "Effective Collision Diameters and Correlation of Some Thermodynamic Properties of Solutions," A.I.Ch.E. Journal 5, 301 (1959).

64. Prausnitz, J. M., W. C. Edmister, and K. C. Chao, "Hydrocarbon Vapor-Liquid Equilibria and Solubility Parameter," A.I.Ch.E. Journal 6, 214 (1960).

65. Prausnitz, J. M., and R. N. Keeler, "Application of the Kihara Potential to High Pressure Phase Equilibria," A.I.Ch.E. Journal 7, 399 (1961).

66. Rao, V. N. K., D. R. Swami, and M. N. Rao, "Vapor-Liquid Equilibrium of Benzene-n-Hexane and Benzene-Cyclohexane Systems," A.I.Ch.E. Journal 3, 191 (1957).

67. Reamer, H. H., and B. H. Sage, "Phase Equilibrium in Hydrocarbon Systems. Volumetric Behavior of Cyclohexane," J. Chem. Eng. Data 2, 9 (1958).

68. Redlich, O., and J. N. S. Kwong, "On the Thermodynamics of Solutions. V. An Equation of State. Fugacities of Gaseous Solutions," Chem. Revs. 44, 233 (1949).

69. Rigas, T. J., D. F. Mason, and G. Thodos," Vapor-Liquid Equilibria. Microsampling Technique Applied to a New Variable Volume Cell," Ind. Eng. Chem. 50, 1297 (1958).

70. Roberts, L. R., and J. J. McKetta, "Vapor-Liquid Equilibrium in the n-Butane-Nitrogen System," A.I.Ch.E. Journal 7, 173 (1961).

71. Robinson, C. S., and E. R. Gilliland, Elements of Fractional Distillation, 4th Ed., McGraw-Hill Book Co., Inc., New York (1950).

72. Rossini, F. D., et al., Selected Values of Physical and Thermodynamic Properties of Hydrocarbons and Related Compounds, Carnegie Institute of Technology, Pittsburgh (1953).

73. Sage, B. H., B. L. Hicks, and W. N. Lacey, "The Methane-n-Butane System in the Two-Phase Region," Ind. Eng. Chem. 32, 1085 (1940).

74. Sattler, H. "The Solubility of Hydrogen in Liquid Hydrocarbons," Chem. Abstr. 36, 18 (1942).

75. Scatchard, G., "Change of Volume on Mixing and the Equations for Non-Electrolyte Mixtures," Trans. Far. Soc. 33, 160 (1937).

76. Silver, H. F., "Vapor-Liquid Equilibrium Ratios in Hydrogen-Hydrocarbon Mixtures," Ph. D. Thesis, University of Michigan (1961).

77. Stewart, D. E., B. H. Sage, and W. N. Lacey, "Volumetric Behavior of Hexane in the Liquid Phase," Ind. Eng. Chem. 46, 2529 (1954).

78. Stuckey, A. N., "On the Development of an Ideal K-Value Correlation for Hydrocarbons and Associated Gases," M. S. Thesis, Oklahoma State University (1963).

79. Taylor, H. S., and S. Glasstone, A Treatise on Physical Chemistry, 3rd Ed., Vol. 2, D. Van Nostrand Co., Inc., New York (1951).

80. Watanabe, K., "Ionization Potentials of Some Molecules," J. Chem. Phys. 26, 542 (1957).

81. Wooley, H. W., R. B. Scott, and F. G. Brickwedde, "Compilation of Thermal Properties of Hydrogen," J. Research Nat. Bur. Standards 41, 379 (1948).

APPENDIX A

CALIBRATION OF PRESSURE BALANCE AND MEASURING CYLINDERS

The Michels pressure balance and measuring cylinders were calibrated by the Meetinstituut Bemetel-T.N.O., Amsterdam (The Dutch Bureau of Standards). The technique used is described briefly below (55). In practice, a master balance is calibrated and periodically checked by the calibration procedure. Other balances are calibrated against the master balance. Each measuring cylinder is used for a relatively short pressure range in order that the effective piston area will be constant within the stated accuracy. In this way corrections due to pressure on the piston and cylinder are avoided.

At all pressures the effective area of a piston is determined by back-calculation.

$$A = \frac{F}{P}$$

where A = effective piston area

F = force acting on the effective piston area

P = pressure acting against the piston

Frictional effects are eliminated in the pressure balance by means of (1) careful levelling of the balance, (2) a controlled oil leak between the piston and cylinder, (3) rotation of the piston and weights by means of a special drive assembly designed to impart negligible sidewise thrust to the piston, (4) loading the weights below the piston, rather than above it, and (5) stabilizing the weight axle by use of a lubricated guide pin at the bottom.

The force acting on the effective piston area is determined from the calibrated weights used on the balance. The pressure is determined at low pressures by measuring the height of mercury in an open column that is connected to the balance via a pressure bench.

At higher pressures a 22-meter mercury column is used in conjunction with a piezometer. The piezometer is filled with nitrogen to a pressure at which the effective area has been determined previously. The weights on the balance are adjusted until the mercury in the piezometer just touches an electrical contact. The mercury column is then interposed between the balance and the piezometer. Weights are added until the mercury in the piezometer again touches the contact. The new pressure can be calculated and the effective areas obtained. In all the above measurements the mercury column and piezometer temperatures are carefully measured and regulated, and corrections are made for oil heights.

Table A-I shows the calibrated weights (masses, actually) of the various rotating parts of the pressure balance. Table A-II lists the effective area and weights for each of the measuring cylinders. In addition to these data, Bemetel-T.N.O. determined that the area of the guide pin is 1.76 sq cm and that the height of oil above the bottom of the guide pin is equal to the oil reservoir height plus 1.6 cm. All measurements refer to operation at 20°C with the piston height indicator at 10 on the scale. Pressures are referred to the center-line of the oil outlet on the measuring cylinder.

TABLE A-I

PRESSURE BALANCE WEIGHT CALIBRATIONS

Item	Mass
Indicator axis plus indicator	0.9957 Kg_m
Cone	0.2468
Oil shield	1.6542
Weight pan	0.6090
Lowest weight with axis of suspension	29.7729
Weight No. 1	25.0131
" " 2	25.0120
" " 3	25.0151
" " 4	25.0138
" " 5	25.0139
" " 6	25.0166
" " 7	25.0141
" " 8	25.0161
" " 9	10.0053
" " 10	5.0005
" " 11	5.0061
" " 12	0.9974
" " 13	1.0036
" " 14	1.0042
" " 15	1.0046
" " 16	1.0044

TABLE A-II

MEASURING CYLINDER CALIBRATIONS

Range of Cylinder	Effective Area	Mass of piston, claw, nut and half-rings
3-20 Kg_m/cm^2	12.512±0.001 cm^2	1.4095 Kg_m
20-50	5.0058±0.0004	0.8817
50-125	2.0004±0.0001	0.6719
125-300	0.83393±0.00004	0.5913
300-600	0.41938±0.00002	0.5598
600-1000	0.24461±0.00001	0.5173

APPENDIX B

CALIBRATION OF GAS COMPRESSOR LEVEL

The pressure in the gas compressor is different than that at the centerline of the measuring cylinder oil outlet due to differences in oil and mercury head. The apparatus shown in Fig. B-1 was used to calibrate the gas compressor level indicator reading as a function of the mercury heights. The manometer was hooked up so as to indicate the position of the mercury inside the gas compressor. Both the upper compartment of the compressor and one leg of the manometer were open to the atmosphere. The levels were measured with a cathetometer. Oil was pumped into the compressor to change the level. The data are given in Table B-I.

From the diagram, Fig. B-1, the pressure at the surface of the mercury in the gas compressor is seen to be

$$P_3 = P_1 + (H_1 - H_2)\,\rho'_{oil} - (H_3 - H_2)\,\rho'_{Hg}, \tag{B-1}$$

$$\text{or } P_3 \equiv P_1 - \Delta P, \tag{B-2}$$

where H = height of interface

ρ' = specific weight of fluid

A plot of the data showed a linear relation between the mercury levels and the level indicator reading. The data were fitted by least squares to obtain

$$H_2 = 32.47 - 0.2536\ h \quad \text{cm} \tag{B-3}$$

$$H_3 = 48.31 - 0.2611\ h \quad \text{cm} \tag{B-4}$$

where h = gas compressor level indicator reading.

The density of the oil was found to be 0.876 gm/cm^3. The mercury density is 13.54 gm/cm^3 at 22.5 C. Then

$$\rho'\text{oil} = 0.876\ \frac{\text{gm}}{\text{cm}^3} \times 0.9991\ \frac{\text{gf}}{\text{gm}} = 0.875\ \text{gf/cm}^3$$

$$\rho'\text{Hg} = 13.54 \times 0.9991 = 13.53\ \text{gf/cm}^3$$

The ΔP term must be multiplied by 0.01422 to convert from gf/cm^2 to psia. Thus

$$\begin{aligned} \Delta P = &\Big\{\big[(32.47 - 0.2536\ h) - 82.40\big]\big[\,0.875\,\big] \\ &+ \big[(48.31 + 0.2611\ h) - (32.47 - 0.2536\ h)\big]\big[\,13.53\,\big]\Big\}(0.01422) \\ = &\ 2.427 + 0.09587\ h \quad \text{psia} \end{aligned} \tag{B-5}$$

Equation B-5 is used to calculate the pressure correction from the gas compressor level.

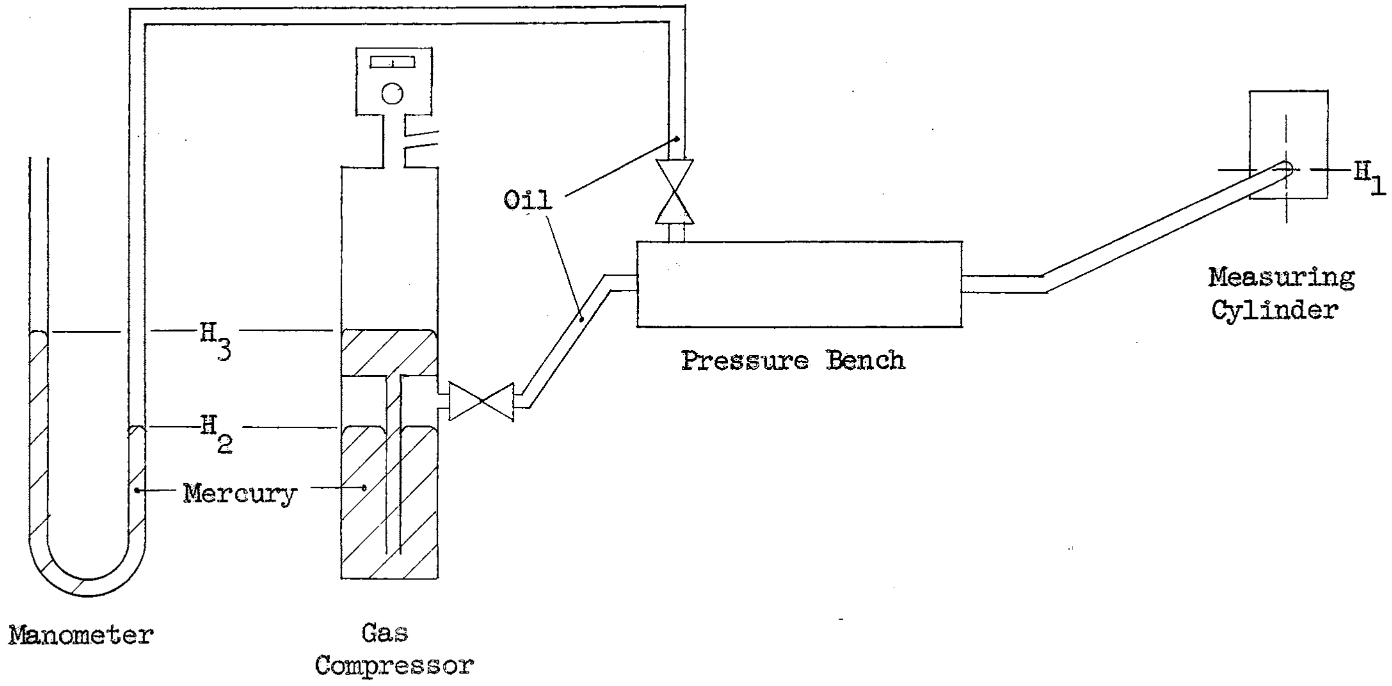

Figure B-1

Gas Compressor Level Calibration Apparatus

TABLE B-I

EXPERIMENTAL DATA FOR CALIBRATION OF GAS COMPRESSOR LEVEL

Room Temp. 22.5°C

Gas Compressor Level Indicator Reading	Manometer Heights in cm	
	Low Side	High Side
17.4	28.08	52.73
25.8	25.92	54.99
33.1	23.98	57.02
40.8	21.95	59.12
49.4	19.81	61.37
57.6	17.79	63.48
66.2	15.60	65.70
72.4	14.10	67.30
79.0	12.39	69.01
83.0	11.31	70.10
89.8	9.67	71.78
95.2	8.30	73.17
100.2	7.08	74.38
19.9	27.53	53.40
18.2	28.07	52.87
23.3	26.58	54.38
37.7	22.90	58.19
61.9	16.80	64.50

Centerline of measuring cylinder oil outlet, 82.40 cm.

APPENDIX C

CALIBRATION OF THERMOCOUPLE

The Chromel-Constantan thermocouple used in this work was calibrated by comparison with a Leeds and Northrup Model 8163 platinum resistance thermometer (Serial No. 1576919). The platinum resistance thermometer was calibrated by the National Bureau of Standards at the oxygen, ice, steam, and sulfur points at a current of 2.0 ma. The calibration data furnished by N. B. S. are as follows:

$$t\ (^{\circ}C) = \frac{R_t - R_o}{\alpha\, R_o} + \delta\left(\frac{t}{100} - 1\right)\left(\frac{t}{100}\right) + \beta\left(\frac{t}{100} - 1\right)\left(\frac{t}{100}\right)^3 \qquad \text{(C-1)}$$

$\alpha = 0.003925305$

$\delta = 1.49166$

$\beta = 0.11037$ (t below 0° C)

$\beta = 0$ (t above 0° C)

$R_o \simeq 25.516$ abs. ohms

where R_o = thermometer resistance at 0° C

R_t = thermometer resistance at t° C

The N.B.S. also furnished a tabulation of t as a function of R/R_o. This tabulation was used to determine the temperature. The value of R_o was determined at the time of a temperature measurement by inserting it into a Dewar flask containing demineralized water and crushed ice made from demineralized water.

The resistance of the platinum resistance thermometer was determined by use of a Leeds and Northrup Model 8069-B Mueller bridge (Serial No. 1550042). Calibration tables were furnished with the Mueller bridge. The detector used was a Leeds and Northrup Model 9834 DC Null Detector.

The Mueller bridge was compared with a standard 10 ohm resistor (L and N Cat. No. 4025-B, Serial No. 1582672) with the following results:

Corrected reading of Mueller bridge	9.9995 ohm
Certified resistance of 10 ohm standard	9.9999±0.0005 ohm

The measured resistance was within the tolerance of the certified value of the 10 ohm standard. The Mueller bridge calibration furnished by L and N was, therefore, used in all subsequent work.

The platinum resistance thermometer was compared with the boiling point of water in a small hypsometer constructed for this purpose. The thermometer was in direct contact with saturated steam boiling from demineralized water. The barometric pressure was measured by use of the U-tube manometer in the air bath. The results are shown below:

R_t (corrected)	35.4458 ohms
R_o (corrected)	25.5150 ohms
Barometric pressure	740.1 mm Hg at 72.5° F or 14.240 psia
Thermometer temperature	210.46° F

Boiling temperature of water at 14.240 psia	210.41° F (43)

The difference in the above temperatures is 0.05° F. and may be due in part to error in the hypsometer temperature reading or the barometric pressure determination. The N.B.S. calibration is made more carefully than was the present comparison and is accepted as being correct.

The thermocouple emf was measured with a Leeds and Northrup Type K-3 potentiometer. The null-detecting device was a Leeds and Northrup Catalog No. 2430 galvanometer. The reference junction and copper lead wire-to-thermocouple junctions were inserted in an ice bath in a Dewar flask. Figure C-1 shows the thermocouple-potentiometer wiring. The emf of the thermocouple could be measured with a precision of ± 0.0002 mv.

The first calibration of the thermocouple was carried out by placing it side by side with the platinum thermometer in a recirculating oil bath. The bath could be used only to about 300° F because the hydrocarbon oil used began to distill at higher temperatures. Some difficulty was encountered in controlling the temperature in the oil bath. The results of this calibration are given in Table C-I and are shown in Fig. C-2. In Fig. C-2 the ordinate, Δ EMF, is the difference between the observed thermocouple emf and the value listed in the standard table for this thermocouple.

Subsequent to the initial calibration, further calibration was made with the platinum resistance thermometer and thermocouple side by side in the thermocouple well in the aluminum block thermostat. The results of the later calibrations are shown in Table C-II and Fig. C-2.

The error in emf for a 0.1 deg. F temperature error is shown for the later points. The later calibrations were considered more nearly accurate since the calibrations were made in place and with stable temperature control. For these reasons the later calibrations were taken to be correct.

Based on the calibrations made in place, the thermocouple readings for operation at various temperatures are shown below.

Temperature, deg. F	Thermocouple emf, mv
150.0±0.1	4.0572±0.0036
250.0±0.1	7.7932±0.0038
320.0±0.1	10.5374±0.0040

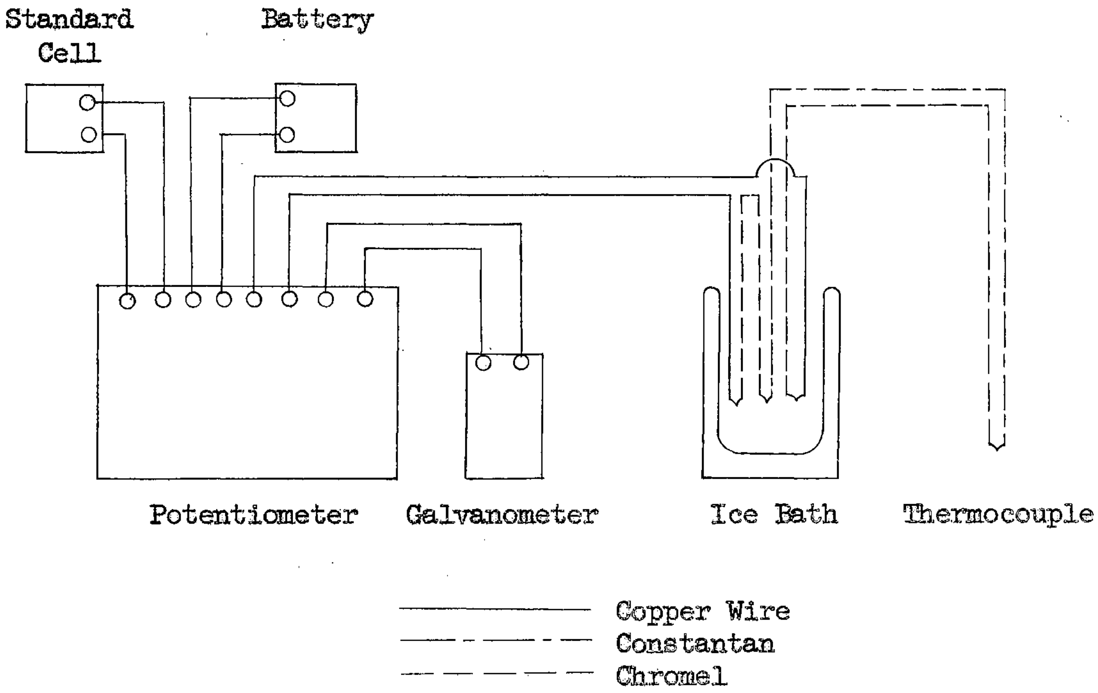

Figure C-1

Diagram of Potentiometer-Thermocouple Circuit

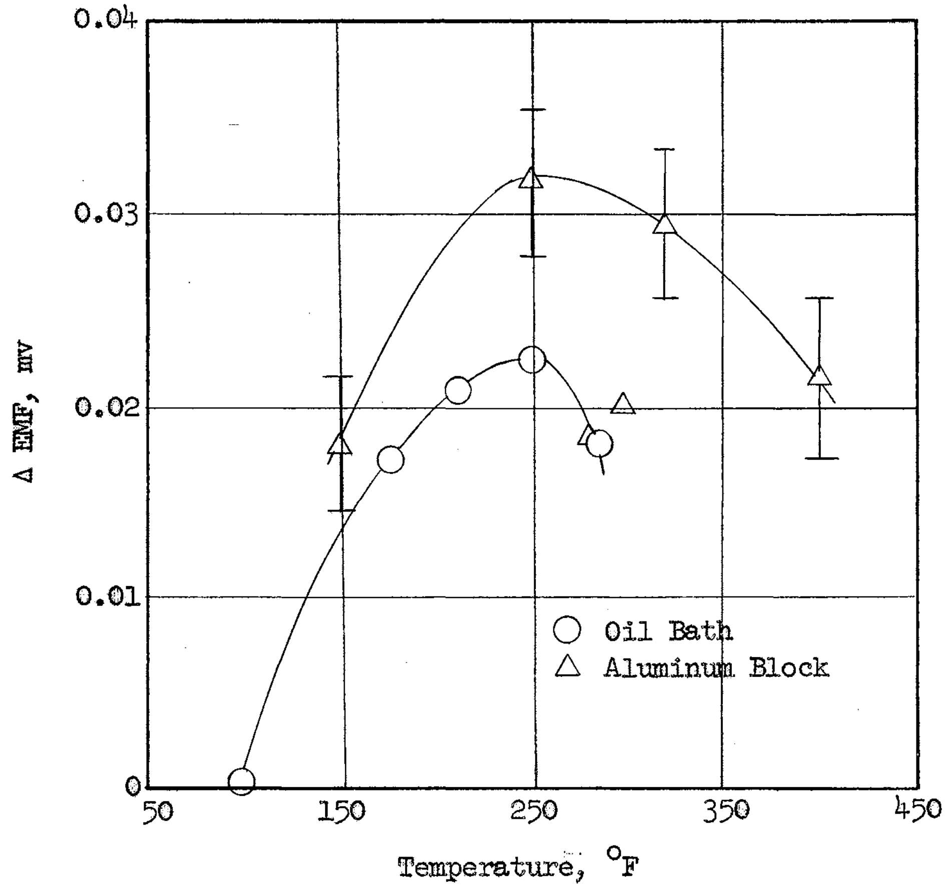

Figure C-2

Thermocouple Calibration Results

TABLE C-I

OIL BATH THERMOCOUPLE CALIBRATION

Resistance Thermometer Temperature, deg F	Observed Thermocouple emf, mv	Tabulated Thermocouple emf, mv	Δ emf, mv
100.58	2.3033	2.3029	0.0004
140.12	3.6978	3.6864	0.0114
175.64	4.9865	4.9694	0.0171
210.28	6.2738	6.2530	0.0208
248.09	7.7106	7.6881	0.0225
281.89	9.0216	9.0038	0.0178

TABLE C-II

ALUMINUM BLOCK THERMOCOUPLE CALIBRATION

Resistance Thermometer Temperature, deg F	Observed Thermocouple emf, mv	Tabulated Thermocouple emf, mv	Δ emf, mv
150.40	4.0715	4.0535	0.0180
248.73	7.7444	7.7127	0.0317
279.63	8.9312	8.9132	0.0180
279.84	9.6485	9.6284	0.0201
320.17	10.5441	10.5148	0.0293
398.86	13.7240	13.7025	0.0215

APPENDIX D

CALIBRATION OF VOLUMETRIC APPARATUS

The quantity of hydrogen collected in the sampling apparatus was calculated from the pressure and volume of the hydrogen. The pressure was read on the U-tube manometer by observing the height in each leg with a cathetometer. The total volume was computed by summing the component volume of each part of the volumetric side of the apparatus. The following discussion describes the volume calibrations.

Analytic Balance Calibrations

Two analytical balances were used in the volumetric calibration work. Voland and Sons Balance No. 18559 (capacity 125 g) was used for small weights. Voland and Sons Balance No. B-125 (capacity 6 Kg) was used for large weights.

Small Balance

Two calibrations were made for the small balance. In the first calibration, the weights used with the balance were calibrated against a standard 50 g weight by the method of Blade (10). At the same time, the rider and vernier on the balance were standardized. An "arm correction" was determined for the balance. Weights from another set were weighed in both pans and the mean value was assumed to be the true weight. In this way corrections for weights made in the left pan were obtained. Arm corrections were applied in the calibration of the balance weights. The calibrated weights were obtained as "apparent mass versus brass." For this reason all buoyancy corrections were made as if the weights were brass. The first calibration was used in the volumetric calibrations.

A second calibration was made by comparison of the balance weights against a Mettler balance. The Mettler balance weights were certified to be Class S. This calibration was repeated later. The results of the calibrations and the arm correction determination are shown in Table D-II and Figures D-1 and D-2. The Mettler calibrations were used in the calculations for sample composition.

Large Balance

Arm corrections were obtained, also, for the large balance. The balance weights were calibrated against the same 50 g standard, since no larger standard was available. Weights up to 100 g in denomination were calibrated on the small balance. Larger weights (nominal 200, 500, 1000, 2000 g) were calibrated on the large balance. Weight and arm corrections are shown in Table D-III and Figure D-3.

Volumetric Calibrations

The method of calculation will be shown for the 25-cc bulb. This bulb was calibrated by filling with water, and again by filling with mercury. The larger bulbs were calibrated only with water. In each case the procedure was first to weigh the bulb empty and open to the air; then to evacuate the bulb and fill it with water. Care was exercised that no bubbles of air were left in the bulb. The bulb was then placed in the air bath. After a few hours at constant temperature, the cock on the bulb was closed. Excess water in the neck of the bulb was removed and the filled weight was determined.

Water Calibration

Empty weight = 47.876 g (corrected for weights and arm)

Density of glass = 2.24 g/cc

Density of air = 0.0012

$$\text{In vacuo mass} = 47.876\left[1 + 0.0012\left(\frac{1}{2.24} - \frac{1}{8.4}\right)\right]$$

$$= 47.895 \text{ g}$$

Weight filled with water at 77.0 °F = 73.250 g

Uncorrected weight of water = 73.25 - 47.90 = 25.35 g

$$\text{Uncorrected water volume} = \frac{25.35 \text{ g}}{0.997 \text{ g/cc}} = 25.4 \text{ cc}$$

$$\text{Volume of glass} = \frac{47.90 \text{ g}}{2.24 \text{ g/cc}} = 21.4 \text{ cc}$$

Total volume = 21.4 + 25.4 = 46.8 cc

$$\text{Apparent density} = \frac{73.25 \text{ g}}{46.8 \text{ cc}} = 1.56 \text{ g/cc}$$

$$\text{In vacuo mass} = 73.250\left[1 + 0.0012\left(\frac{1}{1.56} - \frac{1}{8.4}\right)\right]$$

$$= 73.236 \text{ g}$$

Mass of water = 73.296 - 47.895 = 25.401 g

Density of water at 77.0 °F = 0.99707 g/cc

$$\text{Volume of bulb} = \frac{25.401 \text{ g}}{0.99707 \text{ g/cc}} = \underline{25.476 \text{ cc}}$$

Mercury Calibrations

Empty weight = 47.87 (corrected for weights and arm)

In vacuo mass $= 47.87 \left[1 + 0.0012\left(\frac{1}{2.24} - \frac{1}{8.4}\right)\right] = 47.89$

Weight filled with mercury = 392.70 g

Uncorrected weight of mercury = 392.7 - 47.9 = 344.8 g

Density of mercury at 77.0 °F = 13.5336 g/cc

Uncorrected mercury volume $= \frac{344.8}{13.53} = 25.5$ cc

Total volume = 25.5 + 21.4 = 46.9

Apparent density $= \frac{344.8 \text{ g}}{46.9 \text{ cc}} = 7.35$ g/cc

In vacuo mass $= 392.70 \left[1 + 0.0012\left(\frac{1}{7.35} - \frac{1}{8.40}\right)\right]$

$= 392.71$ g

Mass of mercury = 392.71 - 47.87 = 344.84 g

Volume of bulb $= \frac{344.84 \text{ g}}{13.5336 \text{ g/cc}} = 25.480$ cc

From these two calibrations, the volume of the 25-cc bulb is taken to be 25.48 cc at 77.0 °F, including the stopcock passage. The volumes of the 500-cc, 1-liter and 2-liter bulbs were determined in a similar manner except that water was used in both calibrations. The results are shown in Table D-I.

The volume of the necks of the bulbs was determined by filling them with mercury. The mercury was then removed carefully into a weighing bottle, weighed, and the volume calculated from its mass and density. The neck volumes are also included in Table D-1.

A fifth volumetric bulb was used. This bulb was constructed from a gallon jug, stopcock, and ball-joint as shown in the sketch below.

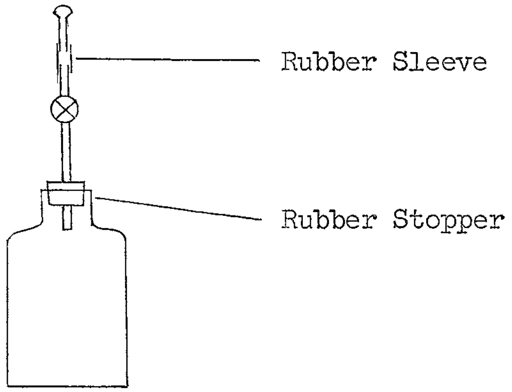

The rubber-to-glass joints were coated with Duco cement to prevent leakage. This bulb, referred to as the 4-liter bulb, was calibrated by expanding air into it. This calibration will be described below.

U-Tube Manometer

The right leg of the U-tube manometer had to be calibrated for volume, since it constituted a part of the volumetric side of the apparatus. This leg was provided with a baked-on reference mark. The calibration was carried out before the manometer was fabricated. The right leg was then joined carefully with the left leg and the U-joint formed. The finished manometer was filled with enough triple-distilled mercury that the level in the right side was well above the U-joint.

The calibration of the manometer leg was made by attaching a stopcock at the bottom. The manometer was filled with mercury, taking care to avoid entrapped air bubbles. A series of measurements were made in which the heights of the mercury and reference mark were measured before and after draining a small amount of mercury into a weighing bottle. The weight and density of the mercury gave the volume of the height increment measured. The data showed that the tube diameter was constant. The data were fitted by least squares to obtain

$$V = 0.2716\ (h_r - h) \qquad \text{(Run 1)}$$
$$V = 0.2718\ (h_r - h) \qquad \text{(Run 2)} \qquad \text{(D-1)}$$

where V = volume <u>below</u> the reference mark, cc
h_r = height of reference mark, cm
h = height of mercury, cm

The difference in the results for the two runs at $(h_r - h) = 40$ cm is only 0.008 cc. The equation for Run 2 was used in calculations.

Capillary Tubing

The remainder of the volumetric side of the sampling apparatus consists of tubing, including that in the manometer leg above the reference mark. The 25-cc and 1-liter bulbs were attached to the side arm ball joints and the stopcock closed on the 1-liter bulb. The air bath temperature was equilibrated at 77.0 °F. The barometric pressure was determined on the U-tube manometer, and the stopcock on the 25-cc bulb was closed. The remainder of the volumetric side was then evacuated. The air in the 25 cc bulb was next allowed to expand into the evacuated lines. The final pressure was observed on the U-tube manometer. Two runs were made, and the calculated volumes agreed within 0.02 cc. A sample calculation follows:

Initial barometric pressure, $P_1 = 739.75$ mm Hg

Initial volume of air, $V_1 = 25.48$ cc

Final pressure, $P_2 = 391.45$ mm Hg

Assuming ideal behavior,

$$V_2 = \frac{V_1\ P_1}{P_2} = 25.48 \left(\frac{739.75}{381.45} \right) = 48.15 \text{ cc}$$

Mercury level in right leg of manometer = 40.35 cm

Height of reference mark = 68.885 cm

Volume in manometer leg
  below reference mark = 0.2718 (68.885 - 40.35) = 7.76 cc

Volume of neck of 25 cc bulb = 0.25 cc

Volume of neck of 1-liter bulb = 0.38 cc

Volume of sampling apparatus to side-
  arms and reference mark = 48.15 - 25.48 - 7.76 - 0.25 - 0.38 =

14.28 cc

The average of the two runs was 14.27 cc.

Four Liter Bulb

The volume of the 4-liter bulb was determined by expansion of air in much the same manner as for the tubing. In this case, however, the 2-liter bulb was used as the air reservoir. Three calibrations were made with the results shown in Table D-I.

TABLE D-I

CALIBRATED VOLUMES OF VOLUMETRIC APPARATUS

Item	Volume, cc	Maximum Estimated Error, cc (±)
25 cc bulb	25.48	0.02
neck	0.25	---
500 cc bulb	445.23	0.06
neck	0.52	---
1-liter bulb	946.63	0.12
neck	0.38	---
2-liter bulb	2048.36	0.24
neck	0.98	---
4-liter bulb	3823.5	6.0
neck	7.25	--
U-tube manometer, below reference mark	Eq. D-1	0.04
Remainder of tubing	14.27	0.1

TABLE D-II

WEIGHT SET NO. 5 CALIBRATIONS

	Calibrated Weight		
Nominal Weight	vs. 50 g Std.	vs. Mettler Class S	vs. Mettler Class S (repeat)
5 mg	5.0 mg	5.1 mg	5.0 mg
10	10.0	10.0	10.0
20	20.0	20.0	20.0
30	30.0	30.1	30.0
50	50.0	50.0	50.0
100	100.1	100.0	100.0
200	200.1	200.0	200.0
300	300.2	300.0	300.0
500	500.1	500.1	500.1
1 g	1.0000 g	0.9999 g	0.9999 g
2	2.0002	2.0000	2.0000
3	3.0001	3.0000	3.0001
5	4.9999	4.9999	4.9999
10	9.9998	9.9998	9.9999
20	20.0002	20.0000	20.0001
30	30.0004	30.0004	30.0004
50	50.0008	50.0004	50.0005
Rider			
Arm 0.1 g	.0998	.1002	.1002
0.2	.1998	.2001	.2001
0.3	.2995	.3001	.3001
0.4	-	.4002	.4002
0.5	.4999	.5002	.5001
0.6	-	.6005	.6002
0.7	.6994	.7002	.7001
0.8	-	.8002	.8001
0.9	.9000	.9002	.9000

TABLE D-III

WEIGHT SET NO. 4775
CALIBRATIONS

Nominal Wt.	Calibrated Weight Vs. 50 g. Std.
1 g	1.00 g
2A	2.01
2B	2.01
5	5.00
10A	10.01
10B	10.01
20	20.00
50	50.00
100A	100.00
100B	99.99
200	200.07
500	500.14
1000	1000.23
2000	2000.54

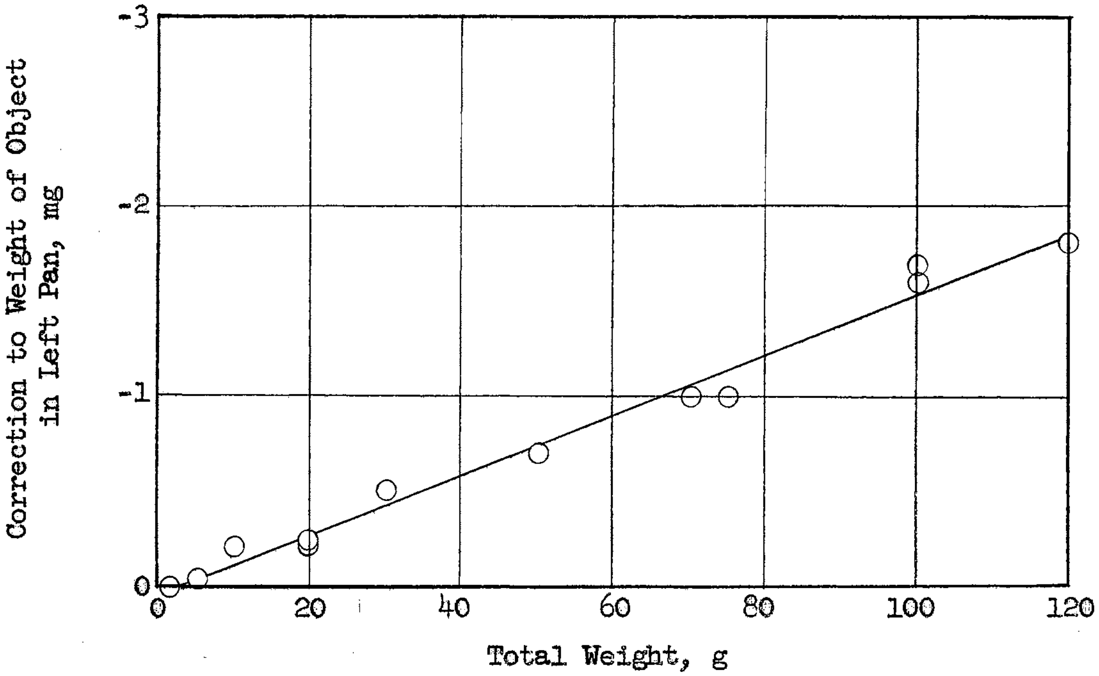

Figure D-1

Voland Balance No. 18559 Arm Correction

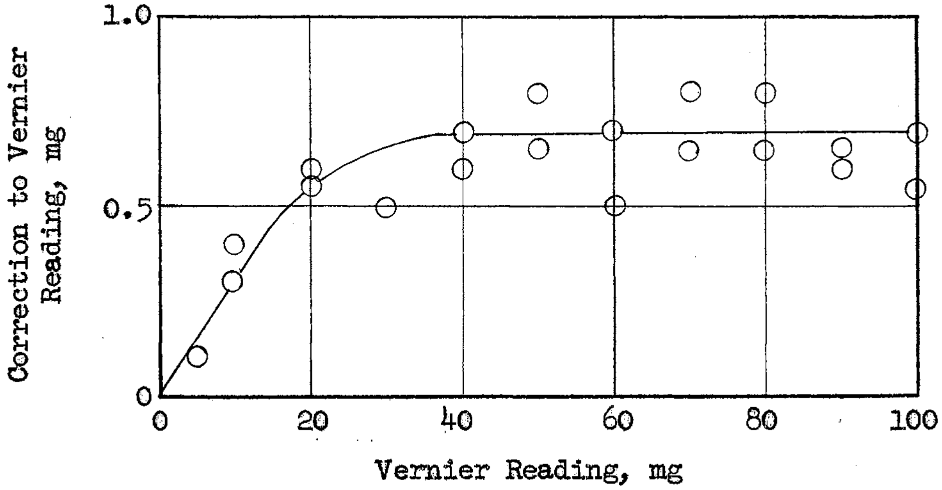

Figure D-2

Voland Balance No. 18559 Vernier Correction

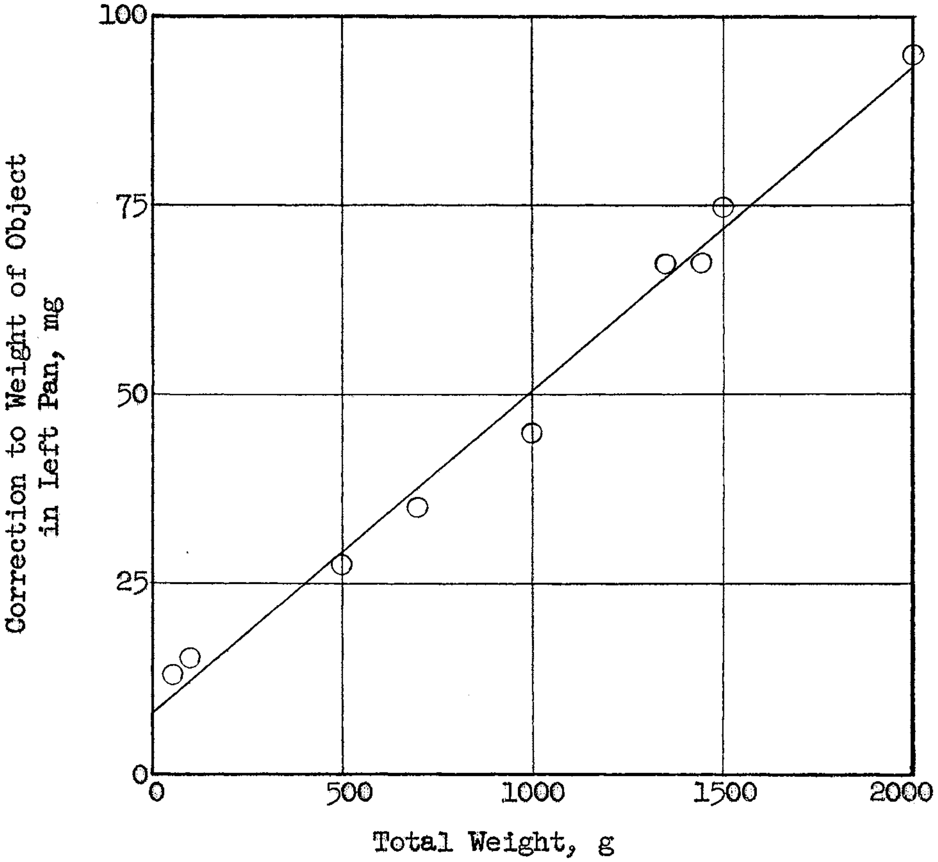

Figure D-3

Voland Balance B-125 Arm Correction

APPENDIX E

EXPERIMENTAL DATA

TABLE E-IA

HYDROGEN-BENZENE EXPERIMENTAL DATA

Run No.	Cell Temp. °F	Phase	Meas. Cyl. Range, Atm	Total Wt. On Balance, Kg Init	Total Wt. On Balance, Kg Final	Oil Level cm	Gas Compr. Level Init	Gas Compr. Level Final	Bal. Temp. °F	Sampling Time, min
3A	280.0	Liq	50-125	254.0801	254.0801	26.8	48.3	48.6	73.3	--
3B	280.0	Liq	50-125	254.0801	254.0801	26.8	48.6	48.8	74	--
3E	280.0	Liq	50-125	254.0801	254.0801	23.9	31.3	31.6	72	--
3F	280.0	Liq	50-125	254.0801	254.0801	23.6	32.0	32.4	75	--
3G	280.0	Liq	50-125	254.0801	254.0801	21.6	32.4	32.2	81	--
3H	280.0	Liq	50-125	254.0801	254.0801	21.6	32.8	32.9	80	--
3I	280.0	Liq	50-125	254.0801	254.0801	21.2	34.7	34.9	73	--
3J	280.0	Gas	50-215	254.0801	254.0801	29.9	36.9	38.8	72	96
3K	280.0	Gas	50-125	254.0801	254.0801	29.6	38.9	40.9	71	7
3L	280.0	Gas	50-125	254.0801	254.0801	29.6	40.9	42.7	73	25.5
3M	280.0	Gas	50-125	254.1351	254.1351	29.4	43.4	45.4	71	41
3N	280.0	Gas	50-125	254.1621	254.1621	29.4	45.6	47.2	72	61
4	320.0	Liq	50-125	58.9666	58.9666	28.9	31.6	31.9	71	--
4	320.0	Gas	50-125	58.9666	58.9936	28.9	32.0	34.9	71	45
5	320.0	Liq	50-125	83.9786	83.9786	29.0	62.1	62.1	73	--
5	320.0	Gas	50-125	83.9786	83.9906	29.0	62.4	64.0	71	50
6	320.0	Liq	50-125	108.9937	108.9937	29.0	78.7	78.8	71	--
6	320.0	Gas	50-125	109.0137	109.0137	29.0	78.9	80.4	75	50
7	320.0	Gas	50-125	184.0380	184.0500	28.4	101.8	103.2	71	25
7	320.0	Liq	50-125	184.0580	184.0580	28.4	103.4	103.8	71	--
8	150.0	Liq	3-20	59.7042	59.7042	27.6	32.0	32.4	71	--
8	150.0	Gas	3-20	59.8042	59.9892	27.7	32.9	36.7	71	25
8	150.0	Gas	3-20	60.0042	61.3016	27.5	36.7	53.6	72	100
9	150.0	Liq	3-20	169.7643	169.7643	27.5	105.3	105.8	72	--
9	150.0	Gas	3-20	169.8143	170.6643	27.2	105.8	116.8	72	42
10	150.0	Liq	20-50	174.2370	174.2370	27.2	31.3	31.3	72	--
10	150.0	Gas	20-50	174.2570	174.4570	26.7	31.8	38.8	71	45

TABLE E-IA (cont'd)

HYDROGEN-BENZENE EXPERIMENTAL DATA

Run No.	Cell Temp. °F	Phase	Meas. Cyl. Range, Atm	Total Wt. On Balance, Kg Init	Total Wt. On Balance, Kg Final	Oil Level cm	Gas Compr. Level Init	Gas Compr. Level Final	Bal. Temp. °F	Sampling Time, min
11	150.0	Liq	50-125	104.4905	104.4905	26.2	71.4	71.5	71	--
12	150.0	Liq	50-125	144.0588	114.0588	26.1	89.8	89.9	71	--
12	150.0	Gas	50-125	144.0728	144.1228	26.1	90.5	94.0	71	22
12	150.0	Gas	50-125	144.1228	144.2328	26.1	94.3	101.3	72	48
13	150.0	Liq	50-125	239.0687	239.0687	25.2	30.6	30.7	73	--
13	150.0	Gas	50-125	239.0787	239.1387	25.1	30.7	35.7	74	45
13	150.0	Gas	50-125	239.1427	239.2027	25.0	35.7	40.7	74	94
14	150.0	Gas	125-300	146.9382	146.9732	24.7	71.1	78.3	74	97
14	150.0	Liq	125-300	146.9832	146.9832	24.6	78.7	79.3	73	--
14	150.0	Gas	125-300	146.9882	147.0232	24.5	79.0	86.0	73	83
15	250.0	Gas	3-20	80.7124	81.9750	24.4	63.6	79.2	74	44
15	250.0	Gas	3-20	81.8570	82.2570	24.3	79.6	85.5	73	22
15	250.0	Liq	3-20	82.3170	82.3170	24.6	85.7	86.0	74	--
16	250.0	Liq	3-20	135.0767	135.0767	24.4	35.8	35.9	73	--
16	250.0	Gas	3-20	135.1267	135.6267	23.5	36.0	42.1	74	30
17	250.0	Gas	20-50	141.0746	141.2746	23.3	99.3	106.8	75	50
17	250.0	Liq	20-50	141.3046	141.3046	23.3	106.9	106.9	73	--
18	250.0	Liq	50-125	140.0062	140.0062	22.7	33.8	33.9	75	--
18	250.0	Gas	50-125	140.0262	140.0962	22.8	35.1	40.7	72	80
19	250.0	Liq	50-125	239.0687	239.0687	22.7	79.0	79.2	74	--
19	250.0	Gas	50-125	239.0787	239.1287	22.6	79.4	84.0	73	78
20	250.0	Liq	125-300	175.9511	175.9511	22.5	106.3	106.5	74	--
20	250.0	Liq	125-300	175.9511	175.9511	22.0	106.7	106.7	77	--
20	250.0	Gas	125-300	175.9511	175.9761	22.0	107.0	112.2	77	61
21	150.0	Gas	50-125	238.9880	239.1080	20.0	26.0	35.8	74	96
21	150.0	Gas	50-125	239.1187	239.2387	20.0	35.9	45.6	78	97
21	150.0	Liq	50-125	239.2637	239.2637	19.5	45.9	46.1	75	--

TABLE E-1A (cont'd)

HYDROGEN-BENZENE EXPERIMENTAL DATA

Run No.	Cell Temp. °F	Phase	Meas. Cyl. Range, Atm	Total Wt. On Balance, Kg Init.	Total Wt. On Balance, Kg Final	Oil Level cm	Gas Compr. Level Init.	Gas Compr. Level Final	Bal. Temp. °F	Sampling Time min.	Equil'n Time, hr
22	150.0	Liq	125-300	146.9574	146.9574	30.4	73.0	73.0	77	--	--
22	150.0	Gas	125-300	146.9624	146.9974	30.5	73.2	80.1	74	147	--
23	150.0	Liq	125-300	234.5056	234.5056	30.3	73.4	73.4	76	--	--
23	150.0	Gas	125-300	234.5076	234.5276	30.2	73.7	78.2	75	101	--
24	150.0	Liq	300-600	206.5418	206.5418	30.0	99.4	99.5	76	--	--
24	150.0	Gas	300-600	206.5418	206.5458	30.0	100.0	103.0	75	80	--
25	150.0	Gas	3-20	60.4042	61.8552	28.9	40.4	58.3	74	110	--
26	150.0	Gas	3-20	166.8661	167.8203	28.8	72.0	83.3	74.5	80	--
27	150.0	Gas	20-50	174.2430	174.5530	28.7	33.8	43.1	73.5	80	--
28	150.0	Gas	50-125	144.0578	144.2128	28.6	90.3	102.5	73	122	--
29	250.0	Gas	3-20	76.9799	77.4299	28.5	22.4	27.9	73	35	--
30	250.0	Gas	50-125	140.0204	140.0954	28.5	34.0	39.5	75	90	--
31	250.0	Gas	50-125	239.0520	239.1070	28.4	76.4	80.6	77.5	72	--
32	250.0	Gas	125-500	175.9476	175.9626	28.6	101.3	104.4	79	80	--
33	250.0	Liq	300-600	176.9203	176.9203	28.7	91.2	91.2	81	--	--
33	250.0	Gas	300-600	176.9203	176.9203	28.7	91.1	92.8	80	100	--
34	250.0	Liq	600-1000	171.8773	171.8773	28.6	99.2	99.4	80	--	--
34	250.0	Gas	600-1000	171.8773	171.8773	28.6	99.7	101.1	77	110	--
35	150.0	Liq	600-1000	172.1273	172.1273	28.4	103.8	103.9	80	--	--
35	150.0	Gas	600-1000	172.1273	172.1293	28.3	105.2	107.9	78.5	170	--
35	150.0	Liq	600-1000	172.1343	172.1343	28.2	109.7	109.8	78.5	--	12
35	150.0	Gas	600-1000	172.1343	172.1443	28.2	110.0	119.6	77.5	112	14

TABLE E-IB

HYDROGEN-BENZENE EXPERIMENTAL DATA

Run No.	Bar. Press., mm Hg Init mm	°F	Final mm	°F	Air Bath U-Tube Manometer Rdgs. First Collection Left	Right	Ref.Mk	Second Collection Left	Right	Ref.Mk	Air Bath Temp., °F	Vol. Bulbs* Attached
3A	733.1	74.5	--	--	651.75	569.5	684.8	718.1	500.8	684.8	77.0	25,500x
3B	739.45	76.2	--	--	800.05	416.20	684.85	--	--	--	77.0	25,500x
3E	--	--	732.55	77.0	760.0	456.95	684.75	--	--	--	77.0	25,500x
3F	--	--	743.85	70.0	809.15	406.3	684.7	--	--	--	77.0	25,500x
3G	746.6	78.5	--	--	777.4	439.3	684.35	--	--	--	86.0	25,500x
3H	--	--	741.7	86.0	779.2	437.45	684.4	--	--	--	86.0	25,500x
3I	--	--	739.7	86.0	788.3	421.1	684.8	--	--	--	86.0	25,500x
3J	--	--	742.5	86.0	759.9	449.8	684.6	--	--	--	86.0	1000,2000
3K	741.75	71.7	742.9	86.0	763.1	446.7	684.65	--	--	--	86.0	1000,2000
3L	740.8	75.7	742.15	86.0	756.2	453.75	684.6	--	--	--	86.0	1000,2000
3M	738.45	72.1	740.1	86.0	758.55	451.2	684.5	--	--	--	86.0	1000,2000
3N	739.3	71.2	741.05	86.0	757.1	452.9	684.6	--	--	--	86.0	1000,2000
4	736.5	74.0	737.1	86.0	641.5	573.05	684.95	--	--	--	86.0	25,500x
4	737.1	86.0	735.2	86.0	709.05	503.1	684.9	--	--	--	86.0	500,1000
5	733.1	74.0	732.9	74.7	770.9	438.85	684.8	--	--	--	86.0	25x,500x
5	732.9	74.7	733.1	86.0	689.2	523.5	684.8	--	--	--	86.0	500,1000
6	737.2	76.9	738.3	86.0	704.85	507.0	684.7	--	--	--	86.0	25,500x
6	735.55	72.8	735.0	86.0	695.2	516.9	684.6	--	--	--	86.0	500x,2000
7	731.95	72.8	730.9	86.0	715.05	504.75	685.0	--	--	--	86.0	25x,2000
7	--	--	738.8	86.0	770.65	447.15	685.0	--	--	--	86.0	25,500x
8	735.3	71.6	736.75	86.0	626.3	597.2	685.4	--	--	--	86.0	25x,500x
8	737.95	72.6	737.95	86.0	702.6	518.35	685.35	--	--	--	86.0	25x,500
8	737.90	72.6	737.15	86.0	697.35	523.8	685.3	--	--	--	86.0	25x,2000
9	737.4	74.3	737.4	86.0	666.8	555.35	685.3	--	--	--	86.0	25x,2000x
9	738.2	73.8	738.0	86.0	663.45	558.65	685.2	--	--	--	86.0	1000,2000

* The letter x by the bulb volume indicates that the stopcock on the bulb was closed.

TABLE E-IB (cont'd)

HYDROGEN-BENZENE EXPERIMENTAL DATA

Run	Bar. Press., mm Hg				Air Bath U-Tube Manometer Rdgs.						Air Bath	Vol. Bulbs*
	Init		Final		First Collection			Second Collection				
No.	mm	°F	mm	°F	Left	Right	Ref.Mk	Left	Right	Ref.Mk	Temp., °F	Attached
10	735.95	71.4	736.2	86.0	704.55	516.2	685.2	--	--	--	86.0	1000x, 2000x
10	735.9	74.9	735.7	86.0	768.25	450.1	685.2	--	--	--	86.0	1000, 2000
11	738.7	71.1	739.75	86.0	697.4	523.65	685.25	--	--	--	86.0	1000x, 2000x
12	740.35	86.0	739.05	86.0	757.85	460.8	685.25	--	--	--	86.0	1000x, 2000x
12	739.3	72.3	741.1	86.0	764.75	453.65	685.2	--	--	--	86.0	1000, 2000
12	740.25	73.6	739.3	86.0	907.8	307.0	685.25	670.5	551.5	685.3	86.0	1000, 2000(x)
13	737.8	72.3	739.4	86.0	773.5	443.95	684.8	--	--	--	86.0	25, 1000x
13	736.7	72.6	736.0	86.0	956.2	257.05	684.75	671.6	549.4	684.75	86.0	1000, 2000
13	736.1	73.0	736.05	86.0	958.1	255.25	684.75	675.45	545.35	684.75	86.0	1000, 2000(x)
14	742.75	86.0	741.1	86.0	959.15	253.95	684.7	640.95	580.7	684.65	86.0	2000, 4000(x)
14	741.9	86.0	741.65	86.0	815.15	400.5	684.6	--	--	--	86.0	25, 500x
14	737.0	74.1	738.1	86.0	957.8	255.25	684.6	640.65	581.0	684.6	86.0	2000, 4000(x)
15	740.1	72.0	741.65	86.0	757.0	460.6	684.65	--	--	--	86.0	500, 1000
15	740.1	73.1	741.6	86.0	660.55	560.55	684.65	--	--	--	86.0	500, 1000
15	741.95	71.5	741.35	86.0	626.7	595.25	684.6	--	--	--	86.0	25, 1000x
16	741.9	73.0	742.55	86.0	638.9	582.75	684.65	--	--	--	86.0	25x, 500x
16	741.2	73.9	740.9	86.0	721.65	497.3	684.65	--	--	--	86.0	500, 1000
17	740.5	73.0	739.6	86.0	763.5	453.75	684.65	--	--	--	86.0	1000, 2000
17	740.15	73.9	740.3	86.0	663.6	557.3	684.6	--	--	--	86.0	25x, 1000x
18	738.55	73.6	738.75	86.0	835.0	379.95	684.6	--	--	--	86.0	25x, 1000x
18	739.8	74.4	740.1	86.0	835.0	379.9	684.6	649.45	571.8	684.6	86.0	1000, 2000(x)
19	739.5	73.8	739.8	86.0	703.1	516.45	684.65	--	--	--	86.0	25, 1000x
19	737.35	74.7	737.5	86.0	905.3	308.2	684.6	663.8	556.95	684.6	86.0	1000, 2000(x)
20	736.7	73.8	735.85	86.0	865.9	348.15	684.55	--	--	--	86.0	25, 1000x
20	736.9	86.0	738.55	86.0	768.15	448.9	684.55	--	--	--	86.0	25, 1000x
20	739.9	86.0	738.65	86.0	811.2	391.7	684.5	--	--	--	86.0	2000, 4000

* The letter x in parentheses indicates stopcock was closed on second collection.

TABLE E-IB (cont'd)

HYDROGEN-BENZENE EXPERIMENTAL DATA

	Bar. Press., mm Hg				Air Bath U-Tube Manometer Rdgs.							
Run	Init		Final		First Collection			Second Collection			Air Bath	Vol. Bulbs
No.	mm	°F	mm	°F	Left	Right	Ref.Mk	Left	Right	Ref.Mk	Temp., °F	Attached
21	742.5	74.4	743.25	86.0	951.3	249.5	684.6	634.45	575.05	684.6	86.0	2000,4000(x)
21	743.3	73.2	742.4	86.0	948.4	252.25	684.7	633.8	575.6	684.7	86.0	2000,4000(x)
21	743.35	86.0	743.5	86.0	736.2	469.65	684.7	--	--	--	86.0	25,1000x
22	742.95	74.0	742.1	86.0	745.35	460.1	684.7	--	--	--	86.0	25,1000x
22	741.65	77.6	742.85	86.0	952.05	248.4	684.6	634.1	575.15	684.6	86.0	2000,4000(x)
23	742.3	74.2	741.9	86.0	821.6	381.05	684.7	--	--	--	86.0	25,1000x
23	743.7	86.0	744.0	86.0	952.15	248.3	684.6	634.6	574.55	684.6	86.0	2000,4000(x)
24	742.2	74.9	741.4	86.0	769.9	434.5	684.6	--	--	--	86.0	25,1000x
24	741.25	74.0	740.6	86.0	951.45	249.0	684.6	634.1	575.15	684.6	86.0	2000,4000(x)
25	742.1	72.4	742.15	86.0	693.9	513.9	684.8	--	--	--	86.0	1000x,2000
26	743.7	86.0	744.0	86.0	704.15	503.1	684.75	--	--	--	86.0	1000,2000
27	743.4	71.8	743.3	86.0	809.6	393.75	684.75	--	--	--	86.0	1000,2000
28	743.6	74.3	743.1	86.0	872.95	328.6	684.7	627.7	581.8	684.7	86.0	2000,4000(x)
29	740.15	73.3	740.95	86.0	653.65	555.05	684.6	--	--	--	86.0	500,1000
30	737.6	76.0	738.6	86.0	723.2	483.05	684.6	--	--	--	86.0	2000,4000
31	737.0	74.8	736.4	86.0	756.8	448.1	684.6	--	--	--	86.0	2000,4000
32	735.95	77.0	737.25	86.0	776.4	427.85	684.6	--	--	--	86.0	2000,4000
33	737.15	77.5	737.1	86.0	850.15	351.5	684.55	637.55	571.45	684.55	86.0	25(x),4000x
33	738.05	80.2	739.7	86.0	755.8	449.0	684.5	--	--	--	86.0	2000,4000
34	739.9	77.5	739.55	86.0	857.95	343.6	684.5	716.9	489.4	684.5	86.0	25(x),4000x
34	740.6	86.0	740.8	86.0	809.8	393.05	684.5	--	--	--	86.0	2000,4000
35	739.45	79.1	740.0	86.0	798.75	404.55	684.5	--	--	--	86.0	25,4000x
35	737.9	81.5	739.4	86.0	966.35	233.65	684.5	634.7	574.3	684.5	86.0	2000,4000(x)
35	738.3	78.3	738.85	86.0	817.45	385.05	684.5	--	--	--	86.0	25,4000x
35	738.85	86.0	739.4	86.0	950.2	249.9	684.5	631.6	572.9	684.5	86.0	2000,4000(x)

TABLE E-IC

HYDROGEN-BENZENE EXPERIMENTAL DATA

Run	Trap No. 1		Trap No. 2	
No.	Tare Wt., g	Gross Wt., g	Tare Wt., g	Gross Wt., g
3A	113.9254	114.5324	112.0126	112.1590
3B	113.8920	114.7897	111.9972	112.1450
3E	113.8760	114.7859	111.9665	111.9734
3F	113.8683	115.1390	111.9657	111.9687
3G	113.9435	114.9451	112.0188	112.0206
3H	113.9427	114.9245	112.0202	112.0225
3I	113.9420	115.0080	112.0180	112.0206
3J	113.9076	114.1087	112.0171	112.0170
3K	113.9135	114.1365	111.9790	111.9795
3L	113.9143	114.1251	111.9802	111.9800
3M	113.9243	114.1316	111.9796	111.9809
3N	113.9245	114.1339	111.9800	111.9802
4	113.9258	114.7681	111.9816	111.9818
4	113.8710	114.3623	111.9808	111.9826
5	113.8425	115.1989	111.9811	111.9838
5	113.8381	114.0868	111.9809	111.9815
6	113.8645	115.0933	111.9807	111.9827
6	113.8396	114.1431	111.9178	111.9184
7	113.8890	114.1090	111.9730	111.9746
7	113.8879	115.0605	112.1003	112.1021
8	113.8879	115.1460	112.1006	112.1041
8	113.9243	113.9653	112.1232	112.1232
8	113.9246	114.1354	112.1234	112.1239
9	113.9247	115.8885	112.1230	112.1256
9	113.8603	113.9257	112.1238	112.1241
10	113.8604	115.1829	112.1236	112.1254
10	113.9002	113.9811	112.1247	112.1245
11	113.8992	114.7096	112.1242	112.1252

TABLE E-IC (cont'd)

HYDROGEN-BENZENE EXPERIMENTAL DATA

Run	Trap No. 1		Trap No. 2	
No.	Tare Wt., g	Gross Wt., g	Tare Wt., g	Gross Wt., g
12	113.8985	114.9893	112.1236	112.1251
12	113.9055	113.9424	112.1137	112.1146
12	113.9005	113.9885	112.1130	112.1136
13	113.8981	115.4661	112.1124	112.1146
13	112.7996	112.8472	112.6298	112.6296
13	112.8006	112.8648	112.6294	112.6301
14	112.7986	112.9079	112.6280	112.6282
14	113.8976	115.1987	112.6279	112.7786
14	112.7988	112.9045	112.7202	112.7198
15	112.7983	114.4222	112.7192	112.7195
15	112.7914	113.3542	112.7192	112.7192
15	113.9060	116.2073	112.7186	113.3850
16	113.9048	114.4078	112.7185	112.9821
16	112.7913	113.2181	112.7634	112.7639
17	112.7918	113.2353	112.7632	112.7643
17	112.7908	113.3080	112.7621	112.7623
18	112.7908	114.1018	112.7629	112.7649
18	112.7905	113.1413	112.7624	112.7623
19	112.7909	113.3950	112.7638	112.7637
19	112.7908	113.0992	112.7627	112.7628
20	112.7910	113.4419	112.7627	112.7700
20	112.7916	113.3844	112.7629	112.7642
20	112.7902	113.0684	112.7624	112.7636
21	112.7902	112.9402	112.7615	112.7617
21	112.7900	112.9371	112.7614	112.7620
21	112.7904	114.0388	112.7608	112.7627
22	112.7897	113.7535	112.7611	112.7637
22	112.7901	112.9105	112.7613	112.7615

TABLE E-IC (cont'd)

HYDROGEN-BENZENE EXPERIMENTAL DATA

Run	Trap No. 1		Trap No. 2		Blank	
No.	Tare Wt., g	Gross Wt., g	Tare Wt., g	Gross Wt., g	Tare Wt., g	Gross Wt., g
23	112.7894	113.7819	112.7608	112.7636		
23	112.7891	112.8903	112.7599	112.7594		
24	112.7890	113.2152	112.7593	112.7627		
24	112.7887	112.8758	112.7593	112.7598		
25	112.8136	113.0372	112.7589	112.7590		
26	112.8131	112.9434	112.7589	112.7593		
27	112.8141	112.9177	112.7583	112.7588		
28	112.8492	113.0043	112.7672	112.7675		
29	112.8511	113.4063	112.7695	112.7690		
30	112.8508	113.2034	112.7683	112.7683		
31	112.8509	113.1482	112.7683	112.7688		
32	112.8515	113.0802	112.7685	112.7691		
33	112.8513	113.4546	112.7685	112.7725		
33	112.8510	113.0090	112.7684	112.7687		
34	112.8513	113.2975	112.7680	112.7724		
34	112.8517	113.0370	112.7681	112.7678		
35	112.8723	113.2826	112.7680	112.7712	112.1495	112.1492
35	112.8739	112.9653	112.7692	112.7674	112.1503	112.1487
35	112.9063	113.3498	112.7678	112.7715	112.0949	112.0944
35	113.9356	114.0120	112.0944	112.0952	112.7715	112.7710

TABLE E-IIA

HYDROGEN-CYCLOHEXANE EXPERIMENTAL DATA

Run No.	Cell Temp. °F	Phase	Meas. Cyl. Range, Atm	Total Wt. on Balance, Kg Init	Total Wt. on Balance, Kg Final	Oil Level cm	Gas Compr Level Init	Gas Compr Level Final	Bal. Temp. °F	Sampling Time, min	Equil'n Time, hr
36	150.0	Liq	3-20	80.4431	80.4431	28.0	33.7	33.7	73	--	7
36	150.0	Gas	3-20	80.7135	82.6171	27.9	36.4	60.2	75	153	6
37	150.0	Liq	3-20	168.2247	168.2247	27.8	30.4	30.4	72.5	--	1.5
37	150.0	Liq	3-20	168.2447	168.2447	27.8	30.1	30.1	74.3	--	5
37	150.0	Liq	3-20	168.2447	168.2447	27.7	30.2	30.2	73	--	12
37	150.0	Gas	3-20	168.3447	169.6693	27.7	31.0	47.7	71	155	14
37	150.0	Liq	3-20	169.8037	169.8037	27.7	48.2	48.3	70.5	--	17.5
38	250.0	Liq	3-20	170.0643	170.0643	27.6	51.3	51.3	76	--	2
38	250.0	Liq	3-20	170.0643	170.0643	27.6	51.2	51.2	75.5	--	5
38	250.0	Liq	3-20	170.0643	170.0643	27.6	51.3	51.3	75	--	8
38	250.0	Liq	3-20	170.0643	170.0643	27.6	51.5	51.5	77.5	--	5
38	250.0	Gas	3-20	170.0643	170.6143	27.6	51.4	57.9	76.5	30	11.5
39	250.0	Liq	3-20	80.7135	80.7135	27.4	21.0	21.0	76.3	--	10
39	250.0	Gas	3-20	81.1835	81.6335	27.3	26.3	32.2	76.5	65	11
40	250.0	Gas	20-50	173.4963	173.6713	27.1	42.0	47.0	77	200	11
40	250.0	Liq	20-50	173.6713	173.6713	27.1	47.0	47.2	76.5	--	14
41	250.0	Liq	50-125	139.6080	139.6080	26.9	35.0	35.0	73.5	--	13
41	250.0	Gas	50-125	139.6150	139.6700	26.9	35.4	39.1	71	100	15
42	250.0	Gas	50-125	238.0780	238.1230	26.5	25.0	28.2	70.5	105	9.5
42	250.0	Liq	50-125	238.1230	238.1230	26.5	28.4	28.6	70	--	13.5
43	250.0	Liq	125-300	175.8140	175.8140	26.5	72.6	72.8	72	--	9
43	250.0	Gas	125-300	175.8140	175.8265	26.5	72.9	75.7	71	110	12
44	250.0	Gas	300-600	176.9203	176.9243	26.5	92.8	94.4	74.3	150	12
44	250.0	Liq	300-600	176.9243	176.9243	26.5	94.7	94.7	73.5	--	16
45	250.0	Gas	600-1000	172.1373	172.1393	26.2	101.9	103.2	74	150	10
45	250.0	Liq	600-1000	172.1393	172.1393	26.2	103.5	103.6	72.5	--	15
46	150.0	Liq	20-50	174.2370	174.2370	25.7	46.3	46.3	70.5	--	16
46	150.0	Gas	20-50	174.2870	174.8120	25.7	47.7	64.2	70.5	90	17

TABLE E-IIA (cont'd)

HYDROGEN-CYCLOHEXANE EXPERIMENTAL DATA

Run No.	Cell Temp. °F	Phase	Meas. Cyl. Range, Atm	Total Wt. on Balance, Kg Init	Total Wt. on Balance, Kg Final	Oil Level cm	Gas Compr Level Init	Gas Compr Level Final	Bal. Temp. °F	Sampling Time, min	Equil'n Time, hr
47	150.0	Gas	50-125	149.0133	149.2003	25.2	31.6	45.8	72	150	12
47	150.0	Liq	50-125	149.2053	149.2053	25.2	46.2	46.3	71.5	--	16.5
48	150.0	Liq	50-125	237.2654	237.2654	24.9	32.0	32.2	72	--	12
48	150.0	Gas	50-125	237.2734	237.3934	24.9	32.1	41.3	75	110	14.5
49	150.0	Gas	125-300	175.9476	175.9796	24.8	71.0	77.1	75	125	8
49	150.0	Liq	125-300	175.9826	175.9826	24.9	77.1	77.2	76	--	12.5
50	150.0	Liq	300-600	176.9203	176.9203	24.6	96.0	96.1	72	--	12
50	150.0	Gas	300-600	176.9203	176.9283	24.6	96.0	99.5	72.5	105	14.5
51	150.0	Gas	600-1000	172.3773	172.3793	24.5	102.1	104.6	72	145	10.5
51	150.0	Liq	600-1000	172.3813	172.3813	24.5	104.7	104.8	73	--	13.5
53	150.0	Gas	20-50	175.0520	175.4844	22.8	72.8	89.3	78	--	32
54	150.0	Gas	600-1000	172.3773	172.3823	22.6	104.6	107.0	74	159	12

TABLE E-IIB

HYDROGEN-CYCLOHEXANE EXPERIMENTAL DATA

	Bar. Press., mm Hg				Air Bath U-Tube Manometer Rdgs.							
Run	Init		Final		First Collection			Second Collection			Air Bath	Vol. Bulbs
No.	mm	°F	mm	°F	Left	Right	Ref.Mk	Left	Right	Ref.Mk	Temp., °F	Attached
36	742.75	72.8	744.3	86.0	615.95	593.55	684.45	--	--	--	86.0	25x, 500x
36	740.35	70.4	741.4	86.0	712.0	494.3	684.45	--	--	--	86.0	1000, 2000
37	744.35	70.9	745.05	86.0	622.5	586.75	684.45	--	--	--	86.0	1000x, 2000x
37	743.85	77.7	743.65	86.0	636.5	572.3	684.45	--	--	--	86.0	1000x, 2000x
37	742.8	74.7	744.35	86.0	630.2	578.75	684.4	--	--	--	86.0	1000x, 2000x
37	744.35	86.0	744.2	86.0	752.0	452.55	684.4	--	--	--	86.0	1000, 2000
37	744.4	86.0	744.4	86.0	628.3	580.65	684.4	--	--	--	86.0	1000x, 2000x
38	738.5	73.2	739.85	86.0	630.5	578.3	684.35	--	--	--	86.0	1000x, 2000x
38	740.45	86.0	741.35	86.0	626.6	582.3	684.35	--	--	--	86.0	1000x, 2000x
38	741.6	86.0	741.75	86.0	646.05	562.2	684.35	--	--	--	86.0	1000x, 2000x
38	740.5	75.7	740.5	86.0	632.95	575.75	684.35	--	--	--	86.0	1000x, 2000x
38	741.8	86.0	742.55	86.0	658.0	549.85	684.3	--	--	--	86.0	1000, 2000
39	738.55	75.5	739.55	86.0	614.55	594.55	684.3	--	--	--	86.0	1000x, 2000x
39	737.45	75.6	738.7	86.0	681.95	525.05	684.3	--	--	--	86.0	1000, 2000x
40	737.15	76.7	738.75	86.0	709.0	497.1	684.3	--	--	--	86.0	1000, 2000
40	738.75	86.0	738.75	86.0	748.7	455.8	684.3	--	--	--	86.0	1000x, 2000x
41	743.6	73.2	744.9	86.0	678.1	529.2	684.3	--	--	--	86.0	25, 1000x
41	744.9	86.0	745.7	86.0	758.45	445.75	684.3	--	--	--	86.0	1000, 2000
42	742.1	71.2	742.5	86.0	813.4	388.95	684.3	--	--	--	86.0	1000, 2000
42	742.5	86.0	742.65	86.0	757.65	446.6	684.3	--	--	--	86.0	25, 1000x
43	738.95	73.5	738.8	86.0	825.0	376.8	684.3	--	--	--	86.0	25, 1000x
43	738.8	86.0	739.55	86.0	901.95	298.4	684.3	662.9	544.9	684.3	86.0	1000, 2000(x)
44	737.55	76.4	738.55	86.0	943.7	256.25	684.3	669.4	538.2	684.3	86.0	1000, 2000(x)
44	738.55	86.0	738.7	86.0	868.25	332.6	684.3	770.35	433.55	684.3	86.0	25, 1000x
45	740.7	75.6	741.55	86.0	955.6	244.25	684.4	671.95	535.7	684.4	86.0	1000, 2000(x)
45	741.55	86.0	742.45	86.0	838.05	363.6	684.35	670.25	537.5	684.35	86.0	25, 1000x

TABLE E-IIB (cont'd)

HYDROGEN-CYCLOHEXANE EXPERIMENTAL DATA

Run	Bar. Press., mm Hg Init		Final		Air Bath U-Tube Manometer Rdgs. First Collection			Second Collection			Air Bath	Vol. Bulbs
No.	mm	°F	mm	°F	Left	Right	Ref.Mk	Left	Right	Ref.Mk	Temp., °F	Attached
46	745.85	86.0	746.3	86.0	650.9	557.5	684.5	--	--	--	86.0	25x,500x
46	746.3	86.0	746.5	86.0	784.1	419.6	684.5	--	--	--	86.0	2000,4000
47	742.25	73.8	742.65	86.0	897.9	302.95	684.5	631.75	577.4	684.5	86.0	2000,4000(x)
47	742.65	86.0	742.95	86.0	686.5	520.8	684.5	--	--	--	86.0	25,500x
48	742.5	71.3	743.3	86.0	735.85	469.55	684.5	--	--	--	86.0	25,500x
48	743.3	86.0	743.65	86.0	936.75	263.55	684.5	635.15	573.15	684.5	86.0	2000,4000(x)
49	743.5	73.8	743.05	86.0	950.4	249.7	684.45	636.3	572.5	684.45	86.0	2000,4000(x)
49	743.05	86.0	743.35	86.0	736.7	468.6	684.45	--	--	--	86.0	25,4000x
50	738.2	71.8	738.0	86.0	747.25	457.6	684.5	--	--	--	86.0	25,4000x
50	738.0	86.0	737.85	86.0	961.05	238.9	684.45	637.3	571.45	684.45	86.0	2000,4000(x)
51	741.0	86.0	741.85	86.0	962.7	236.85	684.45	637.4	571.4	684.45	86.0	2000,4000(x)
51	741.85	86.0	741.3	86.0	857.35	343.95	684.45	702.75	503.9	684.45	86.0	25,4000x
53	744.2	78.1	746.5	86.0	789.8	416.8	684.5	--	--	--	86.0	2000,4000
54	744.4	74.0	740.15	86.0	956.0	220.0	683.8	623.1	562.0	683.8	86.0	2000,4000(x)

TABLE E-IIC

HYDROGEN-CYCLOHEXANE EXPERIMENTAL DATA

Run	Trap No. 1		Trap No. 2		Blank	
No.	Tare Wt., g	Gross Wt., g	Tare Wt., g	Gross Wt., g	Tare Wt., g	Gross Wt., g
36	112.8002	113.2710	112.7663	112.7721	112.1452	112.1452
36	112.8343	113.1464	112.7963	112.7975	112.1453	112.1457
37	112.8140	113.2416	112.7957	112.7970	112.1443	112.1447
37	112.8147	113.5645	112.7955	112.7958	112.1449	112.1453
37	112.8144	113.4028	112.7952	112.7953	113.8681	113.8679
37	113.8679	114.0684	112.1191	112.1211	112.7953	112.7964
37	112.8140	113.3562	112.7948	112.7953	112.1208	112.1205
38	112.8133	113.3421	112.7962	112.7987	112.1222	112.1223
38	112.8424	113.2694	112.7960	112.8056	112.1222	112.1222
38	112.8472	113.6268	112.7961	112.8926	112.1220	112.1218
38	112.8553	113.4371	112.7989	112.7992	112.1228	112.1230
38	112.8579	113.3064	112.7977	112.7978	112.1204	112.1203
39	112.8558	113.3484	112.7967	112.8075	112.1204	112.1205
39	112.8237	113.3729	112.2080	112.2077	113.8138	113.8133
40	113.8140	114.0784	112.2079	112.2606	112.7779	112.7776
40	112.8265	114.0391	112.7776	112.7945	114.0784	114.0781
41	112.8860	113.5002	112.7724	112.7729	113.8692	113.8693
41	113.8693	114.1149	112.2578	112.2621	112.7729	112.7730
42	113.9524	114.1689	112.2538	112.2595	112.9491	112.9491
42	112.9491	113.7145	112.7712	112.7743	112.2595	112.2596
43	112.8788	113.5151	112.7724	112.7754	113.8205	113.8204
43	113.8204	114.0566	112.2557	112.2561	113.5151	113.5148
44	113.8575	114.0671	112.2561	112.2577	112.8798	112.8793
44	112.8793	113.4802	112.7728	112.7823	114.0671	114.0668
45	113.8950	114.0851	112.2559	112.2585	112.7755	112.7753
45	112.8740	113.1049	112.7753	112.7840	112.2585	112.2583
46	112.9115	113.3233	112.8188	112.8191	112.1877	112.1875
46	113.8870	114.1048	112.1875	112.1921	112.8191	112.8195

TABLE E-IIC (cont'd)

HYDROGEN-CYCLOHEXANE EXPERIMENTAL DATA

Run	Trap No. 1		Trap No. 2		Blank	
No.	Tare Wt., g	Gross Wt., g	Tare Wt., g	Gross Wt., g	Tare Wt., g	Gross Wt., g
47	113.8673	114.0606	112.1890	112.1915	112.8949	112.8952
47	112.8952	113.8166	112.8206	112.8204	112.1915	112.1917
48	112.9051	113.8183	112.7514	112.7538	112.1767	112.1775
48	113.8725	114.0303	112.1775	112.1794	113.8183	113.8186
49	113.9029	114.0292	112.1767	112.1791	112.7512	112.7511
49	112.9645	113.5181	112.7511	112.7530	112.1791	112.1787
50	112.8643	113.1804	112.7921	112.7936	112.2291	112.2299
50	113.8651	113.9830	112.2299	112.2321	112.7936	112.7939
51	113.8640	113.9881	112.2294	112.2312	112.8831	112.8828
51	112.8828	113.3672	112.8629	112.8702	112.2312	112.2311
53	112.8503	113.0562	112.8078	112.8081	112.2680	112.2680
54	112.9368	113.0726	112.8028	112.8047	112.2662	112.2668

APPENDIX F

SAMPLE CALCULATION OF EXPERIMENTAL DATA

The calculation of p-T-x-y data from the experimental data is shown below. Final calculations were performed on an IBM 1620 digital computer. A listing of the Fortran program used in the calculations is given in Appendix G. The data used in the sample calculation below are those for Run 40. All constants and conversion factors were taken from the API 44 Tables (72).

Temperature

The temperature was determined from the readings on the potentiometer for the chromel-constantan thermocouples. The emf readings for the thermocouple were 7.7932±0.0038 mv. From the thermocouple calibration (Appendix C), this emf corresponds to a temperature of 150.0±0.1°F.

Pressure

The pressure in the equilibrium cell was determined from the pressure balance pressure, corrected for differences in hydrostatic head of oil, mercury, and hydrocarbon. Correction for difference in head for the hydrogen gas was negligible. (The pressure for vapor-sample runs was corrected for pressure drop through the capillary lines. The latter correction was never estimated to be greater than 0.08 psi, and was negligible at pressure greater than 500 psia.) The pressure at the pressure balance was corrected for buoyancy, thermal expansion of the measuring cylinder, and hydrostatic head due to the oil reservoir acting against the guide pin. The barometric pressure was added to obtain absolute pressure.

Note: The pressure calculated in the 1620 program is P_{gc}, the pressure in the gas compressor. Other corrections were made by hand calculations.

$$P_{bal} = (Mg / A\, g_c) + P_{bar} - P_{oil}$$

where P_{bal} = pressure at pressure balance outlet
g = local acceleration due to gravity
g_c = conversion factor, 980.665 $(kg_m)(cm)/(Kg_f)(sec)^2$
M = mass of all rotating parts, corrected for buoyancy
A = effective area of piston, corrected for thermal expansion
P_{bar} = barometric pressure
P_{oil} = pressure correction due to head of oil on guide pin

Local Acceleration Due to Gravity

The local acceleration due to gravity was calculated from the following formula (14):

$$g = 978.0524 \left[1 + 0.005297 \sin^2 \psi - 0.0000059 \sin^2 2\psi + 0.0000276 \cos^2 \psi \cos^2 (\lambda + 25^\circ)\right] - 0.000060h$$

where ψ = latitude
λ = longitude (positive east of Greenwich)
h = feet above sea level.

At Stillwater, $\psi = 36^\circ\ 7'$ N., $\lambda = 97^\circ\ 4'$ W., $h = 930$ ft.

$$g = 979.777 \text{ cm/sec}^2$$

$$g / g_c = 979.777 / 980.665 = 0.999094 \text{ Kg}_f / \text{Kg}_m$$

Buoyancy Correction

The 20-50 kg / cm^2 piston was used along with weights No. 1, 2, 3, 4, 5, 9, 12, 13, 14, 15, plus 250 g in the weight pan. From the data of Appendix A, the total weight, uncorrected for buoyancy is:

Base Weight	33.3816 Kg_m
Piston, etc.	0.8817
Weight No. 1	25.0131
2	25.0120
3	25.0151
4	25.0138
5	25.0139
9	10.0053
12	0.9974
13	1.0036
14	1.0042
15	1.0046
Extra Weights	0.2500
Total	173.4963 Kg_m

Let V = the volume of a steel weight of in vacuo mass M_o.
d = the density of steel = 7.8 gm / cm^2
ρ_1 = density of air at temperature T_1 and pressure P_1
ρ_2 = density of air at 20 C and 1 atm
M = effective mass of M_o in air at T_1 and P_1
M' = effective mass of M_o in air at 20 °C and 1 atm

Then

$$M = V\ (d - \rho_1) = M_o\ (1 - (\rho_1 / d))$$

$$M' = V\ (d - \rho_2) = M_o\ (1 - (\rho_2 / d))$$

$$\text{or } M = M' \left(\frac{1 - \frac{\rho_1}{d}}{1 - \frac{\rho_2}{d}} \right) = M' \left(\frac{d - \rho_1}{d - \rho_2} \right) \cong M' \left(1 + \frac{\rho_2 - \rho_1}{d} \right)$$

The term in parenthesis is the buoyancy correction to M', and the latter is the weight listed in Appendix A. If the ideal gas law is used to calculate air density, then

$$M = M' \left[1 + 0.000155\ (1 - (293\ P_1\ /\ T_1)) \right]$$

In Run 40, $T_1 = 298\ ^{\circ}K$, $P_1 = 0.965$ atm (see below)

$$M = 173.4963\ (1.0000079) = 173.4977\ \text{Kg}$$

Thermal Expansion Correction

The linear expansion coefficient of the steel in the measuring cylinder is $11 \times 10^{-6}\ {}^{o}C^{-1}$. The area expansion coefficient will be twice the linear coefficient. Then

$$A = A' \left[1 + 0.000022\ (T_1 - 293) \right]$$

where A' is the effective piston area at 20 °C

A is the effective piston area at T_1

Thus

$$A = 5.0058\ (1.00011) = 5.0064\ \text{cm}^2$$

Barometric Pressure

The U-tube manometer in the air bath was used to obtain barometric pressure, with one side evacuated to a negligible pressure and the other side open to the atmosphere. In Run 40 the barometric pressure readings were 737.15 mm Hg at 76.7 F before the run, and 738.65 mm Hg at 86.0 F after the run.

$$P_{bar} = h\rho g\ /\ g_c$$

where h = observed barometric pressure, mm Hg

ρ = density of mercury at temperature of reading, gm / cm^3

The density of mercury is a linear function of temperature between 68 and 86°F. The data in Perry (56) were correlated to give

$$\rho = 13.6383 - 0.001361\ t$$

where t = temperature, deg F.

Before the run:

$$\rho = 13.534\ gm / cm^3$$

$$P_{bar} = 737.15\ mm \times \frac{cm}{10\ mm} \times 13.534\ \frac{gm}{cm^3} \times$$

$$\frac{Kg_m}{1000\ gm} \times 0.99909\ \frac{Kg_f}{Kg_m}$$

$$P_{bar} = 0.9968\ Kg_f / cm^2$$

Similarly, after the run:

$$P_{bar} = 0.9980\ Kg_f / cm^2$$

The average barometric pressure was

$$P_{bar} = 0.9974\ Kg_f / cm^2$$

Also

$$P_1 = 0.9974\ Kg_f / cm^2 \times 0.9675\ \frac{atm}{Kg_f / cm^2}$$

$$= 0.965\ atm$$

Oil Level Correction

The height of the oil above the bottom of the guide pin on the pressure balance is equal to the height of oil in the reservoir plus 1.6 cm (Appendix A). The force transmitted to the rotating shaft is

$$F_{oil} = h_o \rho_o A_{gp} \left(g / g_c\right)$$

where h_o = oil level reading + 1.6

ρ_o = density of the balance oil, 0.876 gm/cm^3

A_{gp} = cross sectional area of the guidepin, 1.76 cm^2

The pressure correction due to the oil level is, then,

$$P_{oil} = F_{oil} / A = h_o \rho_o \frac{A_{gp}}{A} \frac{g}{g_c}$$

In Run 40, h_o = 27.1 + 1.6 = 28.7 cm

$$P_{oil} = 28.7 \text{ cm} \times 0.876 \frac{gm}{cm^3} \times \frac{Kg_m}{1000\ g_m} \times \frac{1.76\ cm^2}{5.0064\ cm^2}$$

$$\times \quad 0.99909 \frac{Kg_f}{Kg_m} = 0.0088 \frac{Kg_f}{cm^2}$$

Corrected Balance Pressure

$$P_{bal} = \frac{Mg}{A\ g_c} + P_{bar} - P_{oil}$$

$$= \left(\frac{173.4977\ Kg_m}{5.0064\ cm^2} \times 0.99909 \frac{Kg_f}{Kg_m}\right) + 0.9974 \frac{Kg_f}{cm^2}$$

$$- 0.0088 \frac{Kg_f}{cm^2}$$

$$= 34.6236 + 0.9974 - 0.0088$$

$$= 35.6122 \ Kg_f / cm^2$$ at the centerline of the cylinder outlet

$$P_{bal} = 35.6122 \ Kg_f / cm^2 \times 14.2234 \frac{lb_f / in^2}{kg_f / cm^2} = 506.53 \text{ psia}$$

Correction for Oil and Mercury Heads

The correction for oil and mercury heads in the gas compressor was shown in Appendix B. The equation for the correction is

$$\Delta P_{gc} = 0.09587 \ h_{gc} + 2.427 \text{ psia}$$

In Run 40 the gas compressor level h_{gc}, was 42.0.

$$\Delta P_{gc} = 0.09587 \ (42.0) + 2.427$$

$$= 6.45 \text{ psia}$$

Then $P_{gc} = P_{bal} - \Delta P_{gc}$

$$= 506.53 - 6.45$$

$$= 500.08$$ psia in the gas compressor over the mercury surface

Correction for Hydrocarbon Head

In Run 40 the system was hydrogen-cyclohexane. The density of pure cyclohexane can be used for the liquid phase density with little error, particularly in view of the smallness of this correction. A further simplification is the use of an average value for the density. The value of the density at the boiling point of the pure hydrocarbon was used. The relative error increases with pressure, but represents a smaller absolute error at the higher pressures. The height of the liquid in the cell is known only approximately anyway, and is taken to be 3 in. in all cases, which should be correct within ± 0.5 in.

$$\Delta P_h = h\rho g \;/\; g_c$$

$$= 3 \text{ in.} \times \frac{\text{ft}}{12 \text{ in.}} \times (0.68 \times 62.4)\,\frac{\text{lb}_m}{\text{ft}^3} \times$$

$$0.999\,\frac{\text{lb}_f}{\text{lb}_m} \times \frac{1 \text{ ft}^2}{144 \text{ in.}^2}$$

$$= 0.07 \text{ psia}$$

Then $P = P_{gc} - P_h$

$P = 500.08 - 0.07$

$P = 500.01$ psia

Correction for Pressure Drop in Capillary

For liquid phase runs, no further corrections are necessary. For the gas-phase runs, corrections were estimated for the pressure drop due to the hydrogen flowing through the capillary lines and gas-distributor cone. Calculations showed that expansion and contraction losses were negligible. The Poiseulle equation was used to calculate the pressure drop, since the flow was laminar in all cases.

$$\Delta P'_c = \frac{32\, L v \mu}{g_c\, D^2} \quad \text{gf} \;/\; \text{cm}^2$$

where L = length, cm
v = average velocity, cm / sec
μ = viscosity, poise (g_m / cm - sec)
g_c = 980.7 g_m - cm / sec^2 - g_f
D = diameter, cm

Converting to English units:

$$\Delta P_c = 0.01422 \quad \Delta P'_c \quad lb_f / in^2$$

Now $v = \frac{Q}{A} = \frac{4Q}{\pi D^2}$

Therefore,

$$\Delta P_c = \frac{(0.01422)\ (32)\ (L)\ (4Q)\ (\mu)}{(\pi)\ (980.7)\ (D^4)} = 0.00059\ \frac{LQ\mu}{D^4}$$

Comparison of the gas compressor level change with the volume of hydrogen collected in several runs showed that each division on the level indicator corresponded to 5.2 cm^3. Thus,

$$Q = 5.2\ \frac{\Delta GCL}{\Delta \theta}$$

Where ΔGCL = change in level indicator reading in time $\Delta\theta$ (sec).

Therefore,

$$\Delta P_c = 0.00059\ \left(5.2\ \frac{\Delta GCL}{\Delta\theta}\right)\ \frac{L\mu}{D^4}$$

$$= 0.00307\ \left(\frac{\Delta GLC}{\Delta\theta}\right)\ \frac{L\mu}{D^4}$$

The heated length of capillary was about 92 cm; the cold length, 230 cm. The capillary diameter was 0.06 cm. The gas-distributor cone had two sets of grooves: one set consisted of 6 grooves 0.56 cm in length; the other set contained 12 grooves 0.95 cm in length. The grooves were approximately 0.01 cm in diameter. In Run 40, the temperature in the heated line and cone was 250 °F. The cold length was taken to be 80 °F. Viscosities for hydrogen are from Granet (29).

$$\frac{\Delta GLC}{\Delta \theta} = \frac{5 \text{ divisions}}{68 \text{ min}} \times \frac{\text{min}}{60 \text{ sec}} = 0.00123 \ \frac{\text{div}}{\text{sec}}$$

$$\mu = 0.000107 \text{ poise at } 250 \ ^{\circ}\text{F.}$$

$$\mu = 0.000089 \text{ poise at } 80 \ ^{\circ}\text{F.}$$

$$\Delta P_c = (0.00307)\ (0.00123) \left\{ \left| \frac{710}{540} \right| (0.000107) \left[\frac{92}{(0.06)^4} + \frac{0.56}{(6)\ (0.01)^4} + \frac{0.95}{(12)\ (.01)^4} \right] + \frac{(0.000089)\ (230)}{(0.06)^4} \right\}$$

$$= .02 \text{ psi}$$

$$P = 500.01 - 0.02 = 499.99 \text{ or } \underline{500.0 \text{ psia in cell}}$$

Composition

The liquid- and gas-phase composition calculations are made in the same manner. Only the gas-phase calculations will be shown.

Hydrogen

The hydrogen was collected in the volumetric part of the apparatus. The following volumes were filled with hydrogen in Run 40 (gas-phase). (Volume calibrations are listed in Appendix D.)

1-l. bulb	946.63 cc
neck	0.38
2-l. bulb	2048.36
neck	0.98
Sampling lines to reference mark	14.27

$$\sum(\text{volumes in lines and bulbs}) = \sum V \quad = 3010.62 \text{ cc}$$

To this must be added the amount above the right-hand mercury level, up to the reference mark. From Appendix D, this volume is

$\Delta = 0.02718$ (Ref. mark ht, mm - Right side manometer level, mm)

The reference mark and manometer heights were 684.3 and 497.1 mm, respectively.

$$\Delta = 0.02718\ (684.3 - 497.1) \ = \ 5.09 \text{ cc}$$

$$V = \Delta + \sum V \ = \ 5.09 + 3010.62 \ = \ 3015.71 \text{ cc}$$

The pressure is given by the difference in levels of the manometer legs, which were 709.0 and 497.1 mm Hg. The air bath temperature was 85.9 °F.

$$P \ = \ \frac{h\rho g}{g_c}$$

where $h \ = \ 709.0 - 497.1 \ = \ 211.9 \text{ mm Hg} \ = 21.19 \text{ cm Hg}$

$$P \ = \ (21.19 \text{ cm})\ (13.521 \frac{\text{gm}}{\text{cm}^3})\ (0.99909 \frac{g_f}{g_m})\ (\frac{0.73556 \text{ mm Hg}}{g_f \ / \ \text{cm}^3})$$

$$P = \ 210.5 \text{ mm Hg (at } 0\ ^{\circ}\text{C}).$$

The compressibility factor for hydrogen (81) is given by

$$z \ = \ 1.0 \ + \ 0.000582 \left|\frac{P}{760}\right|$$

$$\text{or} \quad z \ = \ 1.0 + 0.000582 \left|\frac{210.5}{760}\right| \ = \ 1.0002$$

$$R = 82.0567 \frac{\text{cc-atm}}{\text{g mole - }^{\circ}\text{K}} \times \frac{760 \text{ mm Hg}}{\text{atm}}$$

$$= 62,363 \frac{\text{cm}^3\text{-mm Hg}}{\text{g mole -}^{\circ}\text{K}}$$

$$T = \frac{85.9 + 459.7}{1.8} = 303.1 \ {}^{\circ}\text{K}.$$

$$\text{G-moles Hydrogen} = \frac{P\,V}{zRT} = \frac{(210.5)\ (3016)}{(1.0002)\ (62,363)\ (303.1)}$$

$$= 0.03358$$

Hydrocarbon

The hydrocarbon was frozen out into two traps. The traps were emptied of hydrogen by means of the Toepler pump. The amount of hydrocarbon was determined by the difference in the weights of the traps, before and after sampling.

The trap weights were measured by weighing on the Voland and Sons Balance No. 18559. Calculations showed that buoyancy and arm corrections need not be made because of the relatively small change in weight of the traps. Corrections were made for the weights, in case different weights were used in the gross and tare weight determinations. Changes in buoyancy were corrected for in Runs 35 through 54 by weighing a "blank" trap at the same time that the gross and tare weights were observed:

	Tare	Gross
Trap No. 1	113.8140 g.	114.0784 g.
Trap No. 2	112.2079	112.2606
Blank	112.7779	112.7776

These weights were corrected to obtain the amount of hydrocarbon.

	Tare	Gross	Net
Trap No. 1	113.8146 g	114.0794 g.	0.2648 g
Trap No. 2	112.2083	112.2617	0.0534
			0.3182 g Total

The molecular weight of cyclohexane is 84.162.

$$\text{G-moles cyclohexane} = \frac{0.3182 \text{ g}}{84.162} = \underline{0.003781}$$

$$\text{Total g-moles} = 0.03358 + 0.00378 = 0.03736$$

$$\text{Mole-fraction cyclohexane in vapor} = \frac{0.003781}{0.03736} = \underline{\underline{0.1012}}$$

APPENDIX G

FORTRAN LISTING OF

THESIS DATA CALCULATIONS

```
DIMENSION WT(16),PWT(6),A(6),V(13),TAB(2),CF(2),WTMOL(2)
WT(1)=25.0131
WT(2)=25.0120
WT(3)=25.0151
WT(4)=25.0138
WT(5)=25.0139
WT(6)=25.0166
WT(7)=25.0141
WT(8)=25.0161
WT(9)=10.0053
WT(10)=5.0005
WT(11)=5.0061
WT(12)=0.9974
WT(13)=1.0036
WT(14)=1.0042
WT(15)=1.0046
WT(16)=1.0044
PWT(1)=1.4095
PWT(2)=0.8817
PWT(3)=0.6719
PWT(4)=0.5913
PWT(5)=0.5598
PWT(6)=0.5173
A(1)=12.512
A(2)=5.0058
A(3)=2.0004
A(4)=0.83393
A(5)=0.41938
A(6)=0.24461
BWT=33.2816
V(1)=14.27
V(2)=0.11
V(3)=25.48
V(4)=0.25
V(5)=445.23
V(6)=0.52
V(7)=946.63
V(8)=0.38
V(9)=2048.36
```

```
    V(10)=0.98
    V(11)=3823.5
    V(12)=7.25
    V(13)=0.0
    TAB(1)=303.1
    TAB(2)=298.1
    R=62363.1
    CF(1)=.9936
    CF(2)=.9946
    WTMOL(1)=78.114
    WTMOL(2)=84.162
    PRINT 103
  1 ACCEPT TAPE 100,ID,NCYL,OIL,GCL,BALT,ROOMT,CELLT,PBAR1,
       TBAR1
    ACCEPT TAPE 101, PBAR2,TBAR2,NWTS,EXWTS,NSOLV
    W1=BWT+PWT(NCYL)+EXWTS
    DO 5 I=1,NWTS
    ACCEPT TAPE 102,J
  5 W1=W1+WT(J)
    RHO1=13.6383-.001361*TBAR1
    RHO2=13.6383-.001361*TBAR2
    PBAR1=.99909E-4*PBAR1*RHO1
    PBAR2=.99909E-4*PBAR2*RHO2
    PBAV=(PBAR1+PBAR2)/2.
    PAT=.9675*PBAV
    TRM=((ROOMT-32.)/1.8)+273.16
    W=W1*(1.+(1.545E-4*(1.-(PAT*293.16/TRM))))
    TBAL=(BALT-32.)/1.8
    AB=A(NCYL)*(1.+(2.20E-5*(TBAL-20.)))
    PPRIM=.99909*W/AB
    POIL=(1.54*OIL+2.464)/(1000.*AB)
    PENG=14.2234*(PPRIM+PBAV-POIL)
    DELP=(.09587*GCL)+2.427
    PENG=PENG-DELP
    ACCEPT TAPE 105,KW1,KW2,KW3,KW4,KW5
    HMOL=0.0
    DO 10 I=1,KW2
    ACCEPT TAPE 106,HTL,HTR,REFMK
    PMANO=CF(KW1)*(HTL-HTR)
    VOL=0.0
    DO 9 J=1,KW5
    ACCEPT TAPE 107,NVOL
  9 VOL=VOL+V(NVOL)
    VOL=VOL+V(1)+(.02718*(REFMK-HTR))
    HMOLN=(PMANO*VOL)/(R*TAB(KW1)*(1.+5.82E-4*(PMANO/760.)))
 10 HMOL=HMOL+HMOLN
    ACCEPT TAPE 108,W1G,W1T,W2G,W2T
    HCMOL=((W1G-W1T)+(W2G-W2T))/WTMOL(KW3)
    IF (KW4)15,15,14
 14 Y=HCMOL/(HCMOL+HMOL)
    X=0.0
    GO TO 16
 15 X=HMOL/(HMOL+HCMOL)
```

```
      Y=0.0
   16 IF(NSOLV)17,17,18
   17 PRINT 104,ID,CELLT,PENG,X,Y
      GO TO 20
   18 PRINT 109, ID,CELLT,PENG,X,Y
   20 GO TO 1
  100 FORMAT(I2,I1,F4.0,F5.0,F5.0,F5.0,F5.0,F6.0,F4.0)
  101 FORMAT(F6.0,F4.0,I2,F6.0,I1)
  102 FORMAT(I2)
  103 FORMAT(3HRUN,6X7HSOLVENT,3X7HT DEG F,6X4HPSIA,8X4HX H2,
         8X4HY HC/)
  104 FORMAT(I3,3X12H CYCLOHEXANE,1XF6.1,4XF9.2,3XF9.7,3XF9.7)
  105 FORMAT(I1,I1,I1,I1,I1)
  106 FORMAT(F6.0,F6.0,F6.0)
  107 FORMAT(I2)
  108 FORMAT(F8.0,F8.0,F8.0,F8.0)
  109 FORMAT(I3,3X12H   BENZENE  ,1XF6.1,4XF9.2,3XF9.7,3XF9.7)
      END
```

APPENDIX H

THERMODYNAMIC CONSISTENCY TEST USING VIRIAL EQUATION OF STATE

The derivation of equations used in the thermodynamic consistency test proposed by Prausnitz and Keeler (65) can be made by use of fugacities or chemical potentials. The former will be used for illustration.

Consider the vapor-liquid equilibrium between a mixture of a gas (component 1) and a liquid (component 2) at temperature T and pressure P. The fugacity of component 2 in the vapor mixture at T and P is, by Equation III-16,

$$\ln \bar{f}_2^v = \frac{1}{RT} \int_0^P \left(\bar{V}_2^v - \frac{RT}{P} \right) dP + \ln P y_2 \qquad \text{(H-1)}$$

Assume the applicability of the virial equation of state (Equation III-28), truncated after 3 terms.

$$Z = \frac{P\underline{V}}{RT} = 1 + \frac{B}{\underline{V}} + \frac{C}{\underline{V}2} \qquad \text{(H-2)}$$

where $B = y_1^2 B_{11} + 2 y_1 y_2 B_{12} + y_2^2 B_{22}$

$C = y_1^3 C_{111} + 3 y_1^2 y_2 C_{112} + 3 y_1 y_2^2 C_{122} + y_2^3 C_{222}$

Substitution of the virial equation into Equation H-1 gives (79)

$$\ln \bar{f}_2^v = \ln \frac{y_2 RT}{\underline{V}} + \frac{2}{\underline{V}} \left(y_1 B_{12} + y_2 B_{22} \right)$$

$$+ \frac{3}{2\underline{V}^2} \left(y_1^2 C_{112} + 2\, y_1 y_2 C_{122} + y_2^2 C_{222} \right), \qquad \text{(H-3)}$$

or,

$$\bar{f}_2^v = \frac{y_2 RT}{\underline{V}} \exp \left[\frac{2}{\underline{V}} \left(y_1 B_{12} + y_2 B_{22} \right) + \frac{3}{2\underline{V}^2} \left(y_1^2 C_{112} + 2\, y_1\, y_2\, C_{122} + y_2^2 C_{222} \right) \right] . \qquad \text{(H-4)}$$

The fugacity of pure component 2 at its vapor pressure, p_2, is obtained by use of Equation III-16 for the special case of the pure component.

$$\ln f_2^v(p_2) = \frac{1}{RT} \int_0^{p_2} \left(\underline{V}_2^v - \frac{RT}{P} \right) dP + \ln p_2 \qquad \text{(H-5)}$$

The virial equation may be used for pure component 2 to obtain

$$\ln f_2^v(p_2) = \ln \frac{RT}{\underline{V}_2^v} + \frac{2\, B_{22}}{\underline{V}_2^v} + \frac{3\, C_{222}}{(\underline{V}_2^v)^2} , \qquad \text{(H-5A)}$$

or

$$f_2^v(p_2) = \frac{RT}{\underline{V}_2^v} \exp \left[\frac{2\, B_{22}}{\underline{V}_2^v} + \frac{3\, C_{222}}{(\underline{V}_2^v)^2} \right] \qquad \text{(H-6)}$$

At the vapor pressure, p_2, the pure liquid and vapor are in equilibrium, and

$$f_2^L (p_2) = f_2^V (p_2) \qquad \text{(H-7)}$$

Equation III-17, applied to pure component 2 in the liquid phase, gives

$$RT \ln \frac{f_2^L (P)}{f_2^L (p_2)} = \int_{p_2}^{P} \underline{v}_2^L \, dP \qquad \text{(H-8)}$$

or,

$$f_2^L (P) = f_2^L (p_2) \exp \left[\frac{1}{RT} \int_{p_2}^{P} \underline{v}_2^L \, dP \right] \qquad \text{(H-9)}$$

The definition of the activity coefficient gives

$$\gamma_2^L = \frac{\bar{f}_2^L}{x_2 \; f_2^L(P)} \quad . \qquad \text{(H-10)}$$

The standard state is pure component 2 at T and P. Substitution of Equations H-7 and H-9 into Equation H-10 yields

$$\bar{f}_2^L = \gamma_2^L \, x_2 \;\; f_2^V (p_2) \exp \left[\frac{1}{RT} \int_{p_2}^{P} \underline{v}_2^L \, dP \right] \qquad \text{(H-11)}$$

At equilibrium, $\bar{f}_2^L = \bar{f}_2^V$, and the right-hand sides of Equations H-4 and H-11 are equal.

The consistency test of Prausnitz and Keeler makes use of Equations H-2, H-4, H-6, and H-11. Assume for the moment that all necessary virial coefficients except B_{12} are available. Assume also that data for evaluation of Equation H-11 is available (this assumption is discussed below). The only unknown remaining in Equations H-2, H-4, H-6, and H-11 is, then, B_{12}. The consistency test consists of solving these equations for B_{12} for several different experimental points at the same temperature. If the values of B_{12} so derived are reasonably constant, then the volumetric and p-T-x-y data are deemed consistent. (All virial coefficients are functions of temperature only.)

The Prausnitz-Keeler test is based, first of all, on the applicability of the virial equation truncated after two terms. Three terms were carried in the derivations, but terms involving the third virial coefficient are shown to have small effect below. In general, the virial equation truncated after two terms represents volumetric data well only at low pressures. In the particular case of gases and mixtures containing mostly gases, the virial equation truncated after two or three terms represents volumetric data quite well up to moderately high pressures. The latter case was illustrated by Prausnitz and Keeler (65), and is confirmed for n-hexane-hydrogen mixtures in Chapter VI. Thus, the Prausnitz-Keeler test is useful for gas-liquid systems, the case of interest in this thesis.

Another circumstance effectively limits the use of the Prausnitz-Keeler to gas-liquid mixtures. In Equation H-11, γ_2^L must be evaluated. In general, γ_2^L is not available, although it may be estimated by the Scatchard-Hildebrand equation (Equation III-31). In the case of gas-liquid systems at moderate temperatures, x_2 is nearly 1.0 and γ_2^L is approximately 1.0 also. The Scatchard-Hildebrand equation was used to estimate γ_2^L in this work, and its use is shown below to produce small effect in the calculated B_{12} values. It should be stressed that the Prausnitz-Keeler test checks mainly the P-T-y data, since x_2 is close to 1.0 in most cases.

The availability of the data used in Equations H-2, H-4, H-6, and

H-11 was taken for granted above. The sources of the data used in this work are given below.

Virial coefficients may be estimated from generalized correlations, but good experimental data are preferable. Second virial coefficients for benzene and cyclohexane were taken from David et al. (19), who made a thorough investigation of the published data. The second virial coefficient of n-hexane was calculated from the Kihara potential (34). Connolly (18) showed that this potential fitted the experimental data for n-hexane very well, and listed the parameters necessary to calculate B_{22} for n-hexane. Values calculated from the Kihara potential checked well with other literature values. The second and third virial coefficients for hydrogen were taken from Bird et al. (9).

Evaluation of third virial coefficients for the hydrocarbons presented a problem. Experimental values at the temperatures of interest were not available. Values of C_{222} were calculated for several hydrocarbons from API 44 volumetric data (72), and for several other substances from literature data. These calculated C_{222} values compared fairly well with the generalized correlation of Prausnitz (60) at reduced temperatures of 0.88 and above. For this reason C_{222} values were taken from Prausnitz' correlation. These values were taken from an extrapolated portion of the correlation and must be regarded as approximate.

Third virial cross-coefficients were calculated by the following empirical rule.

$$C_{ijk} = (C_{iii}\ C_{jjj}\ C_{kkk})^{1/3} \tag{H-12}$$

Connolly (15) showed that the above rule worked fairly well for hydrogen-hydrocarbon systems.

Vapor pressure data for the hydrocarbons were obtained from the API 44 tables (72). Liquid density data for the hydrocarbons (28, 67, 77) were expressed in the following form for ease of calculation.

$$\underline{V}_2^L = \underline{V}_2^o (1 - \beta P) \tag{H-13}$$

Thus, the integral of Equation H-11 becomes

$$\int_{p_2}^{P} \underline{V}_2^L \, dP = \underline{V}_2^o \left[(P - p_2) - \frac{\beta}{2} (P^2 - p_2^2) \right] \tag{H-14}$$

The parameters δ_1, δ_2, and $\underline{V}_1^L$ in the Scatchard-Hildebrand equation were taken from Prausnitz et al. (64). Values of all parameters used are given in Table H-1.

A sample calculation for Run 17 is given below to illustrate the method.

Experimental Data: Hydrogen-benzene system
$T = 250\ ^oF = 394.3\ ^oK$
$P = 499.4$ psia $= 33.98$ atm
$x_1 = 0.0153$
$y_2 = 0.104$

For pure benzene at its vapor pressure, using B_{22} only,

$RT = (82.06)(394.3) = 32{,}350$ cc-atm/g mole
$p_2 = 44.67$ psia $= 3.04$ atm

Eq. H-2

$$\underline{V}_2^v = \frac{33{,}350}{3.04} \quad 1 - \frac{753}{\underline{V}_2^v}$$

$$\underline{V}_2^v = 9828 \quad \text{cc/g mole}$$

Eq. H-6

$$f_2^V\ (p_2) = \frac{32{,}350}{9828} \exp\left[\frac{2(-753)}{9828}\right] = 2.824 \text{ atm}$$

Eq. H-14

$$\int_{p_2}^{P} \underline{V}_2^L\, dP = 101.3 \left\{ (33.98 - 3.04) - \left|\frac{1.52 \times 10^{-5}}{2}\right| (14.7) \left[(33.98)^2 - (3.04)^2 \right] \right\} = 3.21 \text{ cc-atm/g mole}$$

Eq. H-13

$$\underline{V}_2^L = 101.3 \left[1.0 - (1.52 \times 10^{-5})\ (499.4) \right] = 100.5 \text{ cc/g mole}$$

Eq. III-33

$$\delta_{mix} = \frac{(0.0153)(43.0)(1.8) + (0.9847)(100.5)(8.0)}{(0.0153)(43.0) + (0.9487)(100.5)} = 7.9586\ \frac{\text{cal}}{\text{cc}}^{\frac{1}{2}}$$

Eq. III-32

$$\ln \gamma_2^L = \frac{(100.5)(8.0 - 7.9586)^2}{(1.987)(394.3)} = 0.00022$$

$$\gamma_2^L = 1.0002$$

Eq. H-11

$$\bar{f}_2^V = \bar{f}_2^L = (1.0002)(0.9847)(2.824) \exp\left|\frac{3121}{32{,}350}\right| = 3.063 \text{ atm}$$

The third virial coefficients of Table H-1 are combined by the rule of Equation H-12 to obtain

$$C_{112} = 1492 \quad (\text{cc/g mole})^2,$$

$$C_{122} = 5984 \quad (\text{cc/g mole})^2.$$

Then C is calculated by its definition.

$$C = 842\ (\text{cc/g mole})^2$$

B is also calculated, by definition, as

$$B = (0.896)^2(15.37) + 2(0.896)(0.104)\ B_{12} + (0.104)^2(-753),$$

$$B = 4.213 + 0.1864\ B_{12}.$$

The virial equation becomes

$$\frac{33.98\ \underline{v}}{32,350} = 1 + \frac{(4.213 + 0.1864\ B_{12})}{\underline{v}} + \frac{842}{\underline{v}^2}$$

Eq. H-4

$$3.063 = \frac{(0.104)(32,350)}{\underline{v}} \exp \frac{2}{\underline{v}}\ (0.896)\ B_{12} + (0.104)(-753)$$

$$+ \frac{3}{2\underline{v}^2}\ (0.896)^2(1492) + 2(0.896)(0.104)(5984)$$

$$+ (0.104)^2(24,000)$$

The last two equations are solved by trial-and-error to obtain

$$B_{12} = 12.7 \quad \text{cc/ g mole}$$

The results of a few calculations for benzene at 250°F are given below to show the effect of neglecting the third virial coefficient and liquid activity coefficient.

	B_{12} for H_2-Benzene at 250°F		
Pressure, psia	Calc'd with B, C, and γ_2^L	B and C, $\gamma_2^L = 1.0$	B only, $\gamma_2^L = 1.0$
97.0	-15.2	-15.3	-12.1
499.4	12.7	12.6	14.6
2999	9.4	8.5	15.3

The effect of γ_2^L is shown to be very small at low pressures, and not very important even at 2999 psia. The effect of C is more marked, but probably could be neglected for practical purposes because its use does not improve the constancy of B_{12} (which is the important fact to be checked).

TABLE H-I

PARAMETERS USED IN PRAUSNITZ-KEELER CONSISTENCY TEST

Parameter	Hydrogen 150°F	Hydrogen 250°F	Benzene 150°F	Benzene 250°F	Cyclohexane 150°F	Cyclohexane 250°F	n-Hexane 150°F	n-Hexane 250°F
p_2, psia	--	--	9.179	44.67	9.089	42.86	13.28	59.2
$\underline{V}_i^o$, cc/g mole	37.8	43.0	94.07	101.3	114.5	124.8	139.4	154.5
10^5 β, psia^{-1}	--	--	0.97	1.52	0.905	1.66	1.43	2.98
B_{ii}, cc/g mole	14.80	15.37	-1080	-753	-1194	-814	-1360	-887
C_{iii}, (cc/g mole)^2	394	372	10000	24000	7800	9700	60000	72000
δ_i, (cal/cc)$^{\frac{1}{2}}$	2.5	1.8	8.6	8.0	7.8	7.2	7.0	6.6

APPENDIX J

CHAO-SEADER K-VALUE CORRELATION

The Chao-Seader correlation method (12) is based on the thermodynamic relation

$$K = \gamma_i^L \nu_i^L / \phi_i^V \quad . \qquad \text{(III-26)}$$

The vapor fugacity coefficient is calculated by the Redlich-Kwong equation of state (68).

$$\ln \phi_i^V = (z - 1) \frac{B_i}{B} - \ln (z - BP) - \frac{A^2}{B} \left(\frac{2\,A_i}{A} - \frac{B_i}{B} \right) \ln \left(1 + \frac{BP}{z} \right) \qquad \text{(J-1)}$$

$$\text{where } z = \frac{1}{1-h} - \frac{A^2}{B} \frac{h}{1+h} \qquad \text{(J-2)}$$

$$h = \frac{BP}{z} \qquad \text{(J-3)}$$

$$A = \sum_{i=1}^{N} y_i\, A_i \qquad \text{(J-4)}$$

$$A_i = \frac{0.6541}{P_c^{\,0.5}} \left(\frac{T_c}{T} \right)^{1.25} \qquad \text{(J-5)}$$

$$B = \sum_{i=1}^{N} y_i\, B_i \qquad \text{(J-6)}$$

$$B_i = \frac{0.0867\, T_c}{P_c\, T} \qquad \text{(J-7)}$$

Use of the R-K equation requires only component T_c and P_c values.

The liquid activity coefficient is evaluated by use of the Scatchard-Hildebrand equation.

$$\ln \gamma_i^L = \frac{\underline{V}_i^L}{RT} (\delta_i - \delta_{mix})^2 \qquad \text{(III-31)}$$

where

$$\delta_{mix} = \sum_{j=1}^{N} x_j \underline{V}_j^L \delta_j / \sum_{j=1}^{M} x_j \underline{V}_j^L \qquad \text{(III-31)}$$

For components below their critical temperatures, molal volumes are often available, as well as the information required to evaluate δ_i. Chao and Seader found that sufficient accuracy was obtained in their correlation method by use of a single value of δ_i and $\underline{V}_i^L$ for each component (independent of temperature). They tabulated values of these parameters for many hydrocarbons. Components above their critical temperature required special treatment, as described below.

Chao and Seader used selected experimental equilibrium data to back calculate ν_i^L values for components below their critical temperatures. The ν_i^L values were then fitted to the relation

$$\log \nu_i^L = \log \nu^{(o)} + \log \nu^{(1)}, \qquad \text{(J-8)}$$

where

$$\log \nu^{(o)} = A_o + \frac{A_1}{T_r} + A_2 T_r + A_3 T_r^2 + A_4 T_r^3$$

$$+ (A_5 + A_6 T_r + A_7 T_r^2) P_r$$

$$+ (A_8 + A_9 T_r) P_r^2 - \log P_r, \qquad \text{(J-9)}$$

$$\log \nu^{(1)} = 4.23893 + 8.65808 T_r - \frac{1.22060}{T_r}$$

$$-3.15224\ T_r^3 - 0.025\ (P_r - 0.6). \qquad \text{(J-10)}$$

A single set of A values was used for hydrocarbons heavier than methane.

The parameters $\underline{V}_i^L$ and δ_i could not be evaluated directly for gases (e.g., hydrogen). Values of $\underline{V}_i^L$ were assigned arbitrarily for gases from literature values of their partial molar volumes in various solvents. Values of δ_i and ν_i^L were selected such that the error between calculated and experimental K values was minimized for selected experimental data. In this minimization procedure, use was made of the theoretical fact that ν_i^L is a function of temperature and pressure only and should be the same for a particular gas in solution in any solvent. The derived ν_i^L values for methane and hydrogen gases were fitted to Equations J-8 through J-10, and a set of A values obtained for each of these gases.

Values of A, ω, $\underline{V}_i^L$ and δ_i are tabulated below for the substances of interest in this thesis. The original Pitzer et al. corresponding states correlations did not include hydrogen. Chao and Seader arbitrarily used a value of $\omega = 0$ for hydrogen.

	Hydrocarbons	Hydrogen
A_0	5.75748	1.96718
A_1	-3.01761	1.02972
A_2	-4.98500	-0.054009
A_3	2.02299	0.0005288
A_4	0	0
A_5	0.08427	0.008585
A_6	0.26667	0
A_7	-0.31138	0
A_8	-0.02655	0
A_9	0.02883	0

Substance	ω	$\delta\left(\frac{cal}{cc}\right)^{1/2}$	$\underline{V}^L$, cc/g mole
Hydrogen	0	3.25	31
n-Hexane	0.2927	7.27	131.6
Cyclohexane	0.2032	8.20	108.7
Benzene	0.2130	9.16	89.4

The use of the Chao-Seader correlation necessitates a trial-and-error calculation, since the expressions for Φ_i^V and γ_i^L are composition dependent. For a binary mixture at temperature T and P, trial values of K_1 and K_2 are assumed. Then

$$y_1 = \frac{1-K_2}{K_1-K_2} , \qquad \text{(J-13)}$$

$$x_1 = K_1 x_1 , \qquad \text{(J-14)}$$

$$y_2 = 1-y_1 , \qquad \text{(J-15)}$$

$$x_2 = 1-x_1 . \qquad \text{(J-16)}$$

Equations J-1, etc., may now be used to calculate K values, which are compared to the trial values. The procedure is repeated until the calculated and trial K values are arbitrarily close.

The critical properties used in the Chao-Seader calculations are listed below.

Substance	T_c, °K	P_c, atm	Reference
Hydrogen	33.3	12.80	13
n-Hexane	507.8	29.93	23
Cyclohexane	554.2	38.16	23
Benzene	562.66	48.664	23

APPENDIX K

CALCULATION OF GENERALIZED INTERACTION SECOND VIRIAL COEFFICIENTS

The method of Prausnitz and Benson (63) for predicting interaction second virial coefficients for binary mixtures, in which one component has a low molecular weight and the other a high molecular weight, is an application of a previous pure component second virial coefficient correlation presented by Prausnitz (60). The second virial coefficient correlation is of the form

$$\frac{B}{\underline{V}_c} = \theta_B\left(\frac{T}{T_c}, \omega\right) \tag{K-1}$$

Simple mixture rules were used for $\underline{V}_{c12}$ and ω_{12}.

$$\underline{V}_{c12} = \frac{\underline{V}_{c1} + \underline{V}_{c2}}{2} \tag{K-2}$$

$$\omega_{12} = \frac{\omega_1 + \omega_2}{2} \tag{K-3}$$

The characteristic temperature (which is not a critical temperature in the usual sense, for binary mixtures) to be used in Equation K-1 cannot be calculated from any simple formula. Prausnitz and Benson used the London theory of dispersion forces and experimental values of B_{12} to arrive at a correlation method for this characteristic temperature. The correlating equation is

$$T_{c12} = \frac{\alpha_1 \alpha_2 I_1 I_2}{\beta\, k\, \sigma_{12}^6 (I_1 + I_2)} \qquad \text{(K-4)}$$

where T_{c12} = characteristic temperature of 1-2 interaction, °K.
α = polarizability, cc/molecule
I = first ionization potential, e.v./molecule
k = Boltzmann constant, 8.61 e.v./(molecule-°K)
σ_{12} = collision diameter, or characteristic interaction distance, for 1-2 interaction, cm
β = dimensionless constant, 0.744

Values of α and I may be found for many substances from the literature. Values of σ_{12} for various systems were evaluated by Prausnitz and Benson and correlated as a function of $\underline{V}_c$ for the heavy component for the light components methane, propane, hydrogen, nitrogen, hydrogen sulfide, and carbon dioxide.

The values of the parameters used in this study for calculating interaction second virial coefficients by the above method are listed in Table K-I. The use of the method involves straightforward substitution of these parameters into Equations K-2, K-3, and K-4, the evaluation of T/T_{c12}, and the interpolation of $B/\underline{V}_{c12}$ from the tabulation of Prausnitz.

The evaluation of the parameters in Table K-I is not so straightforward and is discussed here for the sake of clarity. Critical volumes must come from experimental data, and were taken from the API 44 tables (72) for benzene and n-hexane, and the NGSMA data book (53) for cyclohexane. The acentric factors were obtained from Edmister's tabulation (23) for the hydrocarbons. Pseudo values of $\underline{V}_c$ and ω were listed for hydrogen by Prausnitz and Benson.

Ionization potentials for benzene and cyclohexane were listed by

Watanabe (80), and for n-hexane and hydrogen by Prausnitz and Benson. Polarizabilities for the hydrocarbons were evaluated from listed values (21) of the dielectric constant as follows. First, the molar polarizability was calculated from the dielectric constant by the Clausius-Mosotti relation (31).

$$E = \frac{M}{\rho} \frac{e-1}{e+2} \qquad \text{(K-5)}$$

where E = molar polarizability, cc/g mole
M = molecular weight, g/g mole
ρ = density, g/cc
e = static dielectric constant

The molecular dielectric constant is related to the molar dielectric constant by the following equation (31)

$$\alpha = \frac{3\ E}{4\pi\ N_o} \qquad \text{(K-6)}$$

where N_o = Avogadro's number,
6.02×10^{23} molecules/g mole

Prausnitz and Benson listed α and I for hydrogen.

The collision diameters, σ_{12}, were taken, as stated earlier, from the correlation presented by Prausnitz and Benson.

TABLE K-I

PARAMETERS USED IN CALCULATION OF GENERALIZED INTERACTION SECOND VIRIAL COEFFICIENTS

Component	v_c, cc/g mole	ω	σ^3_{12}, cc x 10^{24}	I, ev/molecule	e	α, 10^{25}x cc/molecule
Hydrogen	47.0	0	-	15.4	-	7.9
n-Hexane	368	0.290	96	10.4	1.887	-
Cyclohexane	311	0.186	87	9.88	2.010	-
Benzene	260	0.215	79	9.24	2.263	-

NOMENCLATURE

a_1, a_2 = constants in van Laar equation (Eq. III-37)

B = second virial coefficient

C = third virial coefficient

D = fourth virial coefficient

= number of independent intensive thermodynamic variables (Eq. III-8)

E = energy

F = U-TS+PV = Gibbs free energy

f = fugacity

K = y/x = vapor-liquid equilibrium ratio

N = number of components in a mixture

n = number of moles

P = pressure

p = vapor pressure

R = the gas law constant

S = entropy

T = absolute temperature

U = internal energy

V = volume

x = mole fraction in liquid phase

y = mole fraction in vapor phase

z = $P\underline{V}/RT$ = compressibility factor

z' = quantity defined by Eq. VI-7

Greek Letters

β = liquid compressibility parameter (Eq. VI-10)

γ = $\bar{f}/x\, f^{o}$ = activity coefficient

Δ = change in any quantity

δ = $(E^{VAP}/\underline{V}^{L})^{1/2}$ = solubility parameter

μ = chemical potential

ν = f/P = pure component fugacity coefficient

Φ = number of phases in a closed system

ϕ = $\bar{f}/Py$ = mixture fugacity coefficient

ω = $-[(\log_{10} p_r)_{T_r = 0.7} + 1]$ = acentric factor

Subscripts

BZ = quantity associated with benzene

C = quantity evaluated at the critical point

CH = quantity associated with cyclohexane

i, j, k = quantity associated with component *i*, *j*, or *k*

MIX = quantity associated with a mixture

r = quantity reduced by dividing by the corresponding critical quantity

1 = quantity associated with component 1 (lighter component)

= quantity evaluated at condition 1

2 = quantity associated with component 2 (heavier component)

= quantity evaluated at condition 2

_(bar) = quantity per mole

Superscripts

E = quantity in excess of value for ideal mixing

ideal = quantity associated with mixture in which there are no nonidealities due to mixing

L = quantity associated with liquid phase

v = quantity associated with gas phase

VAP = quantity associated with vaporization to the ideal gas state

o = quantity evaluated in a reference state

(o) = quantity associated with a simple fluid

(1) = quantity associated with deviations from simple fluid behavior

* = quantity evaluated at infinite dilution

¯(bar) = partial molal quantity

= quantity associated with a component of a mixture

',″,‴ = quantities associated with different phases in a closed system

Abbreviations

BWR = Benedict-Webb-Rubin

RK = Redlich-Kwong

VITA

Richard Eugene Thompson

Candidate for the Degree of

Doctor of Philosophy

Thesis: INVESTIGATION OF VAPOR-LIQUID EQUILIBRIA FOR HYDROGEN-SIX CARBON HYDROCARBONS

Major Field: Chemical Engineering

Biographical:

Personal Data: Born in Parsons, Kansas, October 15, 1929, the son of James A. and Ruby E. Thompson. Married to Marilyn Short, Bartlesville, Oklahoma, in December, 1951. Father of two children: Gary and Julia Thompson.

Education: Attended elementary school in Bartlesville, Oklahoma; graduated from College-High School, Bartlesville, in 1947; received Bachelor of Science degree in Chemical Engineering from Oklahoma State University in 1951; received a Master of Science, with a major in Petroleum Refining Engineering, from Colorado School of Mines in 1959; completed requirements for the Doctor of Philosophy degree in August 1963.

Organizations: American Institute of Chemical Engineers (Associate Member)

Professional Experience: Employed as an engineer with Phillips Petroleum Company, 1951-1953; employed as an engineer with The Dow Chemical Company, Texas Division, 1953-54. Served in the U. S. Army, 1954-56. Employed in the summer of 1959 with Esso Research Laboratories.